# HEREDITARY DEAFNESS AND MAST CELL TUMORS IN DOGS: SEQUENCE ANALYSIS OF CANDIDATE GENES FROM THE MELANOCYTE DEVELOPMENT PATHWAY

By

Daniel Zemke

A DISSERTATION

Submitted to
Michigan State University
in partial fulfillment of the requirements
for the degree of

DOCTOR OF PHILOSOPHY

Department of Microbiology and Molecular Genetics

2003

ABSTRACT

HEREDITARY DEAFNESS AND MAST CELL TUMORS IN DOGS: SEQUENCE ANALYSIS OF CANDIDATE GENES FROM THE MELANOCYTE DEVELOPMENT PATHWAY

By

Daniel Zemke

The dog is the result of centuries of breeding by humans. Various genetic diseases are prevalent in various breeds of dog as compared to mixed bred dogs. One example is a hereditary sensorineural deafness that is often accompanied by abnormal pigmentation, seen primarily in breeds with merle or white spotting coat patterns. Examination of deaf dogs has revealed an absence of melanocytes in the cochleas of affected ears. Among other functions, melanocytes produce the pigment melanin, which determines coat color. Similar conditions of hearing loss and pigmentation in other species are linked to mutations in genes from the melanocyte development pathway. Mutations in these genes also cause other diseases besides hearing loss and pigmentation. The purpose of this study was to examine selected members of this set of genes at the molecular level in the dog and evaluate their potential role in hereditary deafness and selected other conditions. Candidate genes were selected based on similarity of the phenotype seen in other species to that in the dog. The genes for endothelin receptor B (*EDNRB*), microphthalmia-associated transcription factor (*MITF*), *KIT* and its ligand (*KITLG*) were examined by sequencing the entire coding region in 1 normal and 7 deaf dogs. No causative mutations were found during the course of the sequencing, however other features such as alternative splicing events, single nucleotide polymorphisms

(SNPs), a microsatellite, and a pseudogene were identified. SNPs in *KIT* and *EDNRB* were not found to be associated with deafness in the Jack Russell Terrier. It appears unlikely that any of the candidate genes are responsible for deafness in dogs. In addition to deafness, the *KIT* gene was examined for its involvement in mast cell tumors. Examination of 88 tumors revealed duplications and deletions that appeared to be associated with tumors of higher grade. Duplications similar to those in this study result in constitutive activation of KIT. Other activating mutations of *KIT* have been shown to result in tumor formation. Further study is needed to determine the exact nature of its involvement, including the effect of drugs targeting such activation on the biological behavior of these tumors.

TABLE OF CONTENTS

LIST OF TABLES

LIST OF FIGURES

# CHAPTER 1

# LITERATURE REVIEW

Humans have been responsible for the genetic manipulation of a number of plant and animal species. Individuals that exhibit desirable phenotypic traits are preferentially used for breeding, and breeding from individuals with undesirable traits is avoided. The domestic dog is the result of thousands of years of such selective breeding. Although all dogs share a single common ancestor, the American Kennel Club recognizes 145 different breeds, and it has been suggested that over 1,000 breeds exist worldwide.[2,53] Many of these breeds were specifically bred to perform certain tasks, and the number of breeds reflects the varied roles that dogs play in human societies. To ensure that particularly advantageous traits become permanently established, breeders generally resort to some measure of inbreeding. Dogs with champion status are often bred to multiple partners, including their own offspring and siblings. Formal breed clubs generally discourage mating between dogs of different breeds. The effect of inbreeding is to increase the frequency of certain alleles at a trait locus and increase the number of homozygotes for a particular allele. Unfortunately, this means that the frequency of normally rare recessive traits, some of which may be disadvantageous, can be quite high within a particular breed.

In many dog breeds, there is often an increased risk of inheriting one or more genetic diseases, due to the decreased gene pool that results from inbreeding. For example, the Labrador Retriever is prone to progressive retinal atrophy and narcolepsy, and the German Shepherd is prone to spinal muscle atrophy and hemophilia.[13] Inherited diseases in dogs are known for nearly every organ system in the body. These diseases may be fatal, disabling, or merely uncomfortable to an affected dog. The cost of treatment in some cases can be so high that the dog may be euthanized. Unfortunately,

the genetics of these diseases are often not well understood, and those recognized as recessive traits are hard to remove from the population because breeders do not have a means to identify carriers. Some breeders ignore or deny the fact that there are problems within their breed. As a result, many continue the same breeding practices that created the problem in the first place. Molecular biology, however, can be used to specifically identify the genetic basis of a trait of interest. This would provide the ability to screen for carriers and lower the frequency of undesirable traits by removing carriers from the breeding population. If a mutation leading to the production of an abnormal protein is shown to cause a particular disease, this may yield the opportunity to develop methods of prevention or treatment. For example, a mutant protein that is constitutively active could be treated with drugs that inhibit it. If a disease if found to have to the same molecular basis in both humans and dogs, development of a treatment for dogs may also result in a treatment for humans. The study of a gene at the molecular level can also increase the understanding of its role in complex mammalian systems and how it interacts with other genes.

**Hereditary deafness**

The main focus of this study is hereditary hearing loss, a genetic disease prevalent in a number of dog breeds. There are three main types of hearing loss, categorized by the location of the physiological defect that causes it.[24] Conductive hearing loss stems from defects within the outer and middle ear, including blockage of the ear canal and defects that prevent the conduction of sound from the eardrum to the inner ear. Central hearing loss is due to defects in the brain and auditory nerves that prevent the proper reception or

processing of auditory stimuli. Sensorineural hearing loss is the result of defects within the inner ear that prevent the detection of sound. Sensorineural hearing loss is further classified into two subcategories based on which tissues within the inner ear are affected. Neuroepithelial deafness is the result of defects within the sensory hair cells and their supporting tissues alone. Cochleosaccular deafness is the result of degradation of multiple tissues within the cochlea and saccules, often including the hair cells as well.

Other criteria used to evaluate hearing loss are its heritability, age of onset, progressiveness, and whether or not it is syndromic.[24] Hereditary hearing loss can be passed from parent to offspring and is caused by mutations within the DNA of the individual. Acquired hearing loss is caused by outside factors and cannot be inherited. The normal hearing loss that occurs at old age is considered to be acquired hearing loss. Other non-hereditary causes of hearing loss include physical trauma and exposure to various chemicals. Congenital hearing loss is deafness that is apparent at birth or soon after, whereas other forms of hearing loss do not appear until later in life. In progressive hearing loss, the severity of the loss increases with time. Non-progressive hearing loss does not change in severity. Finally hearing loss can be syndromic on non-syndromic. In syndromic hearing loss, other systems of the body are affected in addition to the auditory system. Non-syndromic hearing loss refers to cases where deafness is the only symptom.

Acquired deafness cannot be passed from one individual to another, and therefore does not present any threat to the population as a whole. Because hereditary deafness can be propagated through a lineage, it is important to discover the underlying cause and screen for it within breeding stock. In dogs, congenital deafness has been reported in at least 69 breeds.[74] However, inheritance has not been proven in some of these breeds,

therefore the actual number with hereditary deafness is unknown. Hereditary deafness in different breeds may also have different etiologies; therefore a broad study of hereditary deafness in all dogs is not feasible. The focus of this study was on hereditary deafness in breeds that show inheritance of the merle (for example Collies and Australian Cattle Dogs) and spotting (for example Boxers and Dalmatians) coat color loci.[73,80] These breeds share a common pattern of deafness that is hereditary, cochleosaccular, congenital, non-progressive, and syndromic. Hearing loss, when present, can occur in either one ear (unilateral) or both ears (bilateral).

The frequency of deafness is different in each breed and may even vary between different populations within a breed. Hereditary deafness has been best described in the Dalmatian. In one estimate, 8% of Dalmatians have bilateral deafness and 22% have unilateral deafness.[74] The mode of inheritance in Dalmatians is unclear because different studies have produced conflicting results. Some studies have suggested that deafness is due to a single autosomal recessive gene with incomplete penetrance.[32,56] Another study suggests that multiple loci are involved and that unilateral and bilateral deafness may have different genetic causes.[23] Some studies have found that deafness is significantly more prevalent in females than in males.[38] The mode of inheritance in other breeds has not been extensively reported, however one study of the Australian Cattle Dog suggests that 2 recessive genes may be involved.[73]

The canine ear continues to develop after birth, and the ear canal does not open until about 2 weeks of age.[73] Testing is usually not performed until at least 6 weeks of age, when mature hearing patterns have been established and the processes leading to the

form of deafness under study are complete. The preferred way to assess hearing loss is the brainstem auditory evoked response (BAER) test, also known as the brainstem auditory evoked potential (BAEP) or auditory brainstem response (ABR).[73] An auditory stimulus is sent to the ear by earpieces in the form of a series of clicks. Electrodes positioned on the head receive the electrical signal produced in response to this stimulus, and the signals from multiple stimulatory clicks are recorded and processed by a computer. Sample results from a BAER test are shown in Figure 1. In a normal auditory response, 4 or 5 distinct peaks are produced corresponding to passage of the signal through different parts of the nervous system. The first peak is produced in the cochlea

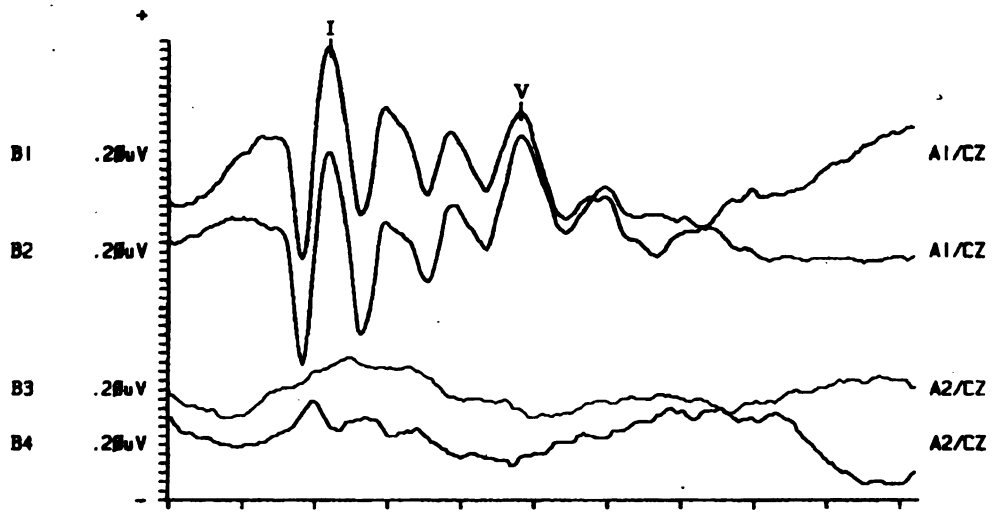


Figure 1. BAER test results from a Catahoula Leopard Dog with unilateral deafness. Two recordings were made from each ear. The upper two lines are from the right ear and show a normal auditory response. The lower lines show the lack of a response for the deaf left ear. The position of peaks I and V are shown on the graph.

and the adjacent end of the cochlear nerve, and the remaining peaks are produced in different parts of the brain. If the first peak is present but any of the following peaks are absent, central hearing loss is indicated. Absence of the first peak indicates either sensorineural or conductive hearing loss. A physical examination of the ear can be used to ensure that the stimulus was properly transmitted to the cochlea and rule out conductive hearing loss. Alternatively, a stimulus can be transmitted through bone directly to the cochlea.

A diagram of the inner ear is shown in Figure 2. The cochlea consists of three fluid filled chambers. The scala vestibuli and scala tympani contain a fluid known as perilymph, and the cochlear duct contains a fluid known as endolymph. In a normal ear, sound vibrations entering the ear impact upon the tympanic membrane and are transmitted to the scala vestibuli by the action of the bones of the middle ear on the oval window.[73] The resulting pressure waves in the perilymph of the scala vestibuli travel the length of the cochlea, return via the scala tympani, and exit at the round window. This movement of pressure waves causes a shearing force on the sensory hair cells within the organ of Corti of the cochlear duct. The stereocilia of these hair cells, which are embedded in the tectorial membrane, are deflected. This open ion channels within the hair cells that allows potassium ions from the endolymph to enter. The influx of potassium ions depolarizes the hair cells, causing them to release neurotransmitters that stimulate neighboring nerve endings. The electrical impulses generated travel along the cochlear nerve to the brain and are interpreted as sound. High frequency sounds maximally stimulate the basal turns of the cochlea and low frequency sounds stimulate the apical turns. This allows the brain to distinguish different frequencies of sound.

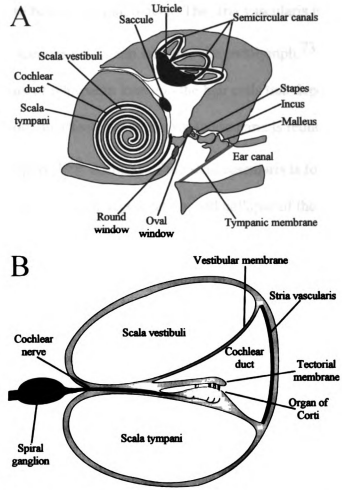


Figure 2. Auditory structures of the middle and inner ear. (A) Overall view of the middle and inner ear structures. (B) Cross section view of the cochlea. Diagrams are based on structures published by Evans, 1993, but have been modified.

The pathology in deaf dogs has been found to be similar in the Dalmatian, Collie, Border Collie, Australian Shepherd, and Great Dane.[33,40,48] These represent breeds with inheritance at both the spotting and merle loci. The earliest detectable defect in affected ears of deaf dogs is a degeneration of the stria vascularis in the cochlea of the inner ear (Figure 2).[41] This degeneration can be seen as early as one day after birth, and

is therefore considered to be a congenital defect. The stria vascularis is a layer of highly vascularized tissue that secretes potassium ions into the endolymph.[73] As previously mentioned, it is the influx of potassium ions into the hair cells that depolarizes them and leads to nerve stimulation. In affected ears, the stria vascularis is reduced in thickness with little or no blood supply.[5,48] Atrophy of the stria vascularis is followed by collapse of the vestibular membrane, hair cell degeneration, and collapse of the saccule. In later stages, cell loss has also been noted in the spiral ganglion that is a part of the auditory nerve. Further examination reveals that pigmentation in the stria vascularis due to melanocytes is diminished.[48]

Melanocytes are found within the stria vascularis as part of a layer of intermediate cells that lies between the marginal epithelial cells that line the inner surface of the cochlea and the basal cells that supply them with nutrients. In mice, it has been found that marginal cells normally form extensive interdigitations with both the intermediate and basal cells.[70] When melanocytes in the inner ear are absent, it has been found that the extent of interdigitations and number of blood vessels supplying the marginal cells are reduced. The endocochlear potential in these cases is often zero. The endocochlear potential is an ionic gradient that is a result of the secretion of potassium ions by the stria vascularis into the endolymph. This gradient is necessary for the influx of those ions into the hair cells. It is unclear whether melanocytes directly secrete potassium ions or are merely supporting the cells that do.

Another function of melanocytes is the production of the pigment melanin, which is partially responsible for determining the color of the skin, hair, and eyes. Deafness in Dalmatians has been shown to be positively associated with blue eye color and negatively

associated with the presence of colored patches.[23] In many breeds, deaf dogs generally have a larger proportion of white in the coat than normal.[72] In some cases the dog may be completely white. White coat color can be produced by the merle and spotting loci, both of which are associated with deafness. White coat color can also be produced by the albino locus, however this locus is not associated with deafness. The merle phenotype is dominantly inherited, and produces a dilution of color in the heterozygous state.[80] In homozygotes, extreme dilution produces a coat that is nearly completely white. Many breeds that have inherited merle also inherited alleles at the spotting locus; therefore white spots in these breeds may be due to either locus. There is some evidence of reversion of the merle phenotype, and it has been suggested that merle may be due to a transposable element.[66] The tweed and harlequin phenotypes are modifications of the merle phenotype, and harlequin in particular produces white spots.[67,68] The Irish spotting, piebald, and extreme piebald phenotypes result from the inheritance of recessive alleles at the spotting locus.[80] Since the inheritance of deafness is generally considered to be recessive, the spotting locus would therefore appear to be a better candidate than merle.

In one study, melanocytes were undetectable in hair bulbs taken from white areas of a Dalmatian and a nonmerle Shetland Sheepdog, both of which have inherited alleles at the spotting locus.[63] Melanocytes were found in hair bulbs from white areas of a Shetland Sheepdog with the harlequin modification of merle, but they were immature. Homozygous merle dogs were not examined. In contrast, the white hair produced in albinism is the result of mature melanocytes that have no tyrosinase activity.[34] The

absence of melanocytes in the white areas of dog breeds with spotting alleles, and a similar absence of melanocytes in the inner ears of deaf dogs from these breeds, suggests that a common cause might be responsible for both. It is possible that the immature melanocytes seen in the harlequin merle are less capable of surviving in the inner ear. It is also possible that immature melanocytes are exclusive to the harlequin modifier, and that homozygous merles are white due to an absence of melanocytes. The merle locus can't be ruled out as being associated with deafness, therefore, without further studies.

In the Dalmatian, it has been suggested that white coat color, blue eyes, and deafness can all be explained by the action of the spotting locus.[16] The effect of this locus might be a decreased viability of melanocyte precursors. If precursors in the skin or iris die, white hair color or blue eyes result. If precursors in the ear die, deafness results. In places where the precursors manage to survive, normal coloration or hearing results. The randomness in the survivability of these precursors might explain the difficulty in determining the mode of inheritance of deafness. It does not explain, however, why deaf parents are more likely to produce deaf offspring than normal parents.[23] The situation might be the same for the merle locus. This discrepancy might be explained by the inheritance of either modifier genes or mutations within the spotting or merle genes themselves that affect precursor survival and increase the risk of deafness. The genes for spotting, merle, or their modifiers are not known in the dog. Therefore, similar phenotypes of abnormal pigmentation and deafness in other species must be used as models to determine possible candidates for study in the dog.

The dominant spotting (W) phenotype in mice is a coat color variant characterized by reduced or absent pigmentation. Affected mice have a stria vascularis

that is thinner than normal, which is accompanied by a lack of intermediate cells including melanocytes.[21,64] Collapse of the cochlear duct and saccule follow, along with degeneration of the hair cells and nerve fibers. The microphthalmia (mi) locus in the mouse has many different phenotypic alleles, many of which exhibit dilute or white coat color and smaller than normal or absent eyes.[71] Some of these alleles, such as microphthalmia-white (Mi-wh), also have inner ear defects that lead to cochleosaccular deafness. This is interesting with respect to dog breeds that show inheritance of the merle trait. In the Great Dane and Collie, dogs with a predominantly white coat have been seen that exhibit both microphthalmia and deafness.[33]

In the human, Waardenburg syndrome is one potential model for deafness in dogs. Common symptoms include cochleosaccular deafness, patchy white skin, a white forelock of hair, and blue eyes or heterochromia irides.[7] Heterochromia irides refers to a condition in which one eye is normally pigmented and the other eye is blue, or in which the iris of a single eye contains both normal and blue colored segments. There are 4 types of Waardenburg syndrome currently described. Waardenburg syndrome type I (WS1) exhibits the common symptoms plus dystopia canthorum, a facial phenotype in which the eyes are spaced farther apart than normal. Waardenburg syndrome type II (WS2) does not exhibit dystopia canthorum. Waardenburg syndrome type III (WS3) is similar to type I, but with deformities of the limbs. Waardenburg syndrome type IV (WS4), also known as Shah-Waardenburg syndrome, consists of the common symptoms plus aganglionic megacolon. WS1, WS2, and WS3 are dominantly inherited, whereas WS4 is recessively inherited. Since aganglionic megacolon and physical deformities have not been described in deaf dogs, WS2 appears to be the best model for deafness in

dogs. Because of its variegated nature, it has been suggested that the merle locus is a better model of Waardenburg syndrome than spotting.[63] Merle would also be a better model for WS1, WS2, and WS3 because of a similar mode of inheritance. In addition to Waardenburg syndrome, piebaldism in humans also results in a white forelock of hair. In some cases, human piebaldism has been known to exhibit hearing loss.[69] Therefore, this condition should also be considered as a model for what is seen in dogs.

Many of the conditions mentioned above have been linked to mutations within genes that are a part of the melanocyte development and melanin synthesis pathway. This pathway is shown in Figure 3. The genes *PAX3*, endothelin receptor B *(EDNRB)* and its ligand endothelin 3 (*EDN3*), microphthalmia-associated transcription factor (*MITF*), *KIT* and its ligand (*KITLG*), and *SOX10* are all important for the survival, proliferation, migration, and differentiation of melanocyte precursors. Multiple names and symbols are used for these genes between and even within species, depending on the author. In this dissertation, the official human and mouse symbols will be used, except where different in the previously published manuscripts. Waardenburg syndrome types I and III are caused by *PAX3* mutations.[54] Waardenburg syndrome type II is caused by mutations in human *MITF*, and the mouse microphthalmia phenotype is the result of defects in the *Mitf* gene. Waardenburg syndrome type IV is the result of mutations in the *EDNRB*, *EDN3*, and *SOX10* genes. Human piebaldism is caused by *KIT* mutations, and the mouse W phenotype is caused by defects in *Kit*.[76] Due to the number of genes involved, not all could be examined. The *EDNRB*, *MITF*, *KIT*, and *KITLG* genes were chosen as the best candidates for the investigation of deafness in the dog. Diagrams of their gene structures are shown in Figure 4.

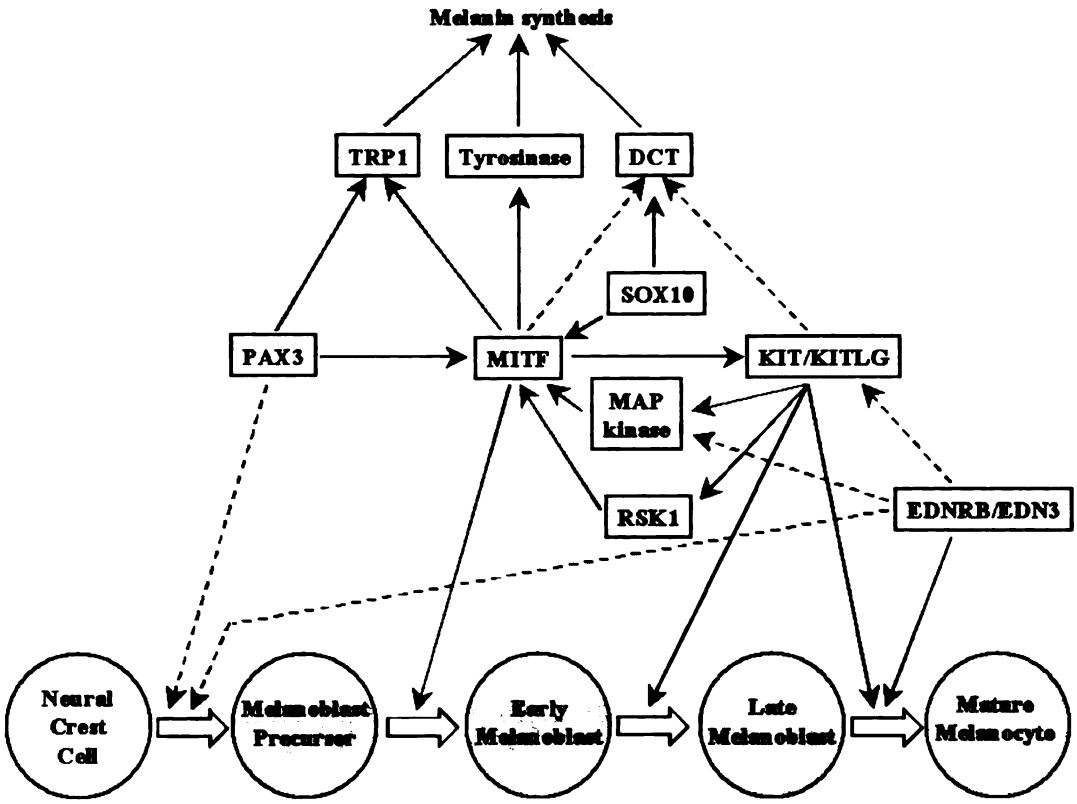


Figure 3. Gene pathway of melanocyte development. The major genes involved are shown in boxes with solid arrows indicating known interactions and dashed arrows indicating proposed interactions. The development pathway of melanocytes is shown at the bottom.

EDNRB

Endothelin was first discovered as a vasoactive peptide of 21 amino acids secreted by endothelial cells that is similar in structure to some neurotoxins that act on membrane ion channels.[81] Three different endothelins are currently known: endothelin 1 (ET1 or EDN1), endothelin 2 (ET2 or EDN2), and endothelin 3 (ET3 or EDN3). Two receptors named endothelin receptor A (EDNRA or ETA) and endothelin receptor B (EDNRB or

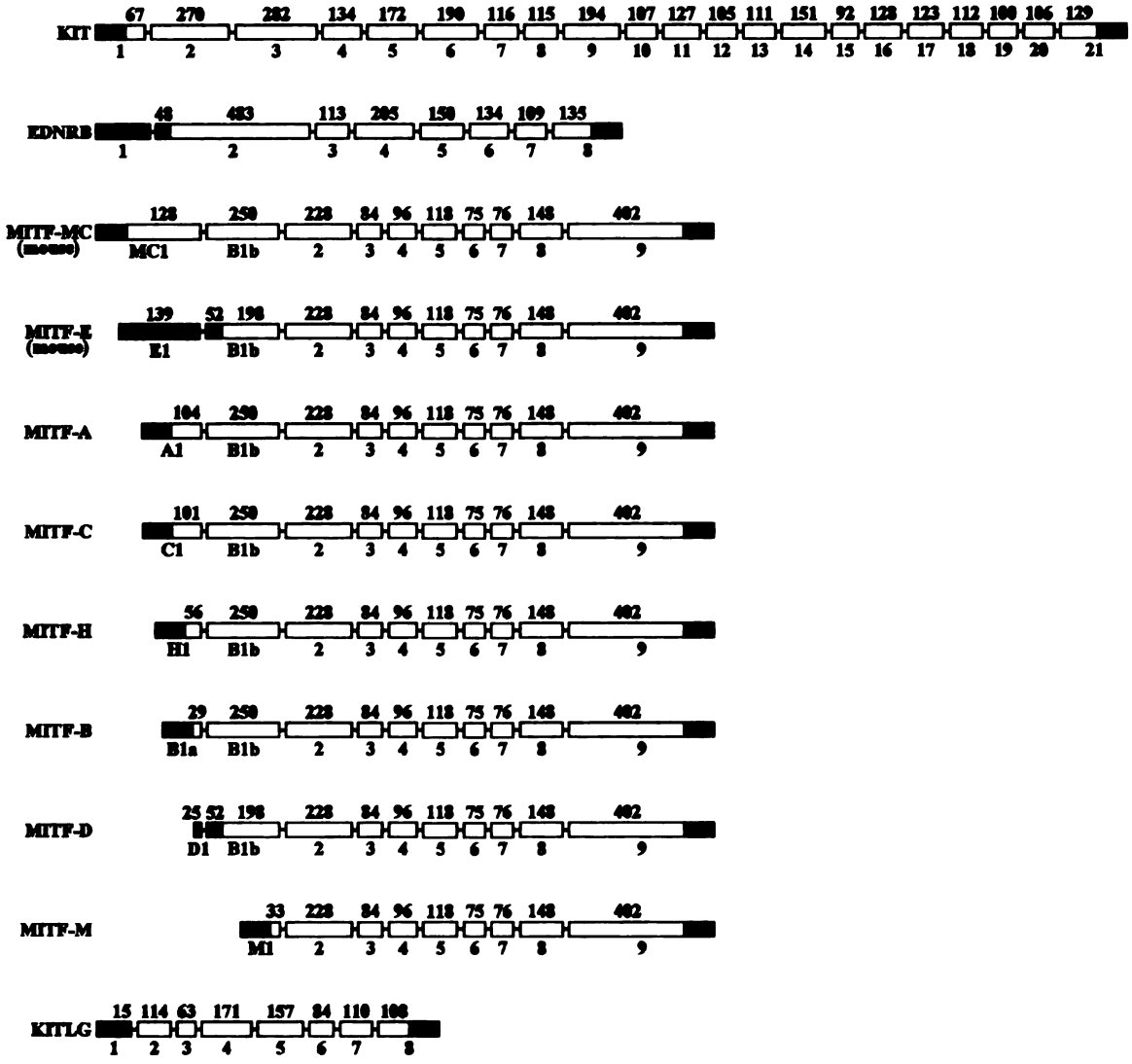


Figure 4. Structures of the mRNAs of the candidate genes. Boxes represent exons. The coding region of each gene is shown in white, untranslated regions in black. Exon designations are shown below each box, and the sizes of the coding sequences in base pairs are shown above. Sizes of untranslated regions are given where known. Sizes are for the human genes, except where noted otherwise. *MITF* isoforms are shown with the optional 18 bp in exon 6 present.

ETB) have been identified that bind to endothelins. A third receptor, endothelin receptor C, has been identified in *Xenopus*.[43] EDNRA binds EDN1 and EDN2 strongly, but has a much weaker affinity for EDN3.[52] EDNRB, on the other hand, binds all three endothelins with equal affinity. Subtypes of EDNRB have been identified in some species that differ in their sensitivity to various competing agents.[12,46]

The EDNRB protein belongs to the G-protein-coupled receptor family and consists of 7 helical transmembrane domains (Figure 5).[52] It is expressed in many tissues, including the brain, kidney, thyroid, liver, uterus, and endothelial cells.[61] The

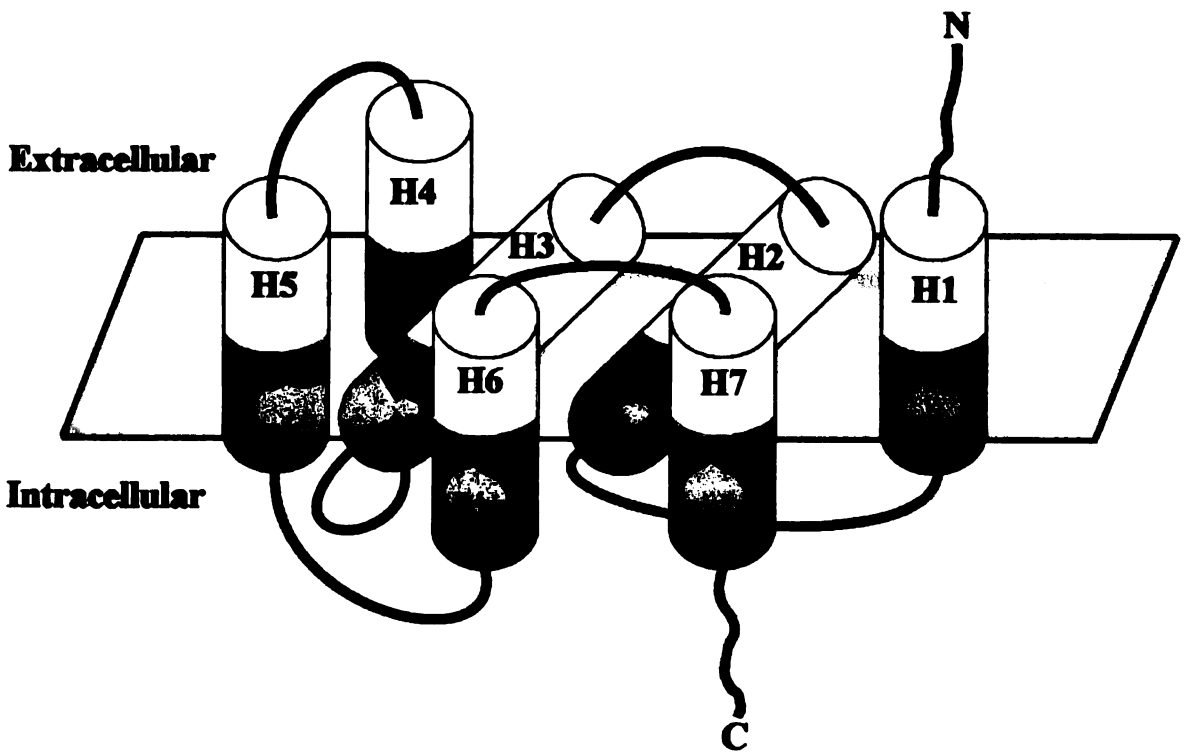


Figure 5. Structure of the EDNRB protein. The transmembrane helices are designated H1 – H7.

*EDNRB* gene has been mapped to Chromosome 13q22 in the human, and *Ednrb* is on Chromosome 14 in the mouse.[39,59] In the human, the *EDNRB* gene has been reported to contain 7 exons.[6] In the rat, however, alternative splicing of a non-coding exon has been seen in the 5' untranslated region and has led to a gene structure consisting of 8 exons.[17,18] The first two exons in the rat structure correspond to exon 1 in the human. For the purpose of this study, the structure in the rat consisting of 8 exons was used. The coding region in the human is 1329 bp in length and codes for a protein of 442 amino acids.[61]

Activation of EDNRB by EDN3 in melanocyte precursors increases their rate of cell proliferation, and temporarily prevents them from differentiating.[44] EDNRB inhibitors have been shown to slow the rate of tumor growth in malignant melanoma cases.[45] EDNRB activation is also responsible for the migration of certain precursor cells from the neural crest during early embryonic development.[42] In particular, the precursors of enteric ganglion cells and melanocytes fail to migrate to distal portions of the body in the absence of proper signaling. A lack of ganglion cells within the distal portions of the gastrointestinal tract leads to a condition known as aganglionic megacolon. In this condition, the large intestine is unable to contract due to a lack of innervation, resulting in intestinal blockage that is often fatal at an early age. Aganglionic megacolon has been found to be caused by mutations within *EDNRB* or within the receptor tyrosine kinase *RET*.[3,29] In humans, aganglionic megacolon is known as Hirschsprung's Disease.

The failure of melanocyte precursors to properly migrate results in abnormal pigmentation, due to a lack of melanocytes within the affected area. In many cases, both innervation of the colon and pigmentation are affected. The piebald-lethal phenotype in the mouse and the spotting lethal phenotype in the rat are both due to deletions in the *Ednrb* gene.[17,39] In the horse, *EDNRB* mutations have been associated with lethal white foal syndrome (LWFS).[82] These foals are the result of matings between horses with the overo coat color phenotype. They have a completely white coat and usually die a few days after birth due to aganglionic megacolon. Mutations in either *EDN3* or *EDNRB* have been found in many Shah-Waardenburg patients.[8,37]

**MITF**

The microphthalmia-associated transcription factor (*MITF*) gene has been mapped human Chromosome 3p14.1-p12.3, and *Mitf* is found on Chromosome 6 in the mouse.[36,75] The entire gene produces two major transcripts of about 5.5 kb and 5.7 kb.[36] A total of 8 *MITF* isoforms are currently known and are produced by alternative splicing of a single *MITF* gene. The coding regions of these isoforms contain 9 exons and range from 1.3 to 1.6 kb in size (Figure 4). All of the isoforms share exons 2 through 9 in common and differ only in their exon 1 sequences. The exon 1 in each isoform consists of a unique 5' end and, except for *MITF-M*, the common sequence segment B1b. An alternative splicing site also exists at the 5' end of exon 6, and results in the optional removal of the initial 18 base pairs of that exon.[36] The effect of this splicing on MITF function is not known.

The different isoforms of *MITF* all have different expression patterns, which are most likely mediated by their different 5' ends. *MITF-M* is expressed exclusively within melanocytes.[76] The *MITF-M* promoter contains binding sites for the *PAX3* and *SOX10* transcription factors, which are also involved in the regulation of pigmentation.[10] *MITF-A* is widely expressed but is enriched in the retinal pigment epithelium.[1] *MITF-H* is also widely expressed but is enriched in the heart. *MITF-C* is expressed in a number of tissues, but not melanocytes.[27] *MITF-D* is primarily expressed in the retinal pigment epithelium. It is also expressed in macrophages and osteoclasts, but not in melanocytes or natural killer cells.[77] *MITF-E* and *MITF-MC* are expressed in mast cells.[58,78] The final isoform, *MITF-B*, has been found in retinal pigment epithelium, melanoma, and cervical cell cancer cell lines by reverse transcription PCR (RT-PCR) only.[79]

The MITF protein consists of a basic-helix-loop-helix-leucine zipper (bHLH-Zip) structure (Figure 6) and is closely related to TFE3 and TFEB, transcription factors that bind the E box in the immunoglobulin heavy chain enhancer.[36] MITF is involved in the differentiation of many cell types, including neural crest-derived melanocytes, mast cells, osteoclasts, and optic cup-derived pigment epithelium.[71] MITF activates the tyrosinase and tyrosinase related protein 1 (*TRP1*) genes of the melanin synthesis pathway (See Figure 3) by binding to an 11 base consensus sequence AGTCATGTGCT, known as the M box, that is present in their promoters.[84] The M box contains within it the consensus sequence CANNTG, known as the E-box, which is recognized by all bHLH-Zip proteins. The DOPAchrome tautomerase (*DCT* or *TRP2*) gene, which is also involved in melanin synthesis, contains an M box in its promoter as well.[15] It is not conclusive, however,

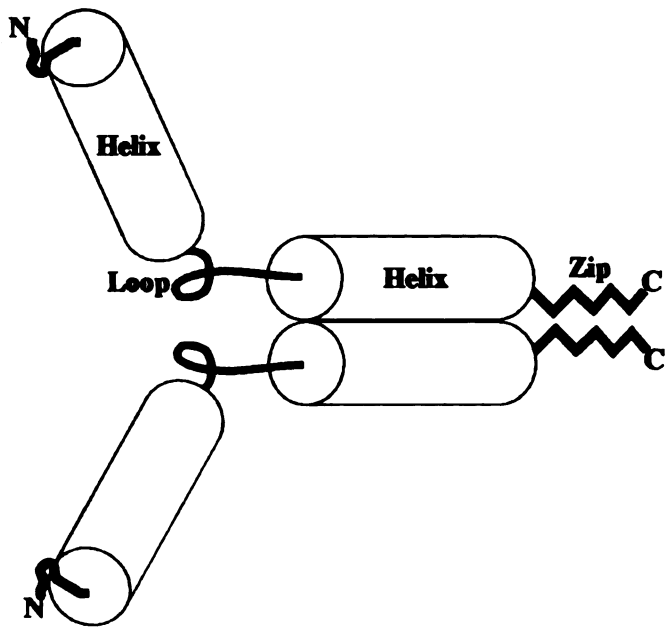


Figure 6. Structure of the MITF protein. Two MITF molecules are shown, depicting a functional homodimer.

whether or not MITF activates *DCT*. MITF also increases the expression of *KIT*, which in turn activates the microtubule-associated protein (MAP) and RSK-1 kinases.[35,76] These kinases phosphorylate MITF at $Ser_{73}$ and $Ser_{409}$, respectively. The phosphorylated MITF recruits the cofactor p300/CBP and is ubiquinated, resulting in a short burst of activity followed by degradation.[62]

A total of 21 *Mitf* mutant alleles are currently known in the mouse.[55] Phenotypic effects may include small or absent eyes, loss of pigmentation or abnormal pigmentation in various parts of the body, deafness, mast cell deficiency, and loss of secondary bone resorption. In the human, *MITF* mutations have been linked to Tietz albinism-deafness

syndrome and Waardenburg syndrome type II, both of which are characterized by deafness and abnormal pigmentation of the hair, skin, or eyes.[76] In the dog, the *MITF* gene is a candidate for both hereditary deafness associated with abnormal pigmentation and microphthalmia.

**KIT/KITLG**

The proto-oncogene *KIT* (sometimes referred to as c-*KIT*) is homologous to the *v-kit* gene found in the Hardy-Zuckerman 4 feline sarcoma virus.[9] *KIT* has been mapped to Chromosome 4q11-q12 in the human, and *Kit* is located on Chromosome 5 in the mouse.[20,83] The gene consists of 20 exons and has a coding region of 2931 bp in the human, encoding 976 amino acids.[83] The *KIT* gene is expressed primarily in the brain, heart, skeletal muscle, kidney, and lungs. The gene product is a membrane bound protein that is a member of the type III receptor tyrosine kinase family, which also includes the receptors for the colony stimulating factor (CSF-1) and platelet-derived growth factor (PDGF).[60] The extracellular portion of the protein consists of 5 immunoglobulin-like folds (Figure 7).[14] The 3 folds closest to the amino terminus form the ligand-binding domain, and the fourth fold is believed to be necessary for dimerization. The intracellular portion of the protein consists of a juxtamembrane domain and a tyrosine kinase domain. The ATP binding and phosphotransferase regions of the tyrosine kinase domain are separated by a kinase insert sequence.

The kit ligand (KITLG, Kitl) is alternatively known as the mast cell growth factor (MGF), Steel factor (SF or SLF), and stem cell factor (SCF). The human *KITLG* gene is

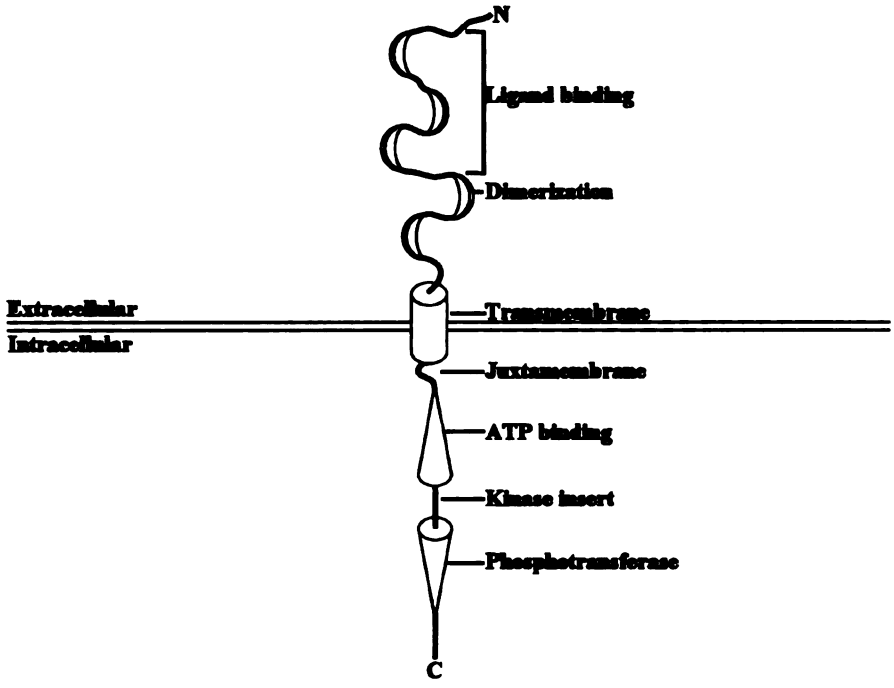


Figure 7. Structure of the KIT protein. The major structural domains are labeled. Immunoglobulin-like folds are indicated as crescent shapes, the transmembrane helix by a cylinder, and the kinase domain by cones.

located on Chromosome 12q22-12q24, and the mouse *Kitl* gene is located on Chromosome 10.[4,19] The *KITLG* gene in humans consists of 8 exons comprising a total coding region of 822 base pairs and encoding 273 amino acids.[51] Exon 6 is alternatively spliced and contains a proteolytic cleavage site after $Ala_{165}$ in the mouse.[14] When exon 6 is present, cleavage at this site removes the transmembrane domain and produces the soluble form of the protein. When exon 6 is absent, the cleavage site is also absent and the membrane-bound form of KITL is produced. The soluble form of KITL in the mouse can be produced by cleavage at either the homologous site in exon 6 or at an alternative

cleavage site in exon 7. Endothelial cells and fibroblasts constitutively express the KITLG protein.[14] KITLG is also expressed in the brain, bone marrow hematopoietic stem cells and stromal cells, skin keratinocytes, gut epithelial cells, the thymus, and the testis. The ratio of soluble to membrane-bound KITLG varies, but the soluble form is the predominant form in most tissues. The structure of the KITLG protein consists of 2 β-pleated sheets and a bundle of 4 α-helices (Figure 8).[14] A total of 4 cysteine residues are present within the KITLG protein and participate in 2 intramolecular disulfide bonds. The cytoplasmic domain, parts of the first, third, and fourth helices, and both disulfide bonds have been determined to be essential for normal function, particularly amino acids 1-141. The active form of KITLG is a homodimer that is heavily glycosylated.

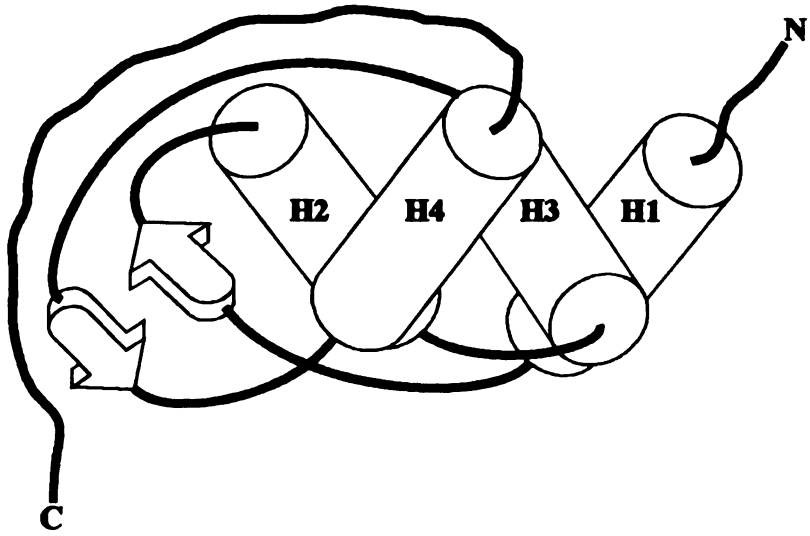


Figure 8. Structure of the KITLG protein. Shown is a single monomer of KITLG; the functional form is a homodimer. The cylinders labeled H1 – H4 depict helices. Arrows depict beta pleated sheets.

Normal signaling by the KIT receptor is the result of KITLG binding. Upon binding of KITLG, KIT dimerizes, which induces its autophosphorylation activity.[14] Activation of KIT results in the initiation of multiple signal cascades. The phosphorylated KIT phosphorylates and activates JAKs, which are non-transmembrane tyrosine kinases.[11] The JAKs further activate the signal transducers and activators of transcription (STAT) proteins STAT1α, STAT5A, and STAT5B, causing them to dimerize, translocate to the nucleus, and bind to specific promoter response elements. Activated KIT also results in the activation of MITF as described above. Signalling by KIT/KITLG is involved in the development and maturation of a number of cell types, including hematopoietic stem cells, mast cells, germ cells, and melanocytes.

Mutations that decrease the activity of KIT may result in anemia, a reduced number of mast cells, decreased fertility, or a lack of pigmentation.[14] Lack of pigmentation is usually displayed as a patch of white hair or skin, and is usually the result of a complete lack of melanocytes within the affected area. Human piebaldism, the white spotting phenotype in mice, the white belt and dominant white phenotypes in pigs, and roan coat color in horses are all associated with mutant KIT.[28,30,31,49,50] Mutations that increase KIT activity are associated with mast cell leukemia and mastocytosis with associated hematologic disorders.[26,57] In the human mast cell leukemia cell line, these mutations were found to result in constitutive phosphorylation of KIT in the absence of KITLG.[26] Similar results have also been obtained for the mutation found in a canine mastocytoma cell line.[47] The association between KIT and mast cell tumors will be discussed in later chapters. *KITLG* mutations have been linked to the roan coat color

phenotype in certain breeds of cattle.[65] *Kitl* mutations are also the basis for the Steel phenotype in the mouse, which involves abnormal pigmentation.[25] Other mutations may cause anemia, a lack of mast cells, and decreased fertility.[14]

**References**


1. Amae S, Fuse N, Yasumoto K, Sato S, Yajima I, Yamamoto H, Udono T, Durlu YK, Tamai M, Takahashi K, Shibahara S. Identification of a novel isoform of microphthalmia-associated transcription factor that is enriched in retinal pigment epithelium. Biochem Biophys Res Commun 247:710-715, 1998.

2. American Kennel Club. The complete dog book, 19th ed., pp. 19-23. Howell Book House, New York, NY, 1997.

3. Amiel J, Attié T, Jan D, Pelet A, Edery P, Bidaud C, Lacombe D, Tam P, Simeoni J, Flori E, Nihoul-Fékété C, Munnich A, Lyonnet S. Heterozygous endothelin receptor B (EDNRB) mutations in isolated Hirschsprung disease. Hum Mol Genet 5:355-357, 1996.

4. Anderson DM, Williams DE, Tushinski R, Gimpel S, Eisenman J, Cannizzaro LA,Aronson M, Croce CM, Huebner K, Cosman D, Lyman SD. Alternate splicing of mRNAs encoding human mast cell growth factor and localization of the gene to chromosome 12q22-q24. Cell Growth Differ 2:373-378, 1991.

5. Anderson H, Henricson B, Lundquist PG, Wedenberg E, Wersall J. Genetic hearing impairment in the Dalmatian dog. Acta Otolaryngol (Stockh) Suppl 232:1-34, 1968.

6. Arai H, Nakao K, Takaya K, Hosoda K, Ogawa Y, Nakanishi S, Imura H. The human endothelin-B receptor gene. Structural organization and chromosomal assignment. J Biol Chem 268:3463-3470, 1993.

7. Asher JH Jr, Friedman TB. Mouse and hamster mutants as models for Waardenburg syndromes in humans. J Med Genet 27:618-626, 1990.

8. Attié T, Till M, Pelet A, Amiel J, Edery P, Boutrand L, Munnich A, Lyonnet S. Mutation of the endothelin-receptor B gene in Waardenburg-Hirschsprung disease. Hum Mol Genet 4:2407-2409, 1995.

9. Besmer P, Murphy JE, George PC, Qiu F, Bergold PJ, Lederman L, Snyder HW Jr, Brodeur D, Zuckerman EE, Hardy WD. A new acute transforming feline retrovirus and relationship of its oncogene v-*kit* with the protein kinase gene family. Nature 320:415, 1986.

10. Bondurand N, Pingault V, Goerich DE, Lemort N, Sock E, Caignec CL, Wegner M, Goossens M. Interaction among *SOX10*, *PAX3* and *MITF*, three genes altered in Waardenburg syndrome. Hum Mol Genet 9:1907-1917, 2000.

11. Brizzi MF, Dentelli P, Rosso A, Yarden Y, Pegoraro L. STAT protein recruitment and activation in c-Kit deletion mutants. J Biol Chem 274:16965-16972, 1999.

12. Brooks DP, DePalma PD, Pullen M, Gellai M, Nambi P. Identification and function of putative $ET_B$ receptor subtypes in the dog kidney. J Cardiovasc Pharmacol 26 Suppl 3:S322-S325, 1995.

13. Brooks M, Sargan DR. Genetic aspects of disease in dogs. *In:* The genetics of the dog, ed. Ruvinsky A, Sampson J, pp. 191-266. CABI, New York, NY, 2001.

14. Broudy VC. Stem cell factor and hematopoiesis. Blood 90:1345-1364, 1997.

15. Budd PS, Jackson IJ. Structure of the mouse tyrosinase-related protein-2/dopachrome tautomerase (*Tyrp2*/*Dct*) gene and sequence of two novel slaty alleles. Genomics 29:35-43, 1995.

16. Cattanach B. The 'dalmatian dilemma': white coat colour and deafness. J Small Anim Pract 40:193-200, 1999.

17. Ceccherini I, Zhang AL, Matera I, Yang G, Devoto M, Romeo G, Cass DT. Interstitial deletion of the endothelin-B receptor gene in the spotting lethal (sl) rat. Hum Mol Genet 4:2089-2096, 1995.

18. Cheng HF, Su YM, Yeh JR, Chang KJ. Alternative transcript of the nonselective-type endothelin receptor from rat brain. Mol Pharmacol 44:533-538, 1993.

19. Copeland NG, Gilbert DJ, Cho BC, Donovan PJ, Jenkins NA, Cosman D, Anderson D, Lyman SD, Williams DE. Mast cell growth factor maps near the steel locus on mouse chromosome 10 and is deleted in a number of steel alleles. Cell 63:175-183, 1990.

20. d'Auriol L, Mattei MG, Andre C, Galibert F. Localization of the human c-*kit* protooncogene on the q11-q12 region of chromosome 4. Hum Genet 78:374-376, 1988.

21. Deol MS. The origin of the acoustic ganglion and effects of the gene dominant spotting ($W^v$) in the mouse. J Embryol Exp Morph 23:773-784, 1970.

22. Evans HE. The ear. *In:* Miller's anatomy of the dog, ed. Evans HE, Miller ME, 3rd ed., pp. 988-1008. WB Saunders, Philadelphia, PA, 1993.

23. Famula TR, Oberbauer AM, Sousa CA. A threshold model analysis of deafness in Dalmatians. Mamm Genome 7:650-653, 1996.

24. Fischel-Ghodsian N, Falk RE. Deafness. *In:* Emery and Rimoin's Principles and Practice of Medical Genetics, ed. Rimoin DL, Connor JM, Pyeritz RE, 3rd ed., vol. I, pp. 1149-1170. Churchill Livingstone, New York, NY, 1996.

25. Flanagan JG, Leder P. The *kit* ligand: a cell surface molecule altered in Steel mutant fibroblasts. Cell 63:185-194, 1990.

26. Furitsu T, Tsujimura T, Tono T, Ikeda H, Kitayama H, Koshimizu U, Sugahara H, Butterfield JH, Ashman LK, Kanayama Y, Matsuzawa Y, Kitamura Y, Kanakura Y. Identification of mutations in the coding sequence of the proto-oncogene c-*kit* in a human mast cell leukemia cell line causing ligand-independent activation of c-*kit* product. J Clin Invest 92:1736-1744, 1993.

27. Fuse N, Yasumoto K, Takeda K, Amae S, Yoshizawa M, Udono T, Takahashi K, Tamai M, Tomita Y, Tachibana M, Shibahara S. Molecular cloning of cDNA encoding a novel microphthalmia-associated transcription factor isoform with a distinct amino-terminus. J Biochem (Tokyo) 126:1043-1051, 1999.

28. Geissler EN, Ryan MA, Housman DE. The dominant-white spotting (*W*) locus of the mouse encodes the c-*kit* proto-oncogene. Cell 55:185-192, 1988.

29. Geneste O, Bidaud C, De Vita G, Hofstra RMW, Tartare-Deckert S, Buys CHCM, Lenoir GM, Santoro M, Billaud M. Two distinct mutations of the RET receptor causing Hirschsprung's disease impair the binding of signalling effectors to a multifunctional docking site. Hum Mol Genet 8:1989-1999, 1999.

30. Giebel LB, Spritz RA. Mutation of the *KIT* (mast/stem cell growth factor receptor) protooncogene in human piebaldism. Proc Natl Acad Sci U S A 88:8696-8699, 1991.

31. Giuffra E, Evans G, Törnsten A, Wales R, Day A, Looft H, Plastow G, Andersson L. The Belt mutation in pigs is an allele at the Dominant white (*I/KIT*) locus. Mamm Genome 10:1132-1136, 1999.

32. Greibrokk T. Hereditary deafness in the Dalmatian: relationship to eye and coat color. J Am Anim Hosp Assoc 30:170-176, 1994.

33. Gwin RM, Wyman M, Lim DJ, Ketring K Jr, Werling K. Multiple ocular defects associated with partial albinism and deafness in the dog. J Am Anim Hosp Assoc 17:401-408, 1981.

34. Halaban R, Moellmann G. White mutants in mice shedding light on humans. J Invest Dermatol 100(2 Suppl):176S-185S, 1993.

35. Hemesath TJ, Price ER, Takemoto C, Badalian T, Fisher DE. MAP kinase links the transcription factor Microphthalmia to c-Kit signalling in melanocytes. Nature 391:298-301, 1998.

36. Hodgkinson CA, Moore KJ, Nakayama A, Steingrímsson E, Copeland NG, Jenkins NA, Arnheiter H. Mutations at the mouse microphthalmia locus are associated with defects in a gene encoding a novel basic-helix-loop-helix-zipper protein. Cell 74:395-404, 1993.

37. Hofstra RMW, Osinga J, Tan-Sindhunata G, Wu Y, Kamsteeg EJ, Stulp RP, van Ravenswaaij-Arts C, Majoor-Krakauer D, Angrist M, Chakravarti A, Meijers C, Buys CHCM. A homozygous mutation in the endothelin-3 gene associated with a combined Waardenburg type 2 and Hirschsprung phenotype (Shah-Waardenburg syndrome). Nat Genet 12:445-447, 1996.

38. Holliday TA, Nelson HJ, Williams DC, Willits N. Unilateral and bilateral brainstem auditory-evoked response abnormalities in 900 Dalmatian dogs. J Vet Intern Med 6:166-174, 1992.

39. Hosoda K, Hammer RE, Richardson JA, Baynash AG, Cheung JC, Giaid A, Yanagisawa M. Targeted and natural (piebald-lethal) mutations of endothelin-B receptor gene produce megacolon associated with spotted coat color in mice. Cell 79:1267-1276, 1994.

40. Igarashi M, Alford BR, Cohn AM, Saito R, Watanabe T. Inner ear anomalies in dogs. Ann Otol Rhinol Laryngol 81:249-255, 1972.

41. Johnsson LG, Hawkins JE Jr, Muraski AA, Preston RE. Vascular anatomy and pathology of the cochlea in Dalmatian dogs. *In:* Vascular Disorders and Hearing Defects, ed. de Lorenzo AJD, pp. 249-295. University Park Press, Baltimore, MD, 1973.

42. Kapur RP, Sweetser DA, Doggett B, Siebert JR, Palmiter RD. Intercellular signals downstream of endothelin receptor-B mediate colonization of the large intestine by enteric neuroblasts. Development 121:3787-3795, 1995.

43. Karne S, Jayawickreme CK, Lerner MR. Cloning and characterization of an endothelin-3 specific receptor (ETC receptor) from Xenopus laevis dermal melanophores. J Biol Chem 268:19126-19133, 1993.

44. Lahav R, Ziller C, Dupin E, Le Douarin NM. Endothelin 3 promotes neural crest cell proliferation and mediates a vast increase in melanocyte number in culture. Proc Natl Acad Sci U S A 93:3892-3897, 1996.

45. Lahav R, Heffner G, Patterson PH. An endothelin receptor B antagonist inhibits growth and induces cell death in human melanoma cells *in vitro* and *in vivo*. Proc Natl Acad Sci U S A 96:11496-11500, 1999.

46. Lecoin L, Sakurai T, Ngo MT, Abe Y, Yanagisawa M, Le Douarin NM. Cloning and characterization of a novel endothelin receptor subtype in the avian class. Proc Natl Acad Sci U S A 95:3024-3029, 1998.

47. London CA, Galli SJ, Yuuki T, Hu ZQ, Helfand SC, Geissler EN. Spontaneous canine mast cell tumors express tandem duplications in the proto-oncogene c-*kit*. Exp Hematol 27:689-697, 1999.

48. Lurie MH. The membranous labyrinth in the congenitally deaf Collie and Dalmatian dog. Laryngoscope 58:279-287, 1948.

49. Marklund S, Kijas J, Rodriguez-Martinez H, Rönnstrand L, Funa K, Moller M, Lange D, Edfors-Lilja I, Andersson L. Molecular basis for the dominant white phenotype in the domestic pig. Genome Res 8:826-833, 1998.

50. Marklund S, Moller M, Sandberg K, Andersson L. Close association between sequence polymorphism in the KIT gene and the roan coat color in horses. Mamm Genome 10:283-288, 1999.

51. Martin FH, Suggs SV, Langley KE, Lu HS, Ting J, Okino KH, Morris CF, McNiece IK, Jacobsen FW, Mendiaz EA, Birkett NC, Smith KA, Johnson MJ, Parker VP, Flores JC, Patel AC, Fisher EF, Erjavec HO, Herrera CJ, Wypych J, Sachdev RK, Pope JA, Leslie I, Wen D, Lin C, Cupples RL, Zsebo KM. Primary structure and functional expression of rat and human stem cell factor DNAs. Cell 63:203-211, 1990.

52. Masaki T, Ninomiya H, Sakamoto A, Okamoto Y. Structural basis of the function of endothelin receptor. Mol Cell Biochem 190:153-156, 1999.

53. Morris D. Dogs. The ultimate dictionary of over 1,000 breeds, pp. 7-12. Trafalgar Square, North Pomfret, VT, 2001.

54. Morton CC. Genetics, genomics and gene discovery in the auditory system. Hum Mol Gen 11:1229-1240, 2002.

55. Mouse Genome Database (MGD), Mouse Genome Informatics Web Site, The Jackson Laboratory, Bar Harbor, Maine. World Wide Web URL: http://www.informatics.jax.org/. Retrieved January 8, 2003.

56. Muhle AC, Jaggy A, Stricker C, Steffen F, Dolf G, Busato A, Kornberg M, Mariscoli M, Srenk P, Gaillard C. Further contributions to the genetic aspect of congenital sensorineural deafness in Dalmatians. Vet J 163:311-318, 2002.

57. Nagata H, Worobec AS, Oh CK, Chowdhury BA, Tannenbaum S, Suzuki Y, Metcalfe DD. Identification of a point mutation in the catalytic domain of the protooncogene c-*kit* in peripheral blood mononuclear cells of patients who have mastocytosis with an associated hematologic disorder. Proc Natl Acad Sci U S A 92:10560-10564, 1995.

58. Oboki K, Morii E, Kataoka TR, Jippo T, Kitamura Y. Isoforms of *mi* transcription factor preferentially expressed in cultured mast cells of mice. Biochem Biophys Res Commun 290:1250-1254, 2002.

59. Puffenberger EG, Hosoda K, Washington SS, Nakao K, deWit D, Yanagisawa M, Chakravart A. A missense mutation of the endothelin-B receptor gene in multigenic Hirschsprung's disease. Cell 79:1257-1266, 1994.

60. Qiu FH, Ray P, Brown K, Barker PE, Jhanwar S, Ruddle FH, Besmer P. Primary structure of c-*kit*: relationship with the CSF-1/PDGF receptor kinase family--oncogenic activation of v-*kit* involves deletion of extracellular domain and C terminus. EMBO J 7:1003-1011, 1988.

61. Sakamoto A, Yanagisawa M, Sakurai T, Takuwa Y, Yanagisawa H, Masaki T. Cloning and functional expression of human cDNA for the $ET_B$ endothelin receptor. Biochem Biophys Res Commun 178:656-663, 1991.

62. Sato S, Roberts K, Gambino G, Cook A, Kouzarides T, Goding CR. CBP/p300 as a co-factor for the Microphthalmia transcription factor. Oncogene 14:3083-3092, 1997.

63. Schaible RH, Brumbaugh JA. Electron microscopy of pigment cells in variegated and nonvariegated, piebald-spotted dogs. *In:* Pigment Cell, vol. 3. Proceedings of the 9th International Pigment Cell Conference, Houston, Texas, January 13-17, 1975, ed. Riley V, pp. 191-200. Karger, Basel, NY, 1996.

64. Schrott A, Spoendlin H. Pigment anomaly-associated inner ear deafness. Acta Otolaryngol (Stockh) 103:451-457, 1987.

65. Seitz JJ, Schmutz SM, Thue TD, Buchanan FC. A missense mutation in the bovine *MGF* gene is associated with the roan phenotype in Belgian Blue and Shorthorn cattle. Mamm Genome 10:710-712, 1999.

66. Sponenberg DP. Germinal reversion of the merle allele in Australian shepherd dogs. J Hered 75:78, 1984.

67. Sponenberg DP. Inheritance of the harlequin color in Great Dane dogs. J Hered 76:224-225, 1985.

68. Sponenberg DP, Lamoreux ML. Inheritance of tweed, a modification of merle, in Australian shepherd dogs. J Hered 76:303-304, 1985.

69. Spritz RA, Beighton P. Piebaldism with deafness: Molecular evidence for an expanded syndrome. Am J Med Genet 75:101-103, 1998.

70. Steel KP, Barkway C. Another role for melanocytes: their importance for normal stria vascularis development in the mammalian inner ear. Development 107:453-463, 1989.

71. Steingrímsson E, Moore KJ, Lamoreux ML, Ferré-D'Amaré AR, Burley SK, Zimring DCS, Skow LC, Hodgkinson CA, Arnheiter H, Copeland NG, Jenkins NA. Molecular basis of mouse *microphthalmia* (*mi*) mutations helps explain their developmental and phenotypic consequences. Nat Genet 8:256-263, 1994.

72. Strain GM. Congenital deafness in dogs and cats. The Compendium on Continuing Education for the Small Animal Practitioner 13:245-251, 1991.

73. Strain GM. Aetiology, prevalence, and diagnosis of deafness in dogs and cats. Br Vet J 152:17-36, 1996.

74. Strain GM. Congenital deafness and its recognition. Vet Clin North Am Small Anim Pract 29:895-907, 1999.

75. Tachibana M, Perez-Jurado LA, Nakayama A, Hodgkinson CA, Li X, Schneider M, Miki T, Fex J, Francke U, Arnheiter H. Cloning of *MITF*, the human homolog of the mouse *microphthalmia* gene and assignment to chromosome 3p14.1-p12.3. Hum Mol Genet 3:553-557, 1994.

76. Tachibana M. MITF: a stream flowing for pigment cells. Pigment Cell Res 13:230-240, 2000.

77. Takeda K, Yasumoto K, Kawaguchi N, Udono T, Watanabe K, Saito H, Takahashi K, Noda M, Shibahara S. Mitf-D, a newly identified isoform, expressed in the retinal pigment epithelium and monocyte-lineage cells affected by Mitf mutations. Biochim Biophys Acta 1574:15-23, 2002.

78. Takemoto CM, Yoon YJ, Fisher DE. The identification and functional characterization of a novel mast cell isoform of the microphthalmia-associated transcription factor. J Biol Chem 277:30244-30252, 2002.

79. Udono T, Yasumoto K, Takeda K, Amae S, Watanabe K, Saito H, Fuse N, Tachibana M, Takahashi K, Tamai M, Shibahara S. Structural organization of the human microphthalmia-associated transcription factor gene containing four alternative promoters. Biochim Biophys Acta 1491:205-219, 2000.

80. Willis MB. Genetics of the Dog, pp. 69-70. Howell Book House, New York, NY, 1989.

81. Yanagisawa M, Kurihara H, Kimura S, Tomobe Y, Kobayashi M, Mitsui Y, Yazaki Y, Goto K, Masaki T. A novel potent vasoconstrictor peptide produced by vascular endothelial cells. Nature 332:411-415, 1988.

82. Yang GC, Croaker D, Zhang AL, Manglick P, Cartmill T, Cass D. A dinucleotide mutation in the endothelin-B receptor gene is associated with lethal white foal syndrome (LWFS); a horse variant of Hirschsprung disease. Hum Mol Genet 7:1047-1052, 1998.

83. Yarden Y, Kuang WJ, Yang-Feng T, Coussens L, Munemitsu S, Dull TJ, Chen E, Schlessinger J, Francke U, Ullrich A. Human proto-oncogene c-*kit*: a new cell surface receptor tyrosine kinase for an unidentified ligand. EMBO J 6:3341-3351, 1987.

84. Yasumoto K, Mahalingam H, Suzuki H, Yoshizawa M, Yokoyama K. Transcriptional activation of the melanocyte-specific genes by the human homolog of the mouse *Microphthalmia* protein. J Biochem (Tokyo) 118:874-881, 1995.

# CHAPTER 2

# CANDIDATE GENE SEQUENCING AND EVALUATION FOR DEAFNESS

## Introduction

The purpose of this study was to determine whether mutations in the candidate genes *EDNRB*, *MITF*, *KIT*, and *KITLG* are responsible for hereditary deafness in dogs. In order to later identify sequence mutations, it was first necessary to obtain the normal sequences of these genes from a dog without deafness. The coding regions of the genes were chosen for study because mutations within them could potentially affect the structure or function of the proteins that they encode. The polymerase chain reaction (PCR) was used to amplify fragments of the coding regions that were then isolated and sequenced. Once the coding region of a gene had been sequenced in a normal dog, it was also sequenced in a number of deaf dogs and examined for sequence differences. In addition to the coding regions, the promoter regions and intronic sequences such as splice sites were also potential sites of mutations causing deafness. PCR was used where possible to obtain introns and untranslated regions where possible and sequence them. Any sequence differences seen were reexamined to determine whether they represented experimental error, neutral polymorphisms, or mutations. Polymorphisms were used as markers to facilitate mapping of the genes and to determine if there was an association between a particular candidate gene and deafness.

## Materials and Methods

Materials and methods for this portion of the study are presented in Chapter 8.

**Results**

*EDNRB*

Prior sequence for the canine *EDNRB* gene was not available; therefore the human and murine sequences were used as a basis for the isolation of the canine homolog. Human *EDNRB* and murine *Ednrb* sequences were retrieved from GenBank (Accession numbers L06623 and NM_007904) and aligned using a software program. It was believed that portions of the gene that were conserved between the human and the mouse were likely to also be conserved in the dog. Regions of high sequence identity between the human and mouse were selected for the placement of primers for the polymerase chain reaction (PCR). Primers were designed to be approximately 20 bp in length with a GC content of about 50%. Where possible, pairing between a certain primer and itself or its opposite primer was limited to no more than 4 consecutive base matches or 8 total. Where sequence differences between the human and mouse were unavoidable, the human sequence was used for the primer.

Initially, 2 sets of primers were designed within individual exons so that they could be amplified from genomic DNA. These primers were first tested on human DNA to ensure that they functioned properly, then on canine DNA. The PCR products obtained were sequenced to determine that they did represent the correct fragments from the *EDNRB* gene. Additional primers were then designed to allow the amplification of the entire coding region of the canine *EDNRB* gene from cDNA in overlapping fragments. The primers designed for this gene are given in Table 1. The fragments used for amplification of the coding region are given in Table 2. Total RNA was extracted from a frozen sample of spleen taken from a Labrador Retriever with normal hearing and

Table 1. Primers designed within *EDNRB* exons. Location is given relative to the start of the canine coding region.

| Name | Sequence | 5' end | Direction |
|---|---|---|---|
| ETB X40F | CCAAGTTTCCCACTGGCGCG | -194 | Forward |
| ETB I1F | TGACCCAAGTGTCCTTGCTT | -90 | Forward |
| ETB I1R | GCTGCTACCTGCTCCAGAA | -1 | Reverse |
| ETB 134F | TAATGACGCCACCCACTAAGA | 134 | Forward |
| ETB 204F | TGCGGAGGTGCCTAAAGGAG | 204 | Forward |
| ETB 298R | AAGTCTCCTTGATCTCGATGGAT | 298 | Reverse |
| ETB 321F | GTCCTGTCTAGTGTTCGTGCTGG | 321 | Forward |
| ETB 365R | AGTGTGGAGTTCCCGATGAT | 365 | Reverse |
| ETB 398BR | CGCATGCACTTGTTCTTGTAGA | 398 | Reverse |
| ETB I2F | GGAGACCTGCTGCACATCA | 436 | Forward |
| ETB I2R | CTTCTGTATGAAAGGCACCA | 546 | Reverse |
| ETB I3F | GCCTCCGTGGGAATCACTGTGT | 547 | Forward |
| ETB 601F | CGAGCTGTTGCTTCTTGGAG | 601 | Forward |
| ETB 661R | CTACTGCTGTCCATTTTGGAACCC | 661 | Reverse |
| ETB I4F | ATTGACTACAAAGGACGTTAC | 733 | Forward |
| ETB 799R | GCATGAAAGCTGTCTTCTGAA | 799 | Reverse |
| ETB I4R | GCAGAAATAGAAACTAAATAGC | 849 | Reverse |
| ETB I5F | GTTGAGAAAGAAGAGTGGCA | 900 | Forward |
| ETB 952F | AGACGGGAAGTGGCCAAAAC | 952 | Forward |
| ETB I5R | AAGCCAGCACAGGGCAAAGA | 1011 | Reverse |
| ETB 1127BR | GAGGCCATATTGATGCCGAT | 1127 | Reverse |
| ETB I7F | ATAGCTCTGTATTTGGTGAG | 1150 | Forward |
| ETB 1233F | ACAGTCCTTAGAGGAAAAGCA | 1233 | Forward |
| ETB 1303R | ACCGGAAGTTGTCATATCCGTGAT | 1303 | Reverse |
| ETB I7R | GTTTTAATGACTTCGGTCCA | 1386 | Reverse |

Table 2. PCR fragments used to obtain the *EDNRB* coding region

| Forward Primer | Reverse Primer | Temperature (°C) | Fragment size (bp) |
|---|---|---|---|
| ETB X40F | ETB 298R | 62 | 493 |
| ETB 204F | ETB 365R | 56 | 162 |
| ETB 321F | ETB 661R | 66 | 341 |
| ETB 601F | ETB 1303R | 58 | 703 |
| ETB I7F | ETB I7R | 52 | 237 |

used for reverse transcription into cDNA. Fragments of the coding region were amplified from the cDNA by PCR, purified by extraction from agarose gels, and sequenced.

The *EDNRB* sequence determined from the normal dog is given in Figure 1. Most of the *EDNRB* coding region sequence has been submitted to GenBank (Accession number AF034530). The coding region is 1329 bp in length and is 94.1% and 83.5% identical to the human and mouse, respectively, at the nucleotide level. At the amino acid level, it is 97.2% identical to the human and 88.2% identical to the mouse. A discrepancy was noted in the sequence obtained from two of the overlapping fragments. The PCR fragments ETB X40F – ETB 298R and ETB 204F – ETB 365R both share bases 224-275 within the coding region. The ETB X40F – ETB 298R fragment showed a single sequence in these bases that closely matches the human sequence. The ETB 204F – ETB 365R fragment also showed a single sequence, but this sequence differed from that of the other fragment. A total of 14 single base differences were seen in the region of overlap between the two fragments, as shown in Figure 2. A total of 8 dogs from different breeds were sequenced in this region and the same results were obtained in all cases. Interpretation of this ambiguity is saved for the discussion.

Sequence from the 3' end of the coding region initially could not be achieved. Rapid amplification of cDNA ends (RACE) was used unsuccessfully in an attempt to obtain this end. The 3' end was eventually obtained by the design of a new set of primers based on human and mouse homology. During the RACE procedure, however, several amplified fragments were isolated and sequenced. The sequence of one of these fragments matched the *EDNRB* cDNA sequence up until the 3' end of exon 6. The first 8 bases of the fragment sequence beyond this point matched the first 8 bases of intron 6 in

Figure 1. Alignment of the cDNA sequences of dog and human *EDNRB* with mouse *Ednrb*. Vertical lines indicate exon breaks and the ends of the coding region. Base positions relative to the start of the canine coding region are given to the left. Nucleotides identical between species are shaded.

Figure 1.

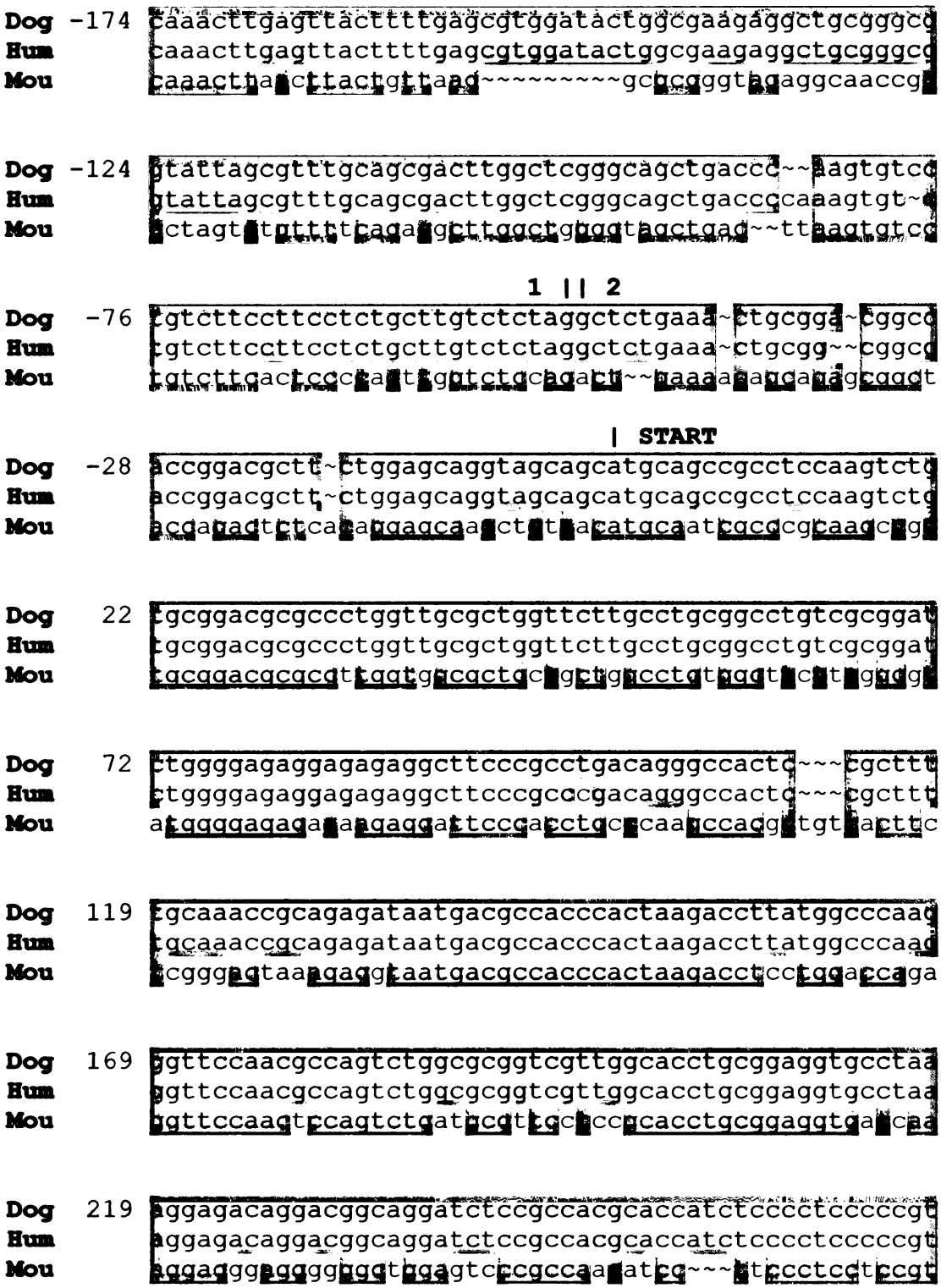
Dog -174
Hum
Mou
Dog -124
Hum
Mou
1 || 2
Dog -76
Hum
Mou
| START
Dog -28
Hum
Mou
Dog 22
Hum
Mou
Dog 72
Hum
Mou
Dog 119
Hum
Mou
Dog 169
Hum
Mou
Dog 219
Hum
Mou

Figure 1 (cont'd).

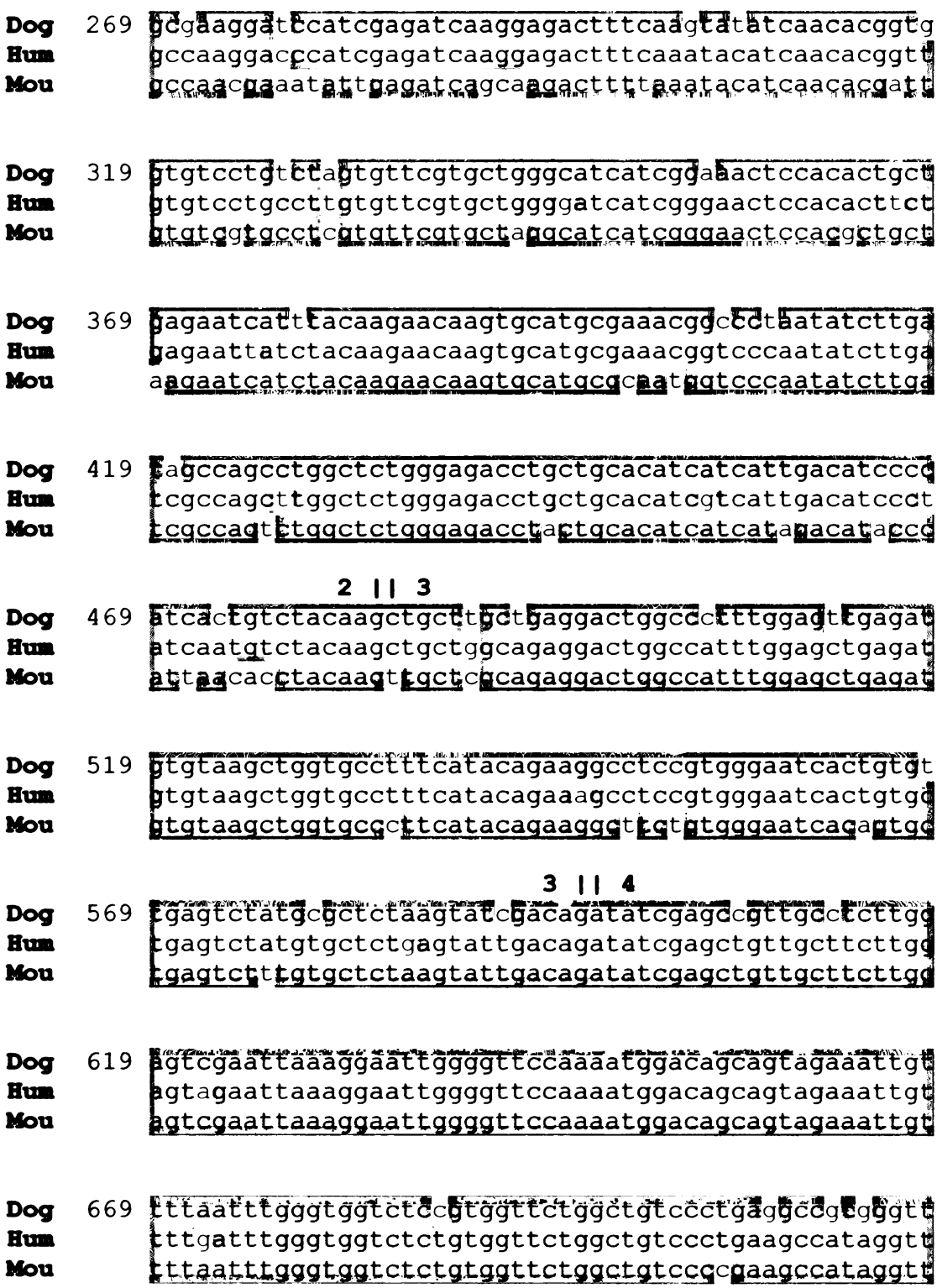

Figure 1 (cont'd).

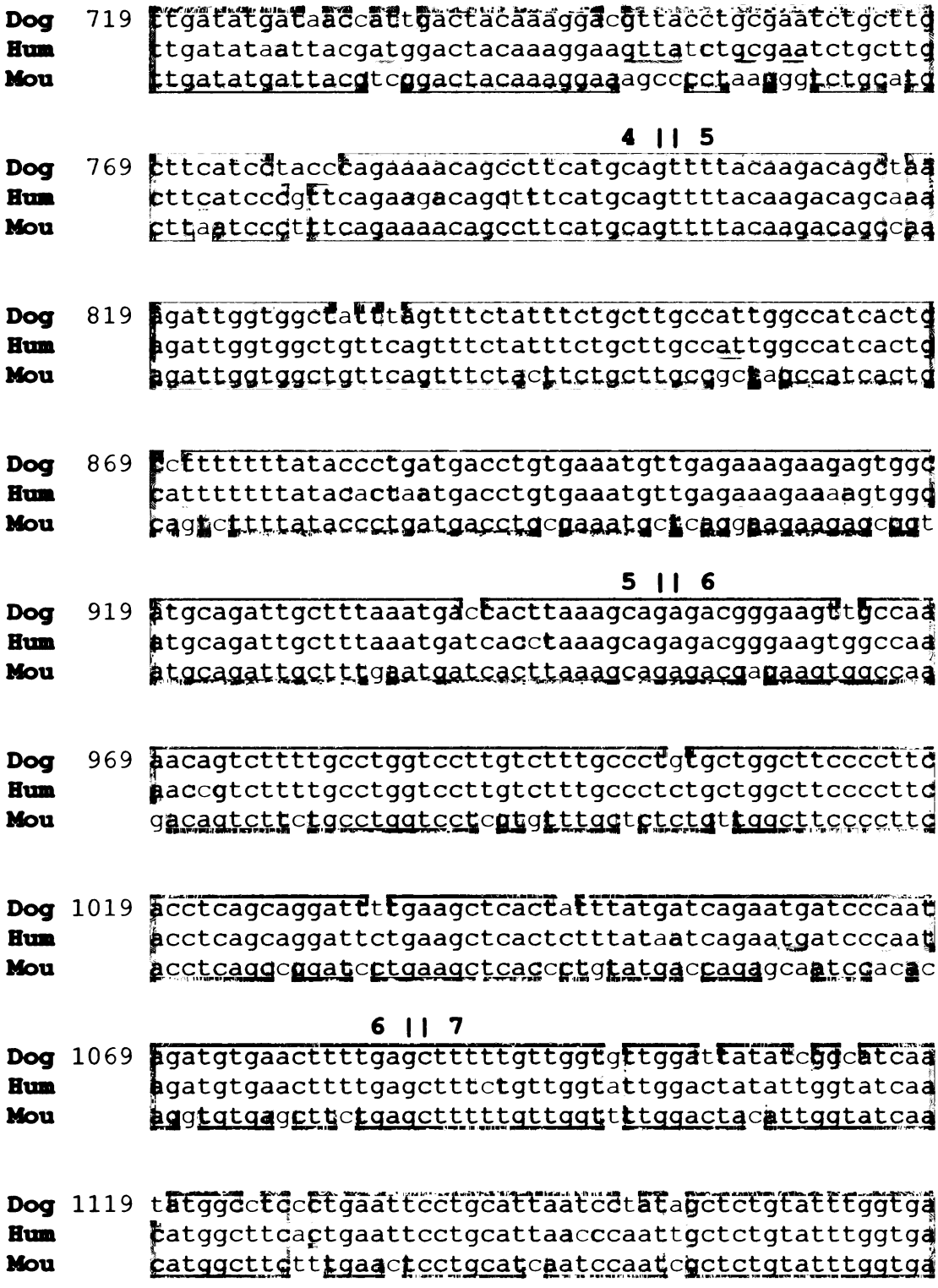

Figure 1 (cont'd).

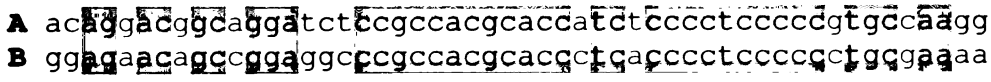


Figure 2. Alternative sequences in canine *EDNRB*. The region shown spans bases 224-275 in the canine coding region. Sequence A was obtained from fragment ETB X40F – ETB 298R and sequence B was obtained from fragment ETB 204F – ETB 365R. Bases that are identical between the sequences of the two fragments are shaded.

the rat; therefore it was thought that this fragment may contain the canine intron 6. The presence of an intron may be explained by genomic DNA contamination of the cDNA preparation or by an unprocessed RNA from which the introns had not been removed. Primers flanking the break separating exons 6 and 7 were used to amplify the intervening intron from genomic DNA. The entire intron was sequenced and found to contain only a single base difference from a sequence in GenBank (Accession number AF026088) identified as canine *EDNRB* intron 4. Comparison of the flanking exonic sequences determined that this represented intron 6 in the numbering scheme used in this study. The sequence obtained is given in Figure 3 and is available from GenBank (Accession number AF134188). Within this intron was found a microsatellite and a single nucleotide polymorphism (SNP). Primers used for investigation of these polymorphisms are given in Table 3. The characterization of these polymorphisms is described in the following chapter. The microsatellite was used to screen a panel of dogs from the DogMap group, and the results were used to locate the *EDNRB* gene to canine Chromosome 22.[7] The manuscript of the resulting publication is provided in the Appendix. Another canine

Figure 3. Sequences from canine *EDNRB* introns. Base numbering is given where introns have been completely sequenced. The remaining introns could not be completely spanned and are shown by partial sequences obtained from the ends, with dots representing the unsequenced central portions. The unsequenced regions are of unknown size due to the unknown size of these introns in the dog. R = G or A.

Figure 3.

**Intron 2**

```
gtaaagggctcctattgacgggagggtgcctagttaggaggagggaggtg
ggagagcctttgggggatcttcttactcaagaagatcatcgcctcctaaa
atcagtgaacattggacataaattc.........................
..................................................
ccactaagtaatgcagttcagagggcactgtgtgaatatctccctaacac
acctcatgtcttctcaatgcag
```

**Intron 3**

```
  1 gtaagagcataaatttaagccaggtatatcctgaacactatactagtgat
 51 tgctatgttacatagaaaataaaccatgtaattcagtaaaagcaggctct
101 gcagcttgacagataattctattttgttcttcag
```

**Intron 4**

```
gtgaattttaccattttctttcctttctgttcttgccttataaatattta
gctactt...........................................
..................................................
ttactttgcatttagtatatagatttttttctacagggaaatgttaatct
tataatactctcttttccatag
```

**Intron 5**

```
gtaagagaacagaagtatgtgctgactcatgattacagtgatgattatga
ataaaaaa..........................................
..................................................
aaaaatgaatttgtagttattttagttctaattcatattaactattcaat
ttaaaggtcagtgttctggatttttacaaataccactgacttttttgtaaa
caatattaagtgttctatttgggaagagagaacgttgtgattatctgaac
catctatttaatttctgactatggttttatttcag
```

Figure 3 (cont'd).

**Intron 6**

```
  1 gtaagaaaggtaaaagagagttttgtaggtaactgccattcagaagtttt
 51 tttcattgatccctttcataggcagagagagagtatcattttgctagtct
101 ttagggagcaaggagtcaagattctcatttttttatcttcacccctattgt
151 agagaaaggaataaaggcgacttatgagaacactgggaatggagagccag
201 agctgtcaaaatgttgagtgggtaccacaattggaaatatcagctccaat
251 tctcctttgcacctcacaaagtcttttctcagccagccccagcacttcca
301 gatgagattttattgtaaaagagagaattgggcatgggcagaagggcatg
351 atgacagagagagagagagagagagacagagacagagagagagacaga
401 gaggggggaaagagagagagaggtcatcattagcaaagaccagtgataaag
451 tcaaaaattatgratatgggtaatttttttcttcacaaaaactcaaaagt
501 ttgcgagaatacatacttaaagcaatgtattgttcacagacatattttgg
551 gtggtttttgcag
```

**Intron 7**

```
gtaggagtatttcaaaataaaaactctttttggcctagcatcaaatataa
cctttccaaactattcatatttctatttaaagacatttcgtaaattgttt
tatagttt.....................................
.............................................
atcacatgtgaactgatgtgaatgtgtaacaagttattttgctttgtaca
g
```

Table 3. Primers designed within *EDNRB* intron 6. Location is given relative to the start of the intron.

| Name | Sequence | 5' end | Direction |
|---|---|---|---|
| ETB I6F | AGGTAACTGCCATTC | 27 | Forward |
| ETB RPTF | GAGAATTGGGCATGGGCAGA | 323 | Forward |
| ETB I6GAF | GACCAGTGATAAAGTCAAAAATCAT | 437 | Forward |
| ETB RPTR2 | TGACTTTATCACTGGTCTTTG | 453 | Reverse |

mapping project has also located *EDNRB* to syntenic group 7, which was later identified as part of Chromosome 22.[2,5]

A 740 bp genomic DNA fragment spanning bases 952-1127 in the coding region and intron 6 was used to probe a canine genomic bacterial artificial chromosome (BAC) library. Clones producing positive signals were cultured, and a single colony from each clone was boiled to make a crude preparation of DNA. One of the clones was determined by PCR to contain the *EDNRB* gene and pure DNA preparations were made of this clone. Primers were designed facing toward exon boundaries to allow sequencing of bordering intronic sequences (Table 1). The BAC clone DNA was directly sequenced using these primers, and the resulting sequences are given in Figure 3. Intron 6 had already been sequenced by other means as mentioned above and intron 3 was small enough to be completely sequenced from the BAC. Partial sequences were obtained at each end of introns 2, 4, 5, and 7, however no sequence could be obtained from intron 1. It is possible that the BAC clone does not contain this portion of the gene.

*MITF*

The *MITF* gene had not been previously sequenced in the dog; therefore, human-mouse homology was used for the design of primers to allow amplification of the canine sequence by PCR. Human *MITF-M* and murine *Mitf-m* sequences for the melanocyte-specific forms were retrieved from GenBank (Accession numbers Z29678 and Z23066) and aligned using a software program. Primer design was performed as previously described. Primer pairs within individual exons were first tested from genomic DNA to ensure that the *MITF* gene could be correctly amplified in the dog, and then additional primers were designed to allow the amplification of the coding region of the gene from cDNA using overlapping fragments. The primers designed for *MITF* within exons are given in Table 4. The fragments used to amplify the coding region of *MITF* are given in Table 5. The same normal Labrador Retriever used for *EDNRB* was also used as a source of cDNA for amplification of *MITF*. The amplification fragments were purified by gel extraction and sequenced.

The sequence obtained from the normal dog is given in Figure 4. The coding region is 1260 bp in length. At the nucleotide level, it is 93.8% identical to the human and 87.6% identical to the mouse. At the amino acid level, it is 97.6% identical to the human and 93.0% identical to the mouse. Two different size bands were obtained for the cDNA fragment MI 206F – MI 955R. These bands were found to represent the different *MITF* forms resulting from the previously mentioned alternative splice site in exon 6.

The 5' end of the *MITF-M* gene could not be obtained from cDNA due to the presence of a second sequence of unknown origin that strongly amplified at the same size. Therefore, the sequence of the 5' end was obtained from genomic DNA. The M1

Table 4. Primers designed within *MITF* exons. Locations are given relative to the start of the canine coding region.

| Name | Sequence | 5' end | Direction |
|---|---|---|---|
| MI I1 MF | GTCTACCGTCTCTCACTGGA | -43 | Forward |
| MI 51F | AAACCCCACCAAGTACCACA | 51 | Forward |
| MI I1R | CTGCCTTTGGGCTTGCTGTA | 90 | Reverse |
| MI 206F | GCGCACCCAACAGCCCCATG | 206 | Forward |
| MI 261R | CTCTTTTTCACAGTTGGAGTT | 261 | Reverse |
| MI I2R | GGCATTCACTTTCCGCCCTG | 307 | Reverse |
| MI I3F | CAGGGCGGAAAGTGAATGC | 288 | Forward |
| MI I3R | ATCCCAGGATTTCTTCATTATA | 409 | Reverse |
| MI I4F | ATAATGAAGAAATCCTGGGA | 389 | Forward |
| MI 431F | TGGCAAATACGTTACCTGTCTCT | 431 | Forward |
| MI I4R | CCTTGGTTGCCATAAAGAT | 485 | Reverse |
| MI 522F | TCCAGCCAACCTTCCCAACA | 522 | Forward |
| MI I6F | TCTGAAGCGAGAGCATTGGC | 580 | Forward |
| MI 613R | TTTGCCTCTCTTTAGCCAATG | 612 | Reverse |
| MI I6R | GGATCATTTGACTTGGGAATC | 710 | Reverse |
| MI I7F | ATTCCCAAGTCAAATGATCC | 691 | Forward |
| MI I7R | GATATAGTCCACAGATGCTT | 762 | Reverse |
| MI I8F | GAAGAAATTGGAGCACGCCA | 813 | Forward |
| MI 887F | GACTTTCCCTTATTCCATCCAC | 887 | Forward |
| MI I8R | CCCGTGGATGGAATAAGTGA | 911 | Reverse |
| MI 955R | GTTCCTGCTTGATGATCCGATTC | 955 | Reverse |
| MI 1232R | CTCATACTGCTCCTCCGGCT | 1232 | Reverse |
| MI X1466R | ATCAAGAAAACCCCTTCAGGTA | 1345 | Reverse |

Table 5. PCR fragments used to obtain the *MITF-M* coding region

| Forward Primer | Reverse Primer | Temperature (°C) | Fragment Size (bp) |
|---|---|---|---|
| MI I1 MF | MI I1R | 58 | 134 |
| MI 51F | MI 261R | 54 | 211 |
| MI 206F | MI 955R | 64 | 750 |
| MI 887F | MI X1466R | 58 | 459 |

Figure 4. Alignment of dog and human *MITF-M* coding region sequences with mouse *Mitf-m* and the canine *MITF* pseudogene (Psg). Vertical lines indicate exon breaks and the ends of the coding region. Base positions relative to the start of the canine coding region are given to the left. Nucleotides identical between species are shaded. The pseudogene sequence given represents the two alleles that contain mutations. The third pseudogene allele is not shown, as the sequence is identical to the normal canine sequence. Y = C or T, M = A or C, W = A or T.

Figure 4.

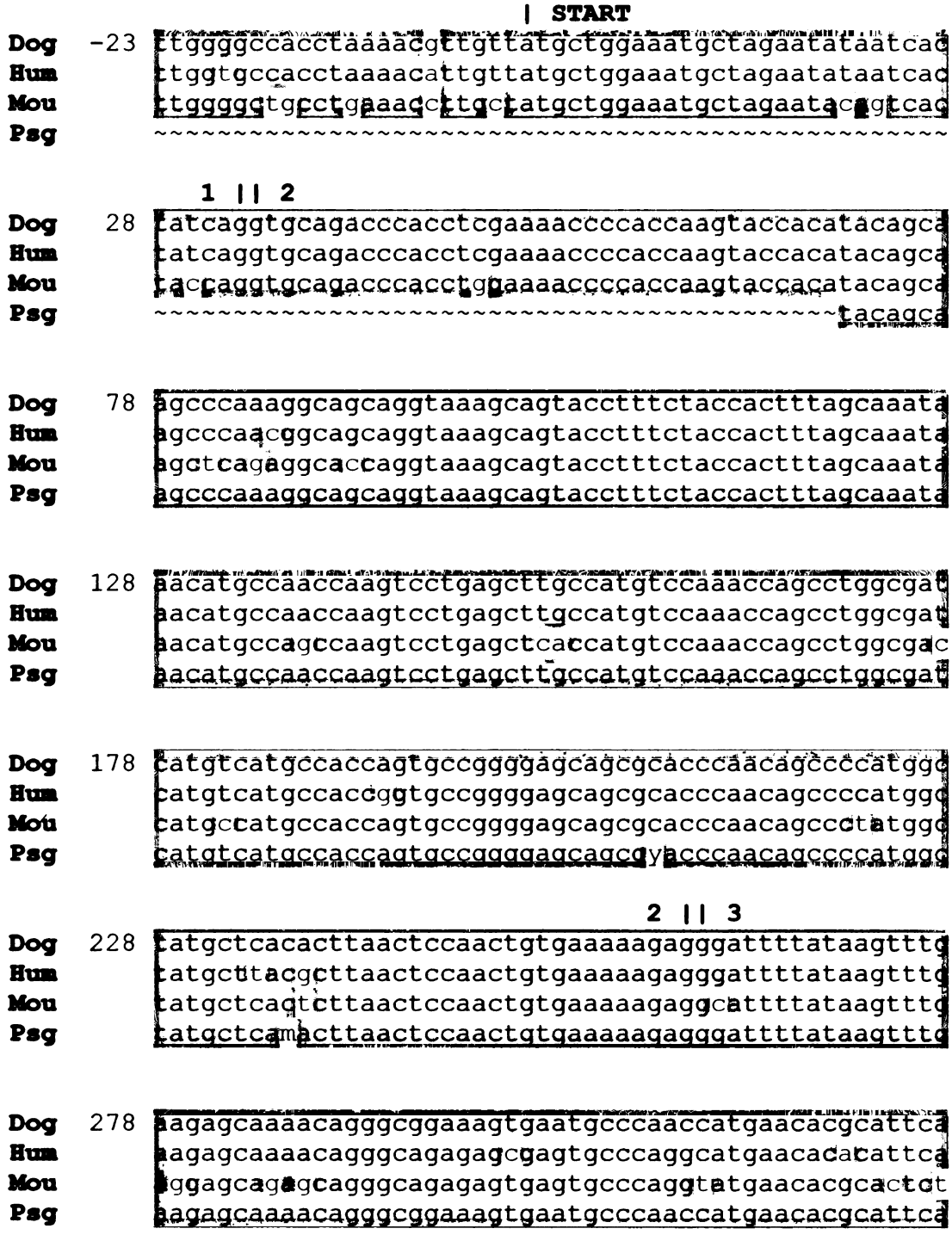
| START
Dog -23
Hum
Mou
Psg
1 || 2
Dog 28
Hum
Mou
Psg
Dog 78
Hum
Mou
Psg
Dog 128
Hum
Mou
Psg
Dog 178
Hum
Mou
Psg
2 || 3
Dog 228
Hum
Mou
Psg
Dog 278
Hum
Mou
Psg

Figure 4 (cont'd).

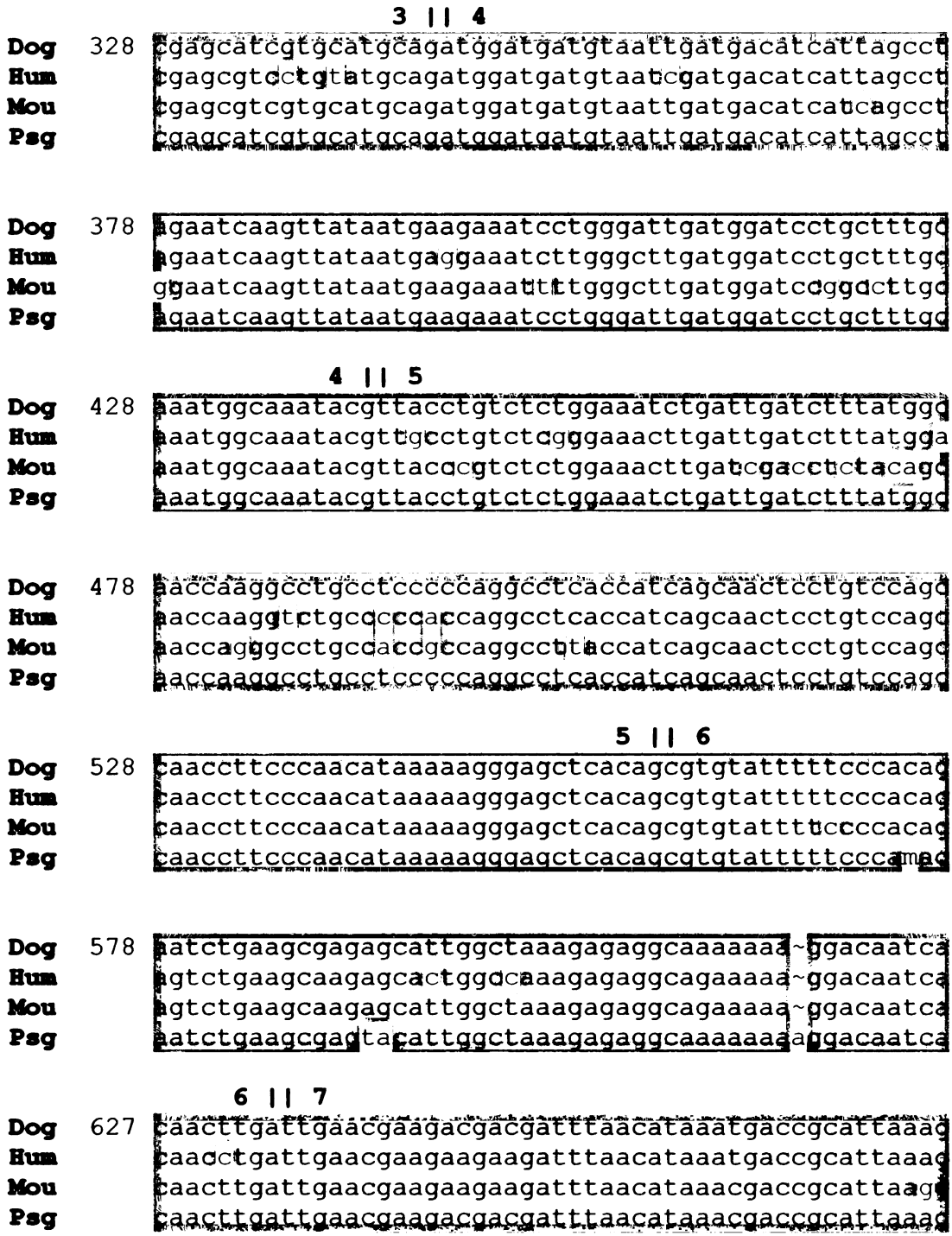

Figure 4 (cont'd).

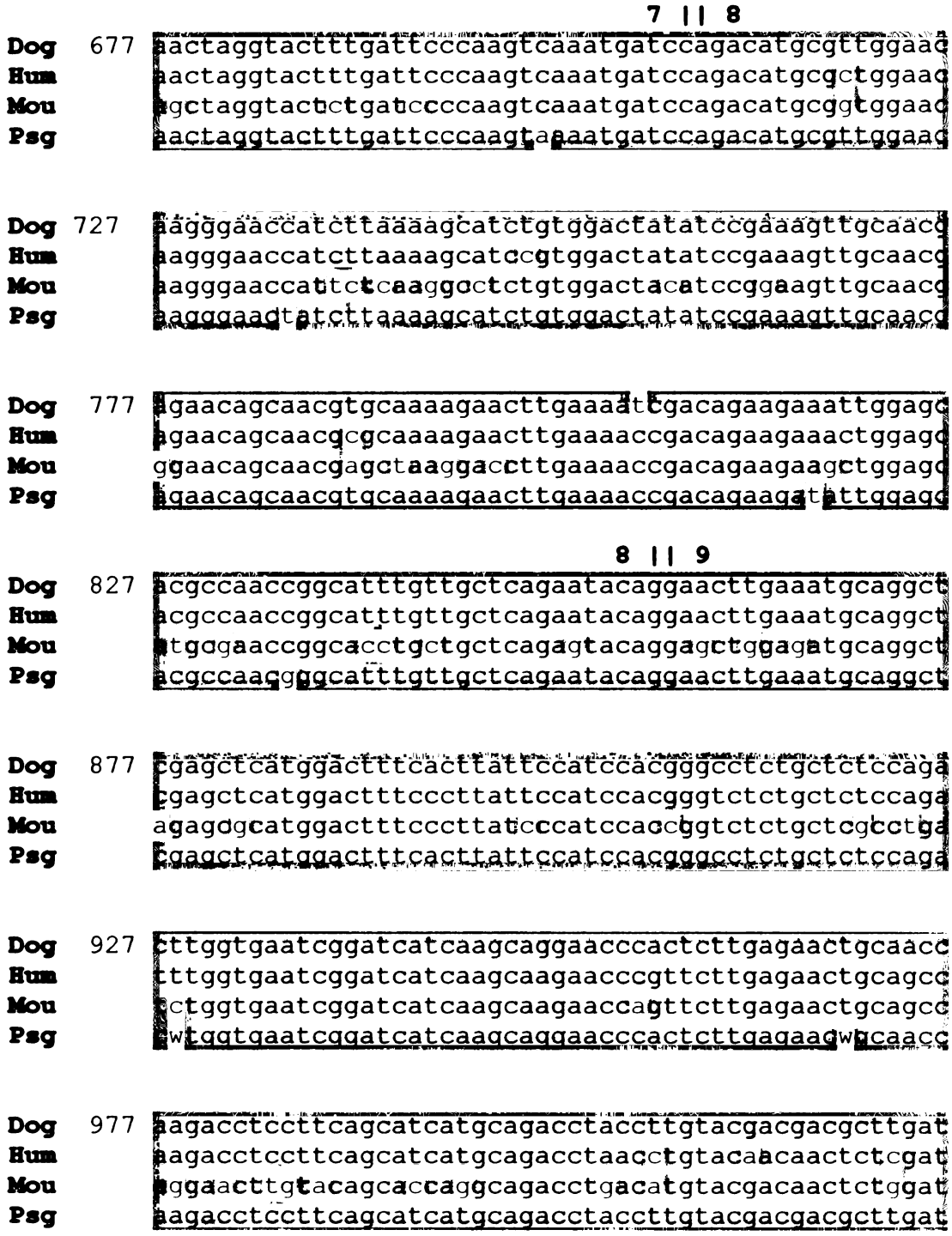

Figure 4 (cont'd).

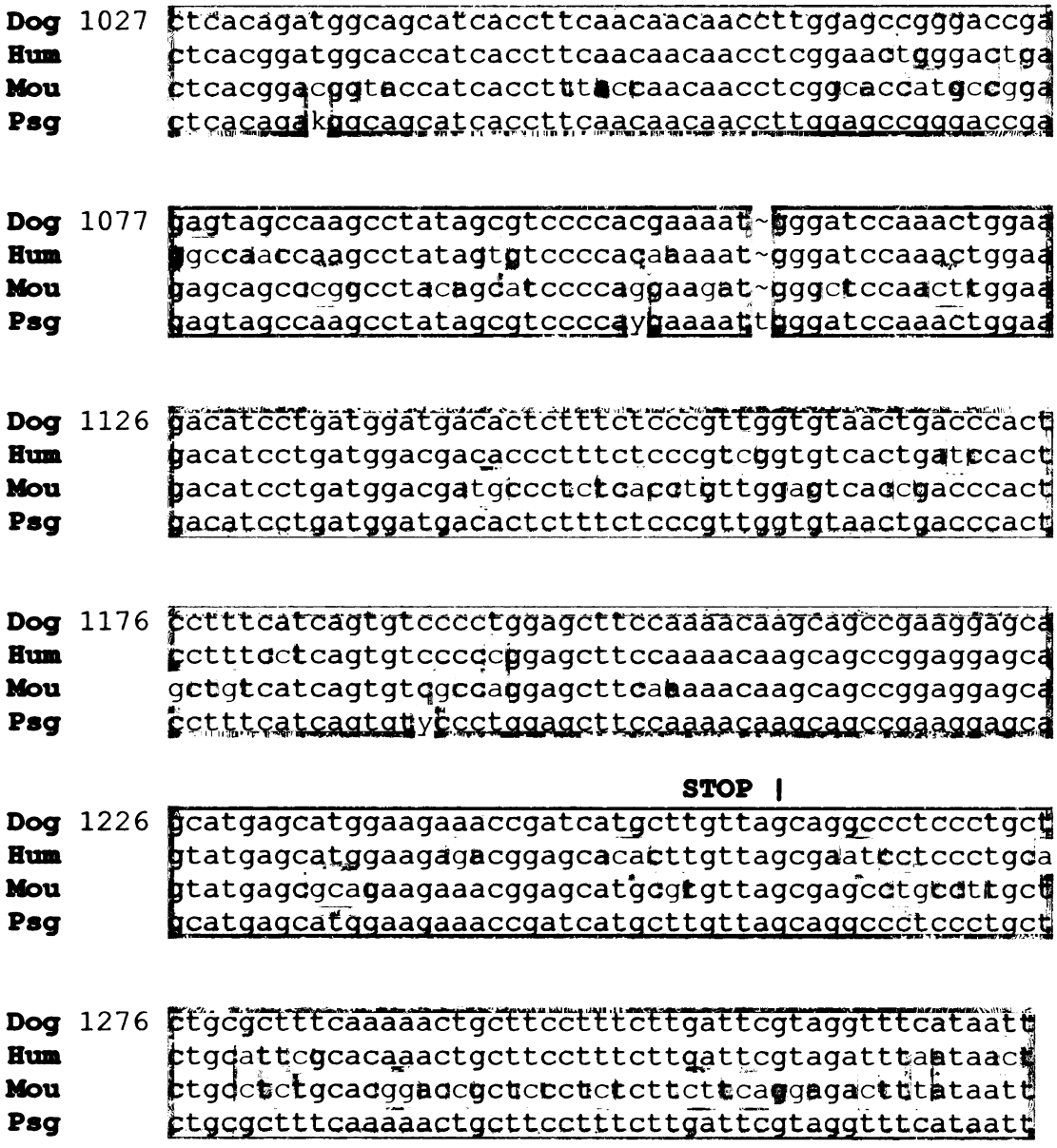

Figure 4 (cont'd).

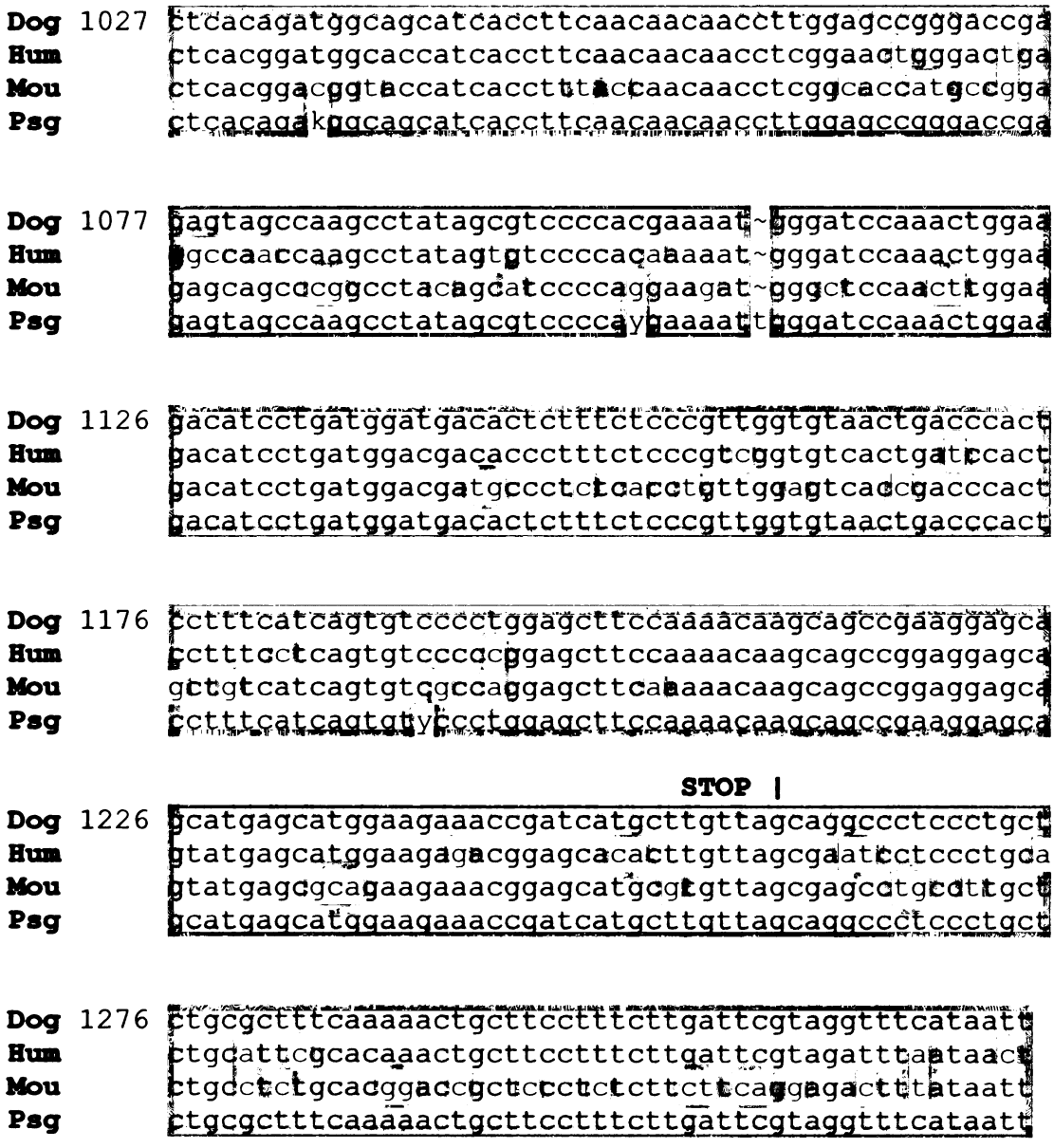

exon of *MITF* is the closest to the rest of the gene within the genomic DNA, therefore it was possible to amplify a fragment containing the M1 exon, the intron following it, and part of exon 2. The entire sequence of the intron was obtained by designing additional primers within the intron itself (Table 6). The sequence obtained is given in Figure 5. RACE was used in an attempt to obtain the 5' alternatively spliced exons from the other *MITF* isoforms. Kidney was used as a source of cDNA because the *Mitf-a*, *Mitf-h*, and

Table 6. Primers designed within *MITF* introns. Position numbers of the 5' end of the primer are given. Positive numbers are relative to the 5' end of the intron and negative numbers are relative to the 3' end.

| Name | Sequence | Intron | 5' end | Direction |
|---|---|---|---|---|
| MI E1R | CTGCACTTACTGGAAAGAG | 1 | 99 | Reverse |
| MI I1BF | AAGGAGGAAAAATACCCTGG | 1 | 187 | Forward |
| MI E2F | AGCCGACCGAACTCACAAA | 1 | 811 | Forward |
| MI I1BR | GTCTAACTCTCAGGATTTGG | 1 | 697 | Reverse |
| MI E2R | CACAGTTGAGTGGGGGAATA | 2 | 70 | Reverse |
| MI I2BF | ACCGGGTTATTGGGTTGTGT | 2 | 160 | Forward |
| MI I2BR | GATGACAAATACGGACAGAG | 2 | -178 | Reverse |
| MI E3F | CATCAGCCTCGTGTGAACAT | 2 | -80 | Forward |
| MI E3R | TCATTACAAAGAGTTACATCC | 3 | 45 | Reverse |
| MI E4F | TTGGGTGGCTTTGCACAGTT | 3 | -63 | Forward |
| MI E4R | GAGAGAACACTGGAAATATC | 4 | 60 | Reverse |
| MI MUTF | TTGCTCAGTAGTTCATTTCTG | 4 | -40 | Forward |
| MI I5BF | GACAAGTGAGGTTATCAAAG | 5 | 51 | Forward |
| MI MUTR | CTTTGATAACCTCACTTGTC | 5 | 70 | Reverse |
| MI I5 3' F | TAGTGTGCGTCATTGTGTGC | 5 | -63 | Forward |
| MI I5BR | CTATAAAACATCTCATTTTC | 5 | -61 | Reverse |
| MI E6F | TGTGCGTCATTGTGTGCCTT | 5 | -60 | Forward |
| MI E6R | TCAATTTCCTCCCAAGAGAT | 6 | 90 | Reverse |
| MI E7F | TAACAAGATACACTAAATGCG | 6 | -69 | Forward |
| MI E7R | TCGCAACAATATGAATAAGCA | 7 | 71 | Reverse |
| MI E8F | GAGTGCTCTGGATAATGAAT | 7 | -73 | Forward |
| MI E8R | AGCGACATATTGGAAACCCT | 8 | 40 | Reverse |
| MI E9F | AATCCTCTGTAAACCACCTCT | 8 | -54 | Forward |

Figure 5. Sequences from canine *MITF* introns. Base numbering is given where introns have been completely sequenced. The remaining introns could not be completely spanned and are shown by partial sequences obtained from the ends, with dots representing the unsequenced central portions. The unsequenced regions are of unknown size due to the unknown size of these introns in the dog. The string of thymine residues at the 3' end of intron 8 causes polymerase slippage, therefore the exact length of this stretch is unknown.

Figure 5.

**Intron 1**

```
  1 gtgagctttattcttattcatatttagtgtctgaaatatatgcaatacat
 51 tgagtaattcacctttcatgttattgtactctttccagtaagtgcaggt
101 ctactactttgatcgtgtttactgtttgataccatgagtatcactgattt
151 aaaggatttttaattctgtattaatgtttataagaaaggaggaaaaatac
201 cctggcggcttaatagtcctgcttttaaaaacacatacatgtaagtgtga
251 ggcatctgaaagaaactgcttcatgtagaattgctttttatgttgagttc
301 aagatcttaattaaaatgttgaataatcatgtccaaatgaaagtgggagg
351 aattaatctacaactagttgatttaatcatcagagtgtttctgtttattt
401 tctacaaccgttttacagctggctcttaaggaggtttgttgttgttgttt
451 ttaaacagaaagctgttctgtttgccaaagaaagtaaaataaattgttat
501 gctccttttttttagattgttgttctgatctcagtaaatcctttcagtcgt
551 gttggggaaaattttgccctccagatggttgcaaattttaaattattaga
601 catgaacaaaagggcacaagttttcaaagagatgtgcagctaattagcag
651 ggaaataaaacagggcaaagtattaccccaaatcctgagagttagacttt
701 aaacttcagtaatatcaaaatccattagcacagtgcctggtacataacag
751 gggcttaataatttattctgttggtggactggccagtctcatgtttgtgc
801 ctgagaaaagagccgaccgaaactcacaaataacggcgctgtcttctctt
851 ccctccgtggctatgttcag
```

**Intron 2**

```
gtaattcatgtctcctcccctctcctgtcttcttacactaaatgaatgtc
tgtcggatattattcccccactcaactgtggactctgcggggccacacac
gccggtctgtgtcccagattctgctatgtggcctccaccctaggcctctt
gacaccatcaccgggttattgggttgtgtggctcaggatggg........
..................................................
tcccctgtgcccaaaccaacctgtcttatttttctctgtccgtatttgtc
atctatcaagctcatttgacggaagttctttctgcattattttatttctc
ggtcagattctactttgtgaaagctttcttagtccatcttgttgctgcac
catcagcctcgtgtgaacatgtcattgaaaagtcatttgcaaatccaagt
catgggctgattttgcttgtgtttttgcag
```

Figure 5 (cont'd).

**Intron 3**

```
gtactgaatgactcggcagtgcaaggatgtaactctttgtaatgagaatc
ta..............................................
..............................................
tctctctttgggtggctttgcacagttttgcttacatttatctctcttc
cattgccctttttcctacag
```

**Intron 4**

```
gtattgatgacttttttttttttttaaagaaaatcttgagatatttcca
gtgttctctccctttccctgaact........................
..............................................
agataaagtctggaatagatctgggtgctagctgaataacctaggaattg
ctcagtagttcatttctgttattgcttctctctctag
```

**Intron 5**

```
gtaaatactggcttgtgtgcctcttcctggggattttctgtttatttttct
gacaagtgaggttatcaaagttgtgacctctagactatt...........
..............................................
gatatggttccatatatatctagaaaatgagatgttttatagtgtgcgtc
attgtgtgccttaaacagttcccgtttctaattacttcattcacgtgcac
ag
```

**Intron 6**

```
gtaagttggttttatgttcatgatgttgatattggagtgaatgttccccc
ttgtatcaaaattgtttaaaatctcttgggaggaaattgatatacat...
..............................................
aggtaatgcacacatggctttaacaagatacactaaatgcgtatgtggtg
ctgttactaatagtcccttcctatgctcttttcttgaag
```

Figure 5 (cont'd)

**Intron 7**

gtgagtacaattccatgttaatctgcatcgtatatttttggtaccttaa
tgcttattcatattgttgcgaaaaatgcacagttatagaaactagagtca
agaagcacccccctctccctttgattccatttctggtatacttct.....
.....
catagttcaacttgtcattgttaccttgtctttagaaattgagtgctctg
gataatgaattttcattgtgcctcaaatcccgaaaaaggttgttttcttc
ctctttgttacag

**Intron 8**

gtatggggcatgtgttgtgtagggtttccaatatgtcgctgacatggagg
tgggaggagaggggatataataagccatgagggacttgatttacatgatt
ctatatagtag.....
.....
ttggtgttatacctcctgtgagtttgaacaaatatgtaataacatgtatg
cgtcattatagtatatcatatatagtactttgccctaaaatcctctgtaa
accacctcttgaaacgtgatttttttttactttattttag

*Mitf-c* isoforms are all expressed in kidney in the mouse.[3] A fragment containing the 5'end of the *MITF-H* isoform was isolated and sequenced to obtain the sequences of the H1 and B1b exons (Figure 6). At the nucleotide level, the H1 exon is 98.2% identical to the human and 91.1% identical to the mouse. The B1b exon is 96.4% identical to the human and 96.0% identical to the mouse.

During the course of sequencing the *MITF* coding region, variations were often seen that seemed to indicate the presence of point mutations and frameshift mutations. When RNA isolated from tissue was treated with DNase prior to reverse transcription, these variations were not seen. This indicated that alternative sequences were being amplified from genomic DNA. In order to further examine these seqeunces, cDNA derived from DNased RNA and genomic DNA treated with RNase were used with PCR primers designed to amplify the coding region of the *MITF* gene and sequenced in 4 dogs. The sequence obtained from cDNA closely matched the human and mouse sequences and was considered to be the normal canine sequence. The fragments amplified from genomic DNA were the same size as those from cDNA, and sequencing confirmed that no introns were present within these fragments. Since the normal genomic *MITF* gene was known to contain introns, it was hypothesized that these alternative products represented a processed pseudogene.

Two of the dogs were found to be homozygous for a sequence that was identical to the normal sequence obtained from cDNA. Since the genomic DNA had been treated with RNase prior to PCR and the introns were absent, this indicates that this sequence is indeed from the pseudogene and not from RNA contamination or the normal genomic copy of *MITF*. In the other two dogs, mutations were seen in the fragments amplified

Figure 6. Alignment of H1 and B1b sequences from dog and human *MITF* with mouse *Mitf*. Base positions relative to the start of the canine coding region in H1 are given to the left. Nucleotides identical between species are shaded.

Figure 6.

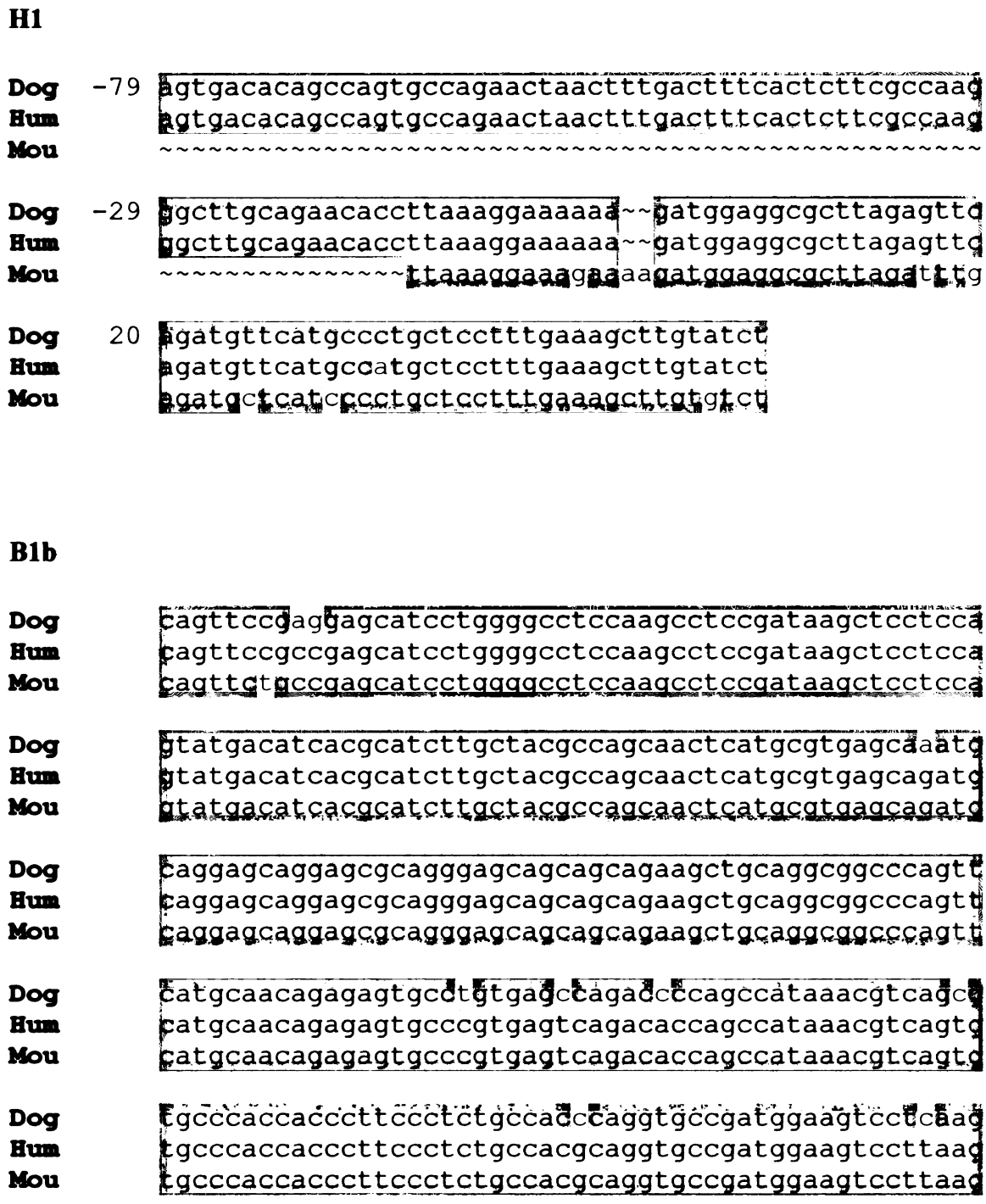
H1
Dog -79 agtgacacagccagtgccagaactaactttgactttcactcttcgccaag
Hum agtgacacagccagtgccagaactaactttgactttcactcttcgccaag
Mou ~~~~~~~~~~~~~~~~~~~~~~~~~~~~~~~~~~~~~~~~~~~~~~~~~~~
Dog -29 ggcttgcagaacaccttaaaggaaaaaa~~gatggaggcgcttagagttg
Hum ggcttgcagaacaccttaaaggaaaaaa~~gatggaggcgcttagagttg
Mou ~~~~~~~~~~~~~~~ttaaaggaaaggaaaagatggaggcgcttagattg
Dog 20 agatgttcatgccctgctcctttgaaagcttgtatct
Hum agatgttcatgccatgctcctttgaaagcttgtatct
Mou agatgctcatccctgctcctttgaaagcttgtgtct
B1b
Dog cagttccgaggagcatcctggggcctccaagcctccgataagctcctcca
Hum cagttccgccgagcatcctggggcctccaagcctccgataagctcctcca
Mou cagttgtgccgagcatcctggggcctccaagcctccgataagctcctcca
Dog gtatgacatcacgcatcttgctacgccagcaactcatgcgtgagcaaatg
Hum gtatgacatcacgcatcttgctacgccagcaactcatgcgtgagcagatg
Mou gtatgacatcacgcatcttgctacgccagcaactcatgcgtgagcagatg
Dog caggagcaggagcgcagggagcagcagcagaagctgcaggcggcccagtt
Hum caggagcaggagcgcagggagcagcagcagaagctgcaggcggcccagtt
Mou caggagcaggagcgcagggagcagcagcagaagctgcaggcggcccagtt
Dog catgcaacagagagtgcctgtgagccagacccagccataaacgtcagcg
Hum catgcaacagagagtgcccgtgagtcagacaccagccataaacgtcagtg
Mou catgcaacagagagtgcccgtgagtcagacaccagccataaacgtcagtg
Dog tgcccaccacccttccctctgccaccaggtgccgatggaagtccttcaag
Hum tgcccaccacccttccctctgccacgcaggtgccgatggaagtccttaag
Mou tgcccaccacccttccctctgccacgcaggtgccgatggaagtccttaag

from genomic DNA. The locations of the mutations are given in Figure 4. These mutations were not seen in the same dogs in fragments amplified from cDNA. The mutations consisted of single base insertions and point mutations. The insertions resulted in frameshifts and one of the point mutations created a stop codon, both of which would be predicted to create a nonfunctional protein. In both of these dogs, the insertions and some of the point mutations were homozygous, but the remaining point mutations were heterozygous. This appears to indicate that two mutant pseudogene forms exist. The homozygous mutations are present on both forms, but the remaining mutations are present on only one of the two forms. Therefore, a total of 3 pseudogene forms were found, two mutants and one apparently normal except for the absence of introns. It is not known whether these represent a single pseudogene with multiple alleles or multiple pseudogenes in different locations.

A 1295 bp MI 51F – MI X1466R cDNA fragment was used to probe the canine genomic BAC library. A total of 14 clones were found by PCR to contain the *MITF* gene. Amplification from these clones using primers that would produce different size fragments from the real gene and the pseudogene indicated that all of the clones contained the real gene. This was also confirmed by sequencing the fragments obtained from the clones. One of the clones was used for the preparation of high quality DNA, and primers were designed facing exonic boundaries to allow the sequencing of bordering intronic sequences (Table 4). The BAC DNA was directly sequenced using these primers and partial sequence was obtained from each end of introns 2-8. The sequences of these introns are given in Figure 6. PCR primers were then designed within the introns facing outward to allow the amplification of individual *MITF* exons and their bordering splice

sites from genomic DNA (Table 6). The primers used to amplify *MITF* exons are given in Table 7. Exons M1 and 2-9 were amplified from the normal Labrador Retriever and sequenced. No differences were seen compared to the sequence obtained from cDNA, confirming that the sequence was correct. As the primers were based within introns, no pseudogene sequence was seen.

In order to further characterize the *MITF* gene, an attempt was made to determine the location of the gene in the canine genome. During the course of sequencing *MITF* in the dog, no polymorphisms were found that would allow it to be mapped in the same manner as *EDNRB*. It was thought that if polymorphisms could be identified in a closely linked gene, mapping of this gene would identify a location that likely contains *MITF* as well. In the current human map, *MITF* is located on Chromosome 3 at a position of approximately 68.5 Mb. The two genes *TMF1* (67.6 Mb) and *ROBO1* (76.6 Mb) flank *MITF* in the human genome. Multispecies primers already existed in the lab for these genes and a canine-hamster radiation hybrid panel was available. The conservation of *MITF* in the clones of this panel was tested by PCR amplification of a genomic fragment

Table 7. PCR fragments used to obtain the *MITF-M* exons.

| Forward Primer | Reverse Primer | Temperature (°C) | Fragment Size (bp) |
|---|---|---|---|
| MI I1 MF | MI E1R | 56 | 175 |
| MI E2F | MI E2R | 56 | 368 |
| MI E3F | MI E3R | 52 | 209 |
| MI E4F | MI E4R | 52 | 219 |
| MI MUTF | MI MUTR | 52 | 228 |
| MI E6F | MI E6R | 52 | 225 |
| MI E7F | MI E7R | 52 | 216 |
| MI E8F | MI E8R | 52 | 261 |
| MI E9F | MI X1466R | 56 | 541 |

containing exon 7 and portions of its flanking introns. This fragment amplifies only from canine DNA and not hamster DNA; therefore the conservation of the canine gene could be determined.

The *TMF1* and *ROBO1* primers were designed to span introns within those genes. Since intron sequences usually are not conserved between species, they were expected to produce fragments of different sizes from dog and hamster. This was confirmed from dog and hamster genomic DNA, however the hamster *Tmf1* fragment was preferentially amplified from the panel clones and canine *TMF1* could not be seen. A canine *TMF1* fragment from genomic DNA was sequenced and new primers were designed within the introns so that the new fragment could only be amplified from canine DNA. The conservation of the canine *TMF1* and *ROBO1* genes were then tested in the panel. A similar pattern of conservation was seen for *MITF* and *TMF1*, whereas the pattern for *ROBO1* was dramatically different. The conservation of the three genes in the panel clones was input into the RHMAP software. Significant linkage was found between *MITF* and *TMF1* (LOD score = 13.09), but not between *MITF* and *ROBO1* (LOD score = 0.06). It appears that *ROBO1* might be located on a different canine chromosome than the other two genes. *MITF* and *TMF1* are both being examined for polymorphisms that could be used for mapping. The conservation of the *MITF* pseudogene is also being tested to determine if it is closely linked to *MITF* or located elsewhere in the genome, but so far has not been successfully amplified from the radiation hybrid panel.

*KIT*

Two canine *KIT* sequences were already available in GenBank (Accession numbers AF044249 and AF099030). The sequence AF044249 was used for the design of PCR primers. The primers were designed for use in both the amplification of the c-*KIT* coding region from cDNA and the potential amplification and sequencing of the introns. The primers designed for the *KIT* gene are given in Table 8, and the fragments used for the amplification of the coding region are given in Table 9. Coding region fragments were amplified, purified and sequenced from the same normal dog as the other genes. The sequence obtained from the dog is given in Figure 7 and is available in GenBank (Accession number AF448148). The coding region of the *KIT* gene is 2940 bp in length. At the nucleotide level, it is 88.3% identical to the human and 81.9% identical to the mouse. At the amino acid level, it is 88.5% identical to the human and 82.0% identical to the mouse. The sequence contained numerous differences from both of the previously published canine sequences. The same sequence was obtained in all dogs tested, indicating that the differences in the published sequences are likely to be sequencing errors and not polymorphisms.

During the sequencing of the coding region, 6 neutral SNPs were found within the gene. None of these polymorphisms correspond to the differences seen with the other two published canine sequences. In addition, introns 10 and 11 were small enough to be amplified and sequenced from genomic DNA. Intron 10 contained 1 SNP, and intron 11 contained 4 SNPs. The locations of the SNPs in the coding region are shown in Figure 7, and the sequences and SNP locations for the introns are given in Figure 8. The sequences of introns 10 and 11 are also available in GenBank (Accession numbers AF448146 and

Table 8. Primers designed for the *KIT* gene. The location is given relative to the start of the canine coding region.

Table 8. Primers designed for the *KIT* gene.

| Name | Sequence | 5' end | Direction |
|---|---|---|---|
| KIT I1F | TCAGAGTCTATCGCAGCCAC | -24 | Forward |
| KIT I1R | TGCTGGATGGATGGATGGGA | 132 | Reverse |
| KIT I2F | TGCACCAACAGAGATGGCTT | 295 | Forward |
| KIT I2R | TTGCCTTCTTTCCCATACAA | 395 | Reverse |
| KIT I3F | GACGGTGCTGTCCAAGAAAT | 585 | Forward |
| KIT I3R | TCAGGAGAGAGCTTGTTTTG | 676 | Reverse |
| KIT I4F | GATGTGTCTAGTTTCGTGGA | 715 | Forward |
| KIT I4R | AATTGAAGTCACCATGATGC | 814 | Reverse |
| KIT I5F | GGATCAGCAAATGTCACAAC | 898 | Forward |
| KIT I5R | ACTCATCATGGGGAAGATAT | 969 | Reverse |
| KIT I6F | AGATTATCCCAAGTCTGACA | 1089 | Forward |
| KIT I6R | TGTAAGTGCCTCCTTCGTTC | 1180 | Reverse |
| KIT I7F | GTGTCCAATTCCGATGTCAA | 1188 | Forward |
| KIT 1241F | CAAAACCAGAAATCCTGACT | 1241 | Forward |
| KIT I7R | TGCAACCACACACTGGAGCA | 1302 | Reverse |
| KIT I8F | TGGTTGCAGGATTCCCAGAG | 1295 | Forward |
| KIT 1355R | CTCTGCTCAGCTCCTGGACA | 1355 | Reverse |
| KIT I8R | ACAGAGACGAGTTTTGCATC | 1408 | Reverse |
| KIT I9F | ACAACAATGTAGGCAGGAGT | 1490 | Forward |
| KIT MutF | CAAATCCATCCCCACACCCTGTTCAC | 1552 | Forward |
| KIT I9R | ACAAAGCCAATCAGCAAAGG | 1598 | Reverse |
| KIT I11F | GAGGAGATCAATGGAAACAA | 1690 | Forward |
| KIT 1731 CT | CAAATCCATCCCCACACCCTGATCAC | 1731 | Forward |
| KIT 1806R | CACTTTCCCGAAGGCACCAGCACCCA | 1818 | Reverse |
| KIT I12F | CTGATTAAGTCGGATGCGGC | 1840 | Forward |
| KIT I12R | TAGGGCTTCTCGTTCGGTTA | 1920 | Reverse |
| KIT I13F | TGTGAATCTTCTTGGAGCGT | 1968 | Forward |
| KIT I13R | AGATCACCATAGCAACAATAT | 2042 | Reverse |
| KIT I14F | AGGAAGATCACGGAGAAGTG | 2090 | Forward |
| KIT I14R | AACGTAAGAAACGCCGGGTT | 2202 | Reverse |
| KIT I15F | GCGTTTCTTACGTTGTGCCA | 2189 | Forward |
| KIT I15R | GCCAACTCATCATCTTCCAT | 2297 | Reverse |
| KIT I16F | AGAGGACTTGCTGAGCTTTT | 2307 | Forward |
| KIT I16R | TTCGACCATGAGTAAGGAGG | 2422 | Reverse |
| KIT I17F | TCTAGCCAGAGACATCAAGA | 2445 | Forward |
| KIT I17R | CAGTTGAAAATGCTCTCAGG | 2540 | Reverse |
| KIT I18F | GAAAGTGATGTCTGGTCCTA | 2554 | Forward |
| KIT I18R | TTTGAATCGACTGGCATCCC | 2642 | Reverse |
| KIT I19F | GGGATGCCAGTCGATTCAAA | 2623 | Forward |
| KIT I19R | AACGTCGGCCTTTTCAGGG | 2759 | Reverse |
| KIT I20F | CAGATCGTGCAGCTAATTGA | 2764 | Forward |
| KIT I20R | AACCAAAAGAACAGGGATCG | 2995 | Reverse |

Table 9. PCR fragments used to obtain the *KIT* coding region.

| Forward Primer | Reverse Primer | Temperature (°C) | Fragment Size (bp) |
|---|---|---|---|
| KIT I1F | KIT I2R | 52 | 419 |
| KIT I2F | KIT I3R | 54 | 382 |
| KIT I3F | KIT I5R | 52 | 385 |
| KIT I5F | KIT I7R | 54 | 405 |
| KIT I7F | KIT I9R | 54 | 409 |
| KIT I9F | KIT I12R | 54 | 419 |
| KIT I12F | KIT I15R | 54 | 457 |
| KIT I15F | KIT I17R | 54 | 352 |
| KIT I17F | KIT I19R | 54 | 315 |
| KIT I19F | KIT I20R | 54 | 373 |

AF 448147). The allele frequencies of the intronic SNPs and one of the SNPs in the coding region were determined as part of a study on mast cell tumors, described in Chapter 6. A 644 bp genomic DNA fragment containing bases 1552-1818 of the canine *KIT* coding region and introns 10 and 11 was used to screen the canine genomic BAC library. A total of 17 clones were found that potentially contain the *KIT* gene and are currently under investigation. This same 644 bp region was found to contain duplications or deletions in some canine mast cell tumors. The analysis of these tumors will be presented in later chapters.

*KITLG*

The human *KITLG* and murine *Kitl* sequences were retrieved from GenBank (Accession numbers NM_000899 and NM_013598) and aligned using a software program. Regions of homology between the human and murine sequences were chosen for the creation of PCR primers as previously described. Primers were designed for use in both the amplification of the coding region from cDNA and the potential

Figure 7. Alignment of the cDNA sequences of dog and human *KIT* with mouse *Kit*. Vertical lines indicate exon breaks and the ends of the coding region. Base positions relative to the start of the canine coding region are given to the left. Nucleotides identical between species are shaded. SNPs in canine c-*KIT* are shown as white capital letters on a black background. R = G or A, Y = C or T.

Figure 7.

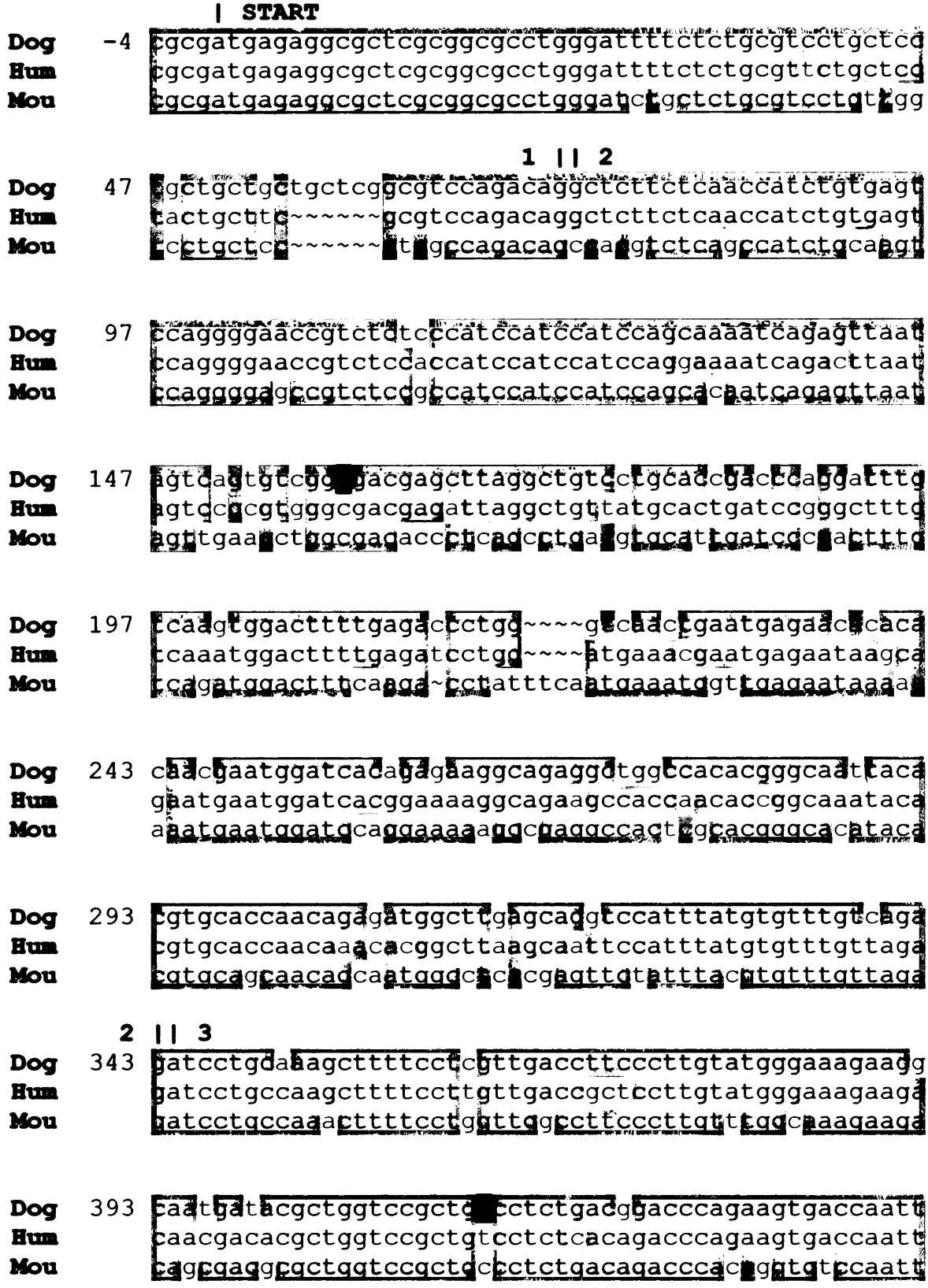
| START
Dog -4 cgcgatgagaggcgctcgcggcgcctgggattttctctgcgtcctgctcg
Hum cgcgatgagaggcgctcgcggcgcctgggattttctctgcgttctgctcg
Mou cgcgatgagaggcgctcgcggcgcctgggatcctgctctgcgtcctgttgg
1 || 2
Dog 47 gctgctgctgctcggcgtccagacaggctcttctcaaccatctgtgagt
Hum tactgcttc~~~~~~gcgtccagacaggctcttctcaaccatctgtgagt
Mou tcctgctcc~~~~~~ttggccagacagcaaggtctcagccatctgcaagt
Dog 97 ccagggggaaccgtctctccatccatccatccagcaaaatcagagttaat
Hum tcagggggaaccgtctccaccatccatccatccaggaaaatcagacttaat
Mou tcagggggagccgtctccgccatccatccatccagcacaatcagagttaat
Dog 147 agtcagtgtccggcgacgagcttaggctgtcctgcaccgacccaggatttg
Hum agtccgcgtgggcgacgagattaggctgttatgcactgatccgggctttg
Mou agttgaaactggcgagacccttcagcctgagtgcattgatccgcactttg
Dog 197 tcaagtggacttttgagacctctgg~~~~gccaactgaatgagaacccaca
Hum tcaaatggacttttgagatcctgg~~~~atgaaacgaatgagaataagca
Mou tcagatggactttcaagaa~cctatttcaatgaaatggttgagaataaaa
Dog 243 caacgaatggatcacagagaaggcagaggctggccacacgggcaattaca
Hum gaatgaatggatcacggaaaaggcagaagccaccaacaccggcaaataca
Mou aaatgaatggatgcaggaaaaaaggcgaaggccactcggcacgggcacataca
Dog 293 cgtgcaccaacagagatggcttgagcaggtccatttatgtgtttgtcaga
Hum cgtgcaccaacaaacacggcttaagcaattccatttatgtgtttgttaga
Mou cgtgcagcaacacacaatgggcccacgagttgtatttacctgtttgttaga
2 || 3
Dog 343 gatcctgdaaagctttcctcgttgaccttcccttgtatgggaaagaaggg
Hum gatcctgccaagctttccttgttgaccgctccttgtatgggaaagaaga
Mou gatcctgccaaactttttcctgttttggccttcccttgttttggcaaagaaga
Dog 393 caatgatacgctggtccgctgcctctgacggacccagaagtgaccaatt
Hum caacgacacgctggtccgctgtcctctcacagacccagaagtgaccaatt
Mou cagcgaggcgctggtccgctgcctctgacagacccacggttgtccaatt

Figure 7 (cont'd).

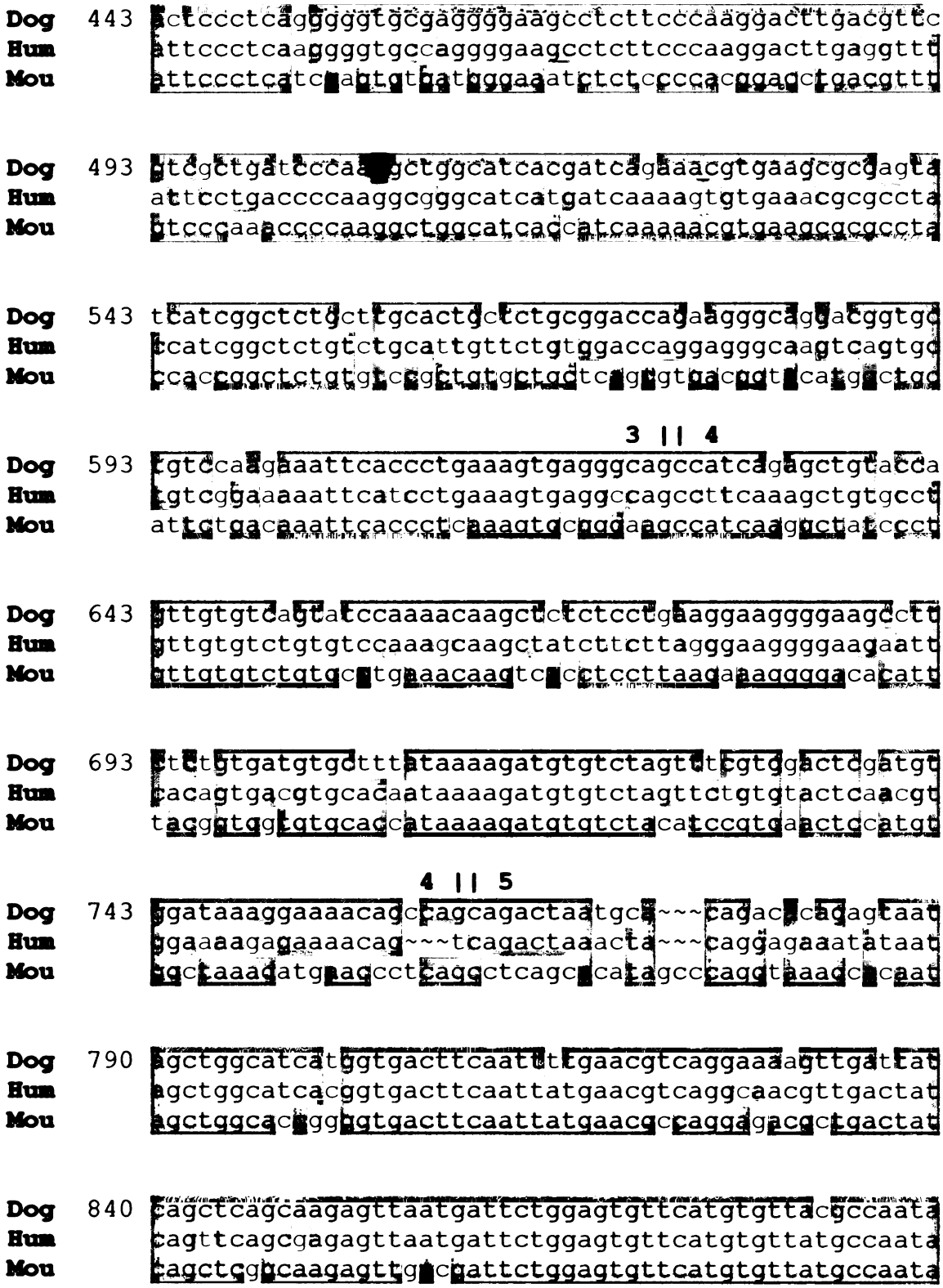

Figure 7 (cont'd).

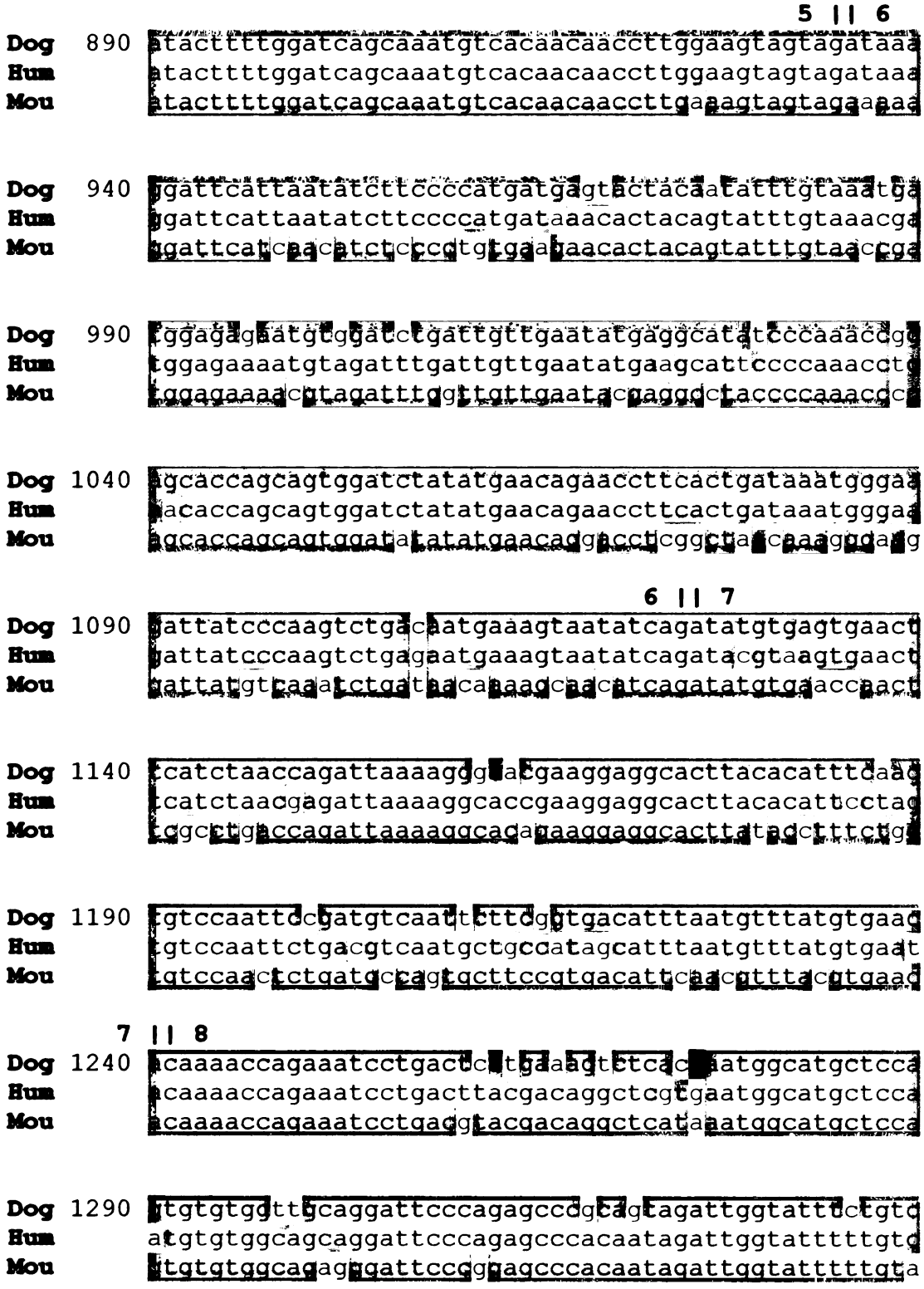

Figure 7 (cont'd).

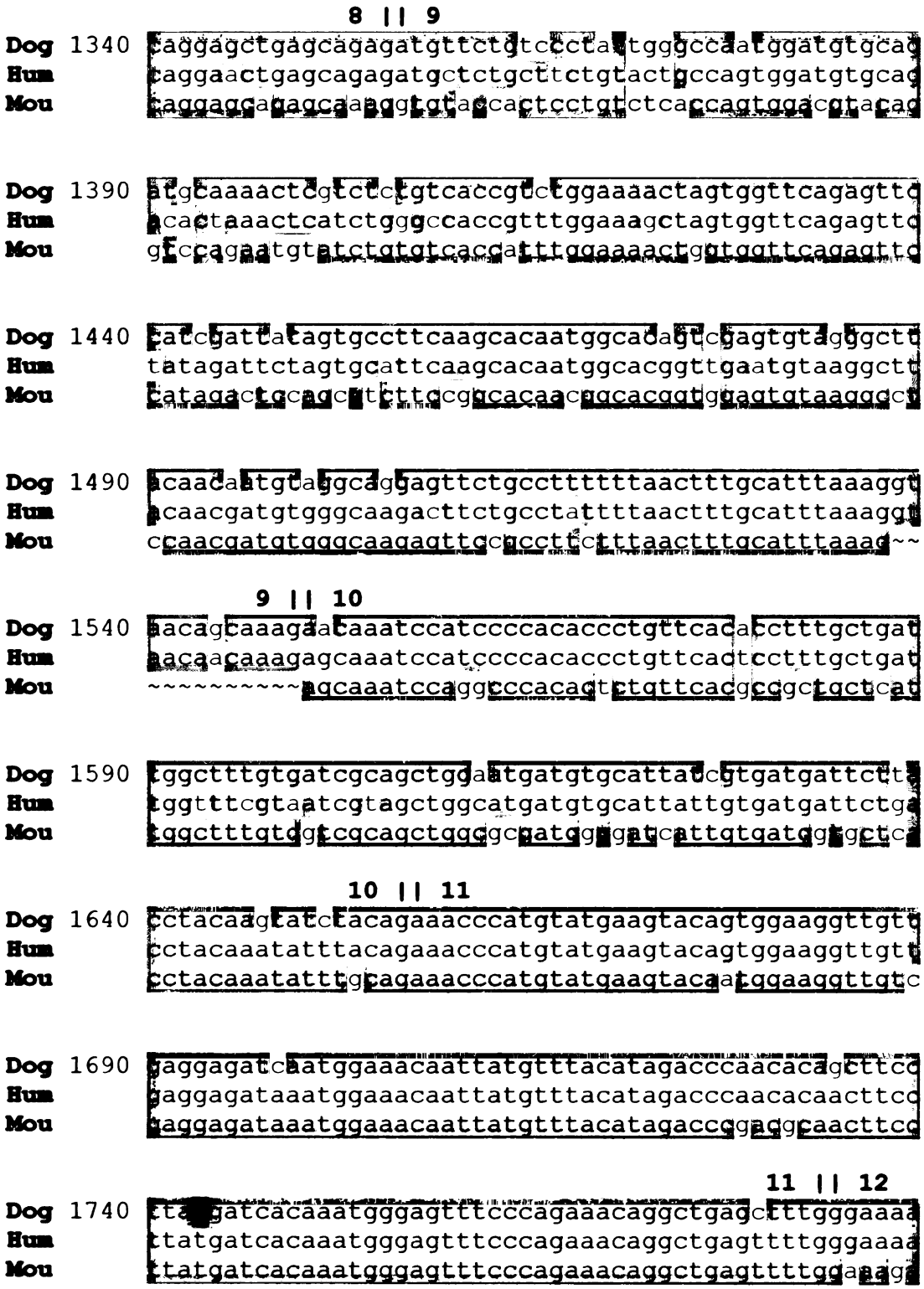

Figure 7 (cont'd).

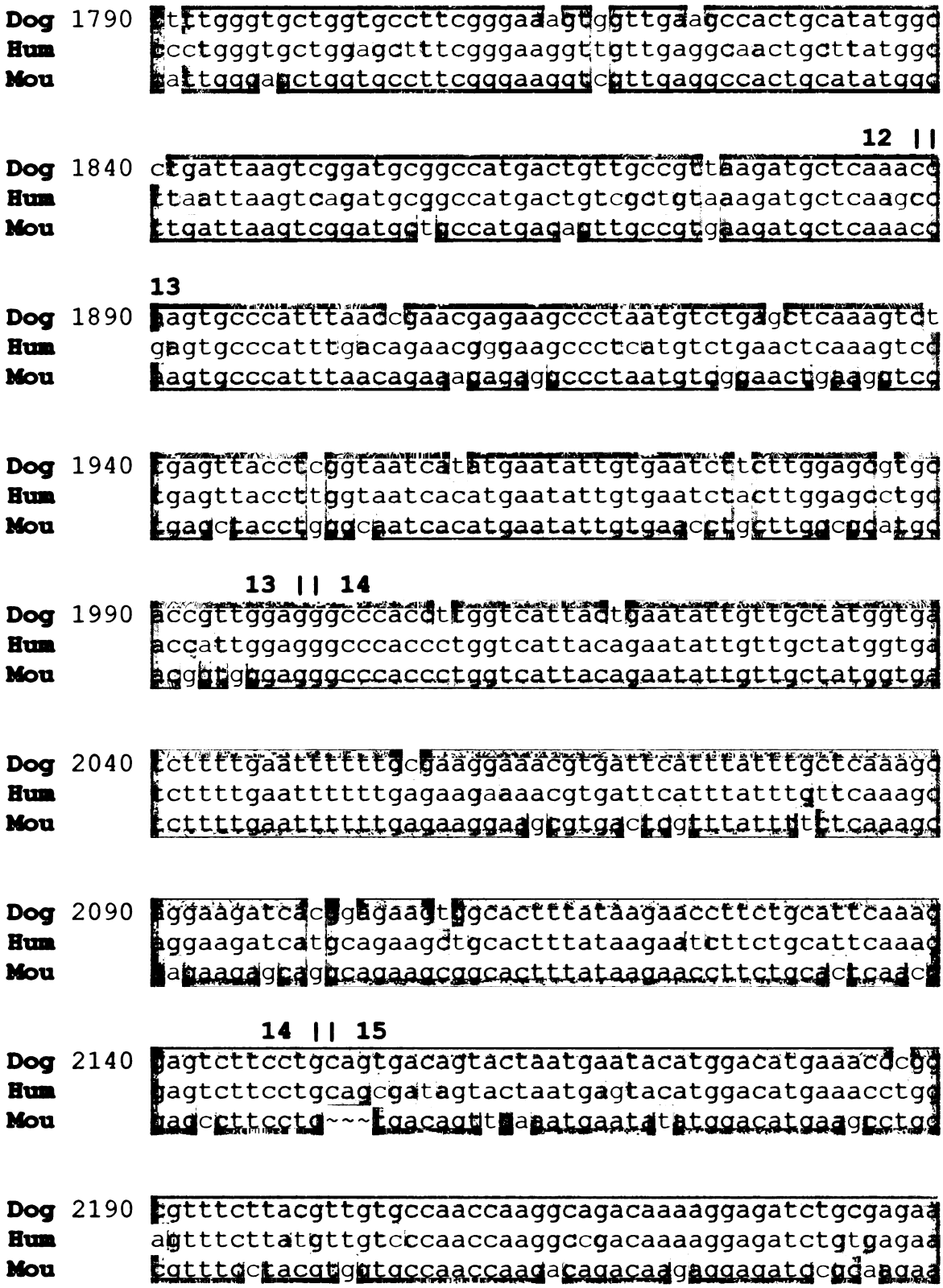

Figure 7 (cont'd).

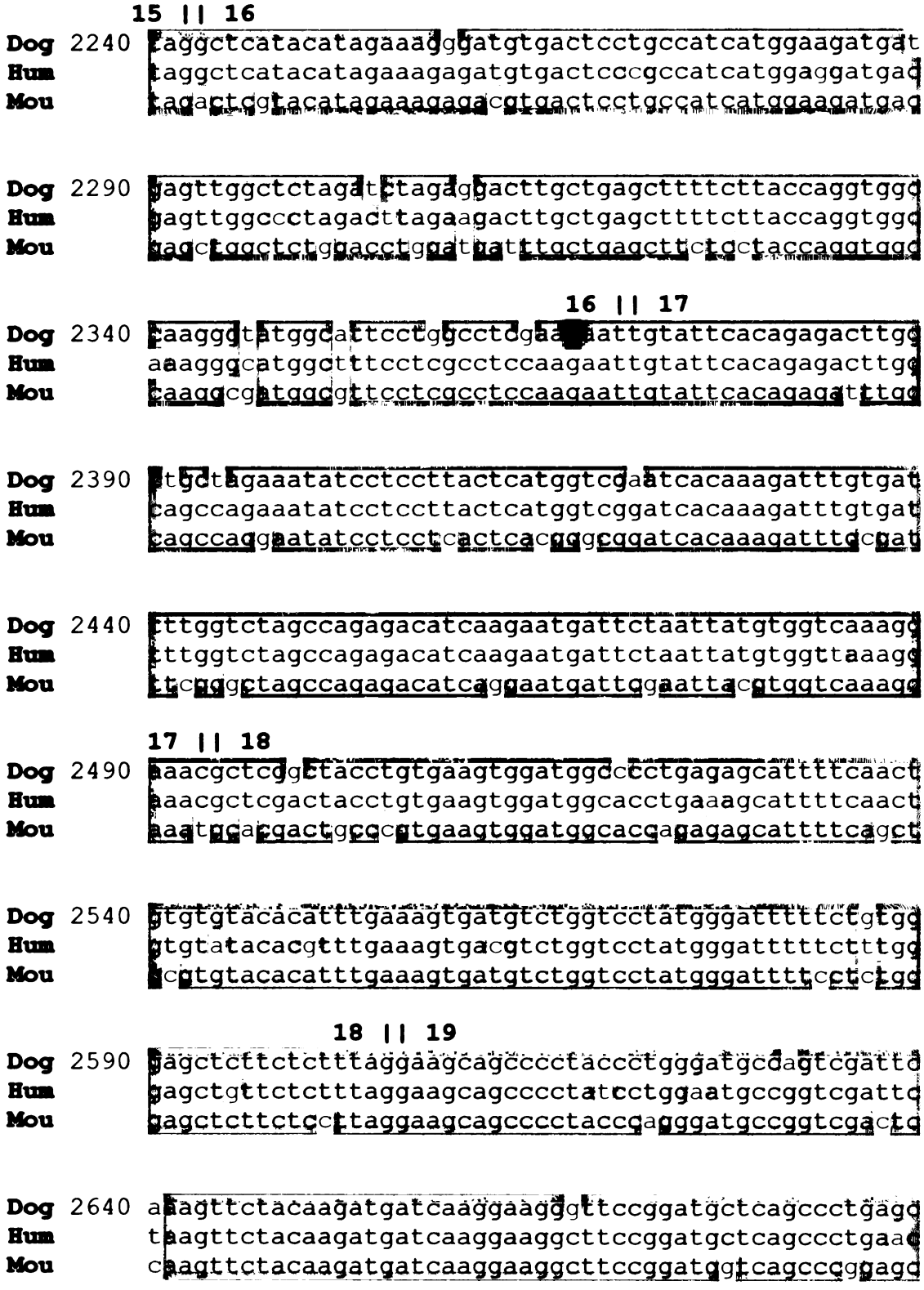

Figure 7 (cont'd).

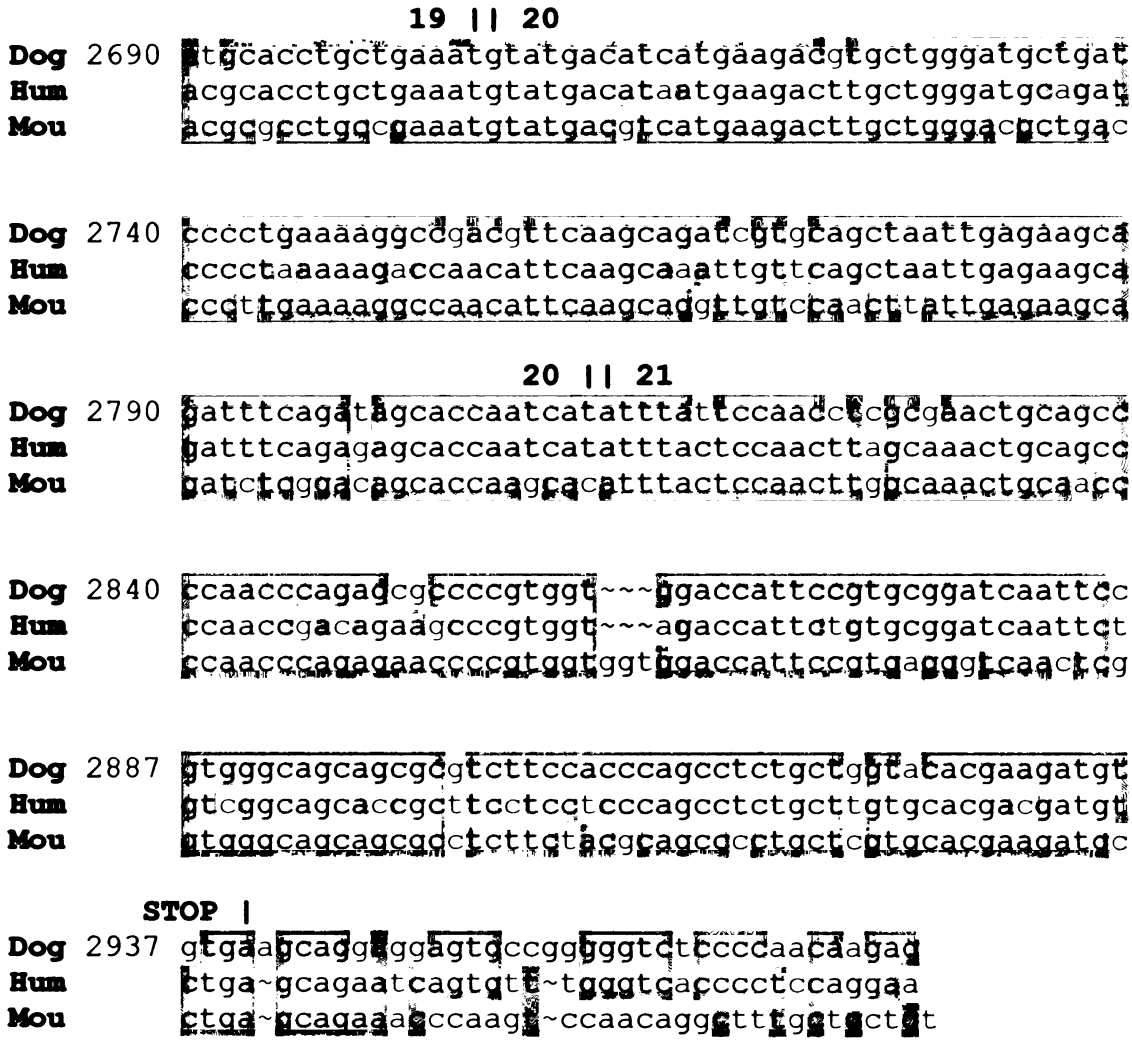

**Intron 10**

```
  1 gtaatcattcatttgttctctaccctaagtgctataatgatcgaaatgtt
 51 attcattaaaagatgatct[redacted]tctctcttttctccccccaccag
```

**Intron 11**

```
  1 gtcagtatgaaa[redacted]aggggctttccatgtaacctttttgtgtacgtgtaac
 51 aatgactttagggaaccccattagcttcctttgttctgttccaactgaga
101 caataagtattttctgtgaagtttcatca[redacted]ttttgatagattcc[redacted]cataa
151 agcaccttatagagaaatgtccttagctggatttgtccttaattccttaa
201 caattccttgattgttgactttgaaattacccagatgctcctttggtcct
251 a[redacted]caccacccctactcttttcttcctttctgcag
```

Figure 8. Sequences of canine *KIT* introns 10 and 11. SNPs are shown as white text on a black background. R = G or A, Y = C or T, K = G or T.

amplification and sequencing of the introns. The primers designed for the *KITLG* gene are given in Table 10, and the fragments used to amplify the coding region are given in Table 11. Fragments of the coding region were amplified, purified, and sequenced from the same normal dog as the other genes. The sequence obtained from the canine *KITLG* coding region is given in Figure 9. The coding region of the canine *KITLG* gene is 825 bp in length. The coding region sequence is identical to a canine *KITLG* sequence that was later found in GenBank (Accession number S53329). It is 91.0% and 87.1% identical to the human and mouse, respectively, at the nucleotide level. At the amino acid level, it is 85.4% identical to the human and 80.7% identical to the mouse.

Table 10. Primers designed for the *KITLG* gene.

| Name | Sequence | 5' end | Direction |
|---|---|---|---|
| MGF I1F | AGCTAAACGGAGTCGCCACA | -57 | Forward |
| MGF I1R | CGAGAGGATTAAATAGGAGC | 67 | Reverse |
| MGF I2F | GGAATCGTGTGACTAATAAT | 89 | Forward |
| MGF I2R | GGACATTTATGAGGGTTATC | 175 | Reverse |
| MGF I3F | GATAACCCTCAAATATGTCC | 156 | Forward |
| MGF I3R | TCCAGAAGATCAGTCAAGCT | 257 | Reverse |
| MGF I4F | ATTCCATCAGATACAAACTTG | 293 | Forward |
| MGF I5R | CTGCAACAGGGGGTAACATA | 571 | Reverse |
| MGF I6F | TATGTTACCCCCTGTTGCAG | 552 | Forward |
| MGF I6R | GCTCCAAAAGCAAAGCCAAT | 704 | Reverse |
| MGF I7F | ATTGGCTTTGCTTTTGGAGC | 684 | Forward |
| MGF I7R | AAACATGAACTGTTACCAGC | 882 | Reverse |

Table 11. PCR fragments used to obtain the *KITLG* coding region.

| Forward Primer | Reverse Primer | Temperature (°C) | Fragment Size (bp) |
|---|---|---|---|
| MGF I1F | MGF I3R | 54 | 314 |
| MGF I3F | MGF I6R | 52 | 546 |
| MGF I6F | MGF I7R | 52 | 331 |

*Analysis of candidate genes' roles in hereditary deafness*

Total RNA was extracted from tissue samples from one deaf dog in each of 7 different breeds: Dalmatian (spleen), Australian Cattle Dog (spleen), Catahoula Leopard Dog (ovary), Boxer (testis), Great Dane (testis), Springer Spaniel (uterus), and Jack Russell Terrier (ovary). The RNA was treated with DNase and reverse transcribed into cDNA. The coding regions of *EDNRB*, *MITF-M*, *KIT*, and *KITLG* were completely sequenced in all 7 dogs. The individual exons of the *MITF-M* gene were amplified and sequenced from genomic DNA in an Australian Shepherd with both deafness and

Figure 9. Alignment of the cDNA sequences of dog and human *KITLG* with mouse *Kitl*. Vertical lines indicate exon breaks and the ends of the coding region. Base positions relative to the start of the canine coding region are given to the left. Nucleotides identical between species are shaded.

Figure 9.

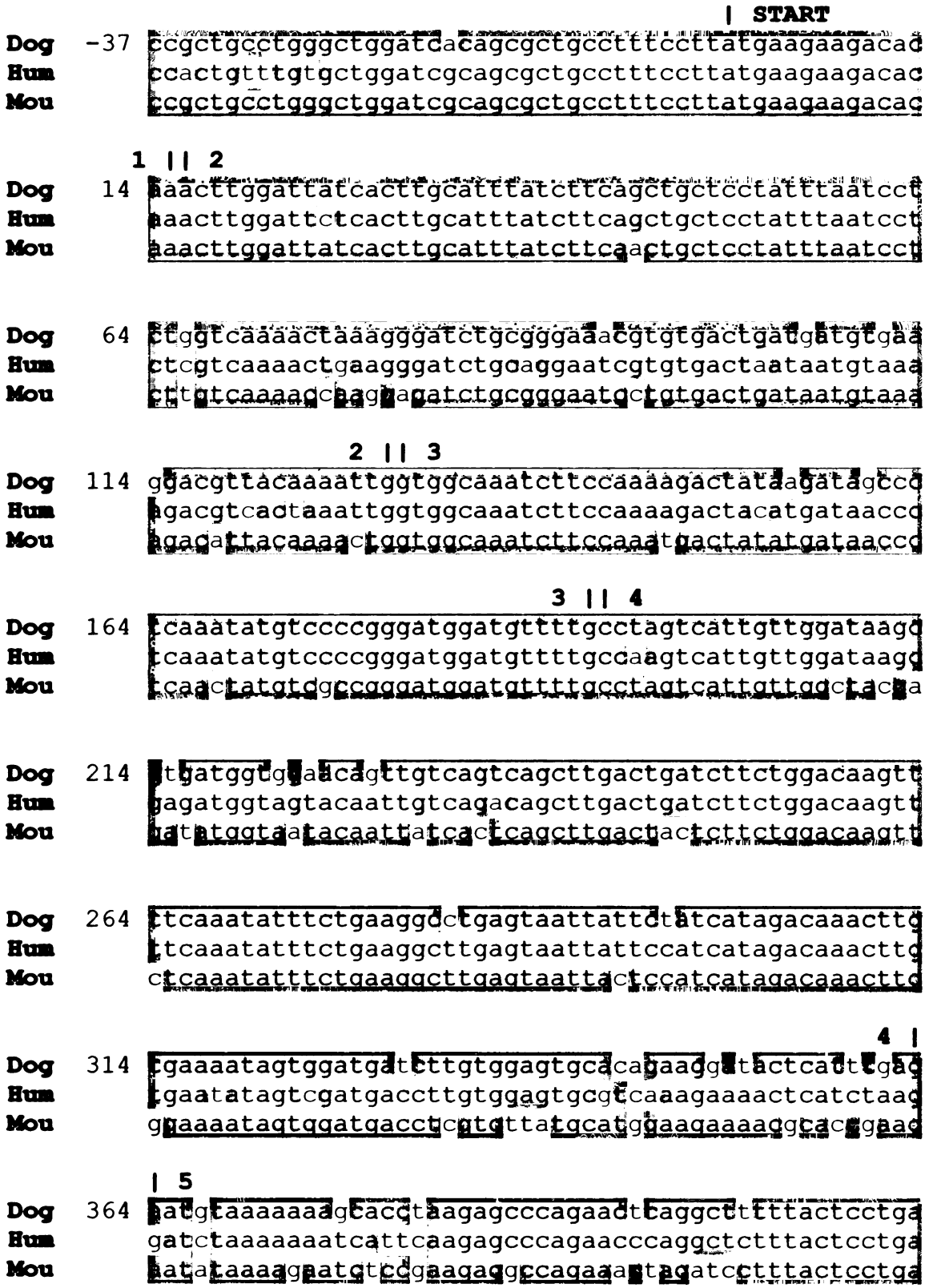

Figure 9 (cont'd).

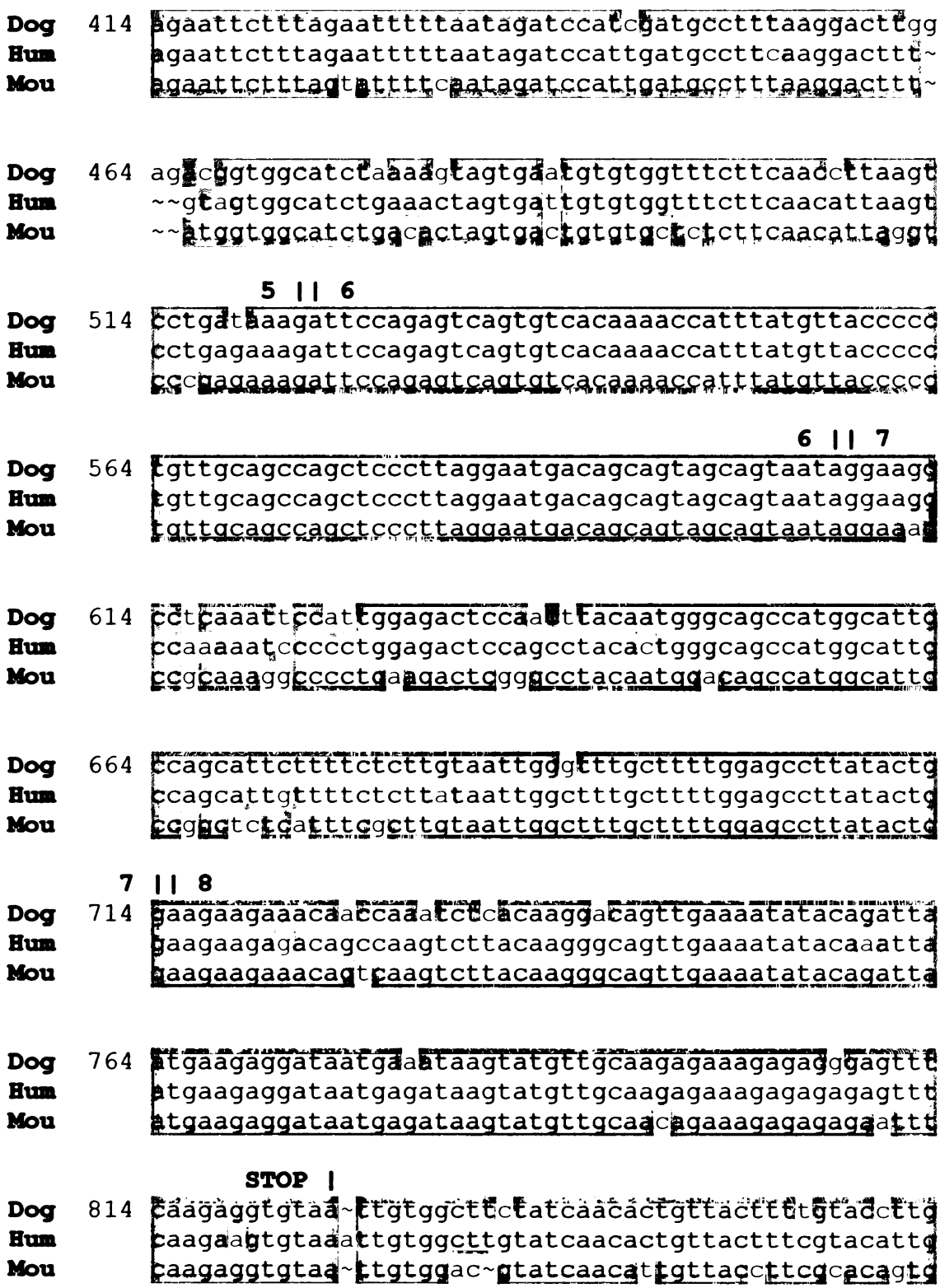

microphthalmia. Individual exons were also amplified from the 7 dogs above. For each exon, the amplified fragments from all 7 dogs were pooled together and the pooled DNA was used as a template for sequencing. An additional 7 deaf Jack Russell Terriers were similarly pooled and sequenced, and 21 other deaf dogs were partially sequenced for *MITF* in pools of 7 as well. No mutations relative to the normal sequences were found for any of the candidate genes in the dogs tested. For those dogs in which individual *MITF* exons were sequenced, no mutations were found in the bordering splice sequences either.

Since polymorphisms had been found for the *EDNRB* and *KIT* genes, these could be used as markers that would allow the investigation of whether either of these genes was associated with deafness. DNA from cheek swabs was available for 59 Jack Russell Terriers, 51 of which belonged to a single pedigree. Among these dogs, 7 were confirmed to be deaf and 41 were confirmed to have normal hearing by BAER testing. The remaining 11 dogs had not been tested, but had not been reported with hearing problems and were considered to be normal. The regions containing the SNPs in intron 6 of *EDNRB* and intron 10 of *KIT* were amplified by PCR for each dog. Restriction digests that would differentially cut each allele determined the genotypes of the two SNPs in each dog. The results of these experiments are shown in Table 12 and Table 13. For the SNP in intron 6 of *EDNRB*, 3 of the deaf dogs were homozygous for a G allele, 1 was homozygous for an A allele, and 3 were heterozygous. The region containing the SNP in intron 10 of *KIT* could only be amplified from 56 dogs. The samples that did not amplify represented 1 normal and 2 deaf dogs. Of the remaining deaf dogs, 2 were homozygous for an A allele, 1 was homozygous for a G allele, and 2 were heterozygous.

Table 12. Genotype results for a SNP in intron 6 of *EDNRB*.

| | GG | GA | AA | Total |
|---|---|---|---|---|
| Deaf | 3 | 3 | 1 | 7 |
| Normal | 18 | 22 | 12 | 52 |
| Total | 21 | 25 | 13 | 59 |

Table 13. Genotype results for a SNP in intron 10 of *KIT*.

| | AA | GA | GG | Total |
|---|---|---|---|---|
| Deaf | 2 | 2 | 1 | 5 |
| Normal | 23 | 18 | 10 | 51 |
| Total | 25 | 20 | 11 | 56 |

A chi-squared analysis could not be performed on the data because expected values among the deaf dogs were less than 5; therefore Fisher's exact test was used to examine the genotype distributions of both SNPs in deaf and normal dogs. The probability that the distribution for the SNP in *EDNRB* was produced by random chance was 1, and the probability for the SNP in *KIT* was 0.823. Therefore, no significant distribution difference was seen, and there does not appear to be an association between genotype at these SNPs and deafness.

**Discussion**

The coding regions of 4 genes were completely sequenced in the dog. Two of these genes had not been previously sequenced in the dog, and mistakes in the published sequences for a third gene were corrected. Partial intronic sequences were obtained for 3 of the 4 genes, and some introns were completely sequenced. Polymorphisms were

identified

mutations

addition, n

the genes.

T

dogs fron

deafness

genes, h

gene, th

splice

obtain

confi

cann

case

the

the

ge

is

w

th

pol

that

identified in two of the genes, and a processed pseudogene was identified in the third. No mutations were found linking any of these genes to hereditary deafness in dogs. In addition, no association was seen between deafness and polymorphic markers in two of the genes.

The absence of mutations within the coding regions of the candidate genes in deaf dogs from 7 breeds indicates that these genes are not likely the cause of hereditary deafness in these breeds. Mutations within the promoter regions or splice sites of these genes, however, may cause altered expression that could lead to deafness. For the *MITF* gene, the splice sites were examined and found to contain no mutations. Most of the splice sites of *EDNRB* are available for screening due to the bordering intronic sequences obtained from a BAC clone. Potential clones have also been identified for *KIT*, which if confirmed could be sequenced to get the splice sites for this gene as well. If mutations cannot be found within the splice sites of the candidate genes, this would strengthen the case for excluding these genes as candidates for deafness in the breeds studied. Although the sequences obtained for the genes in this study extend into the 5' untranslated regions, the promoter sequences of these genes have not yet been obtained. Further study of these genes should include sequencing of the promoters if possible. In the *MITF* gene, each isoform is thought to be under the control of its own specific promoter. It is not known whether any of the other genes may also have multiple promoters. Altered expression of these genes could also be tested for by Northern blots.

No association was seen in the Jack Russell Terrier breed between deafness and polymorphic markers in the *EDNRB* and *KIT* genes. For this experiment, it is assumed that a mutation causing deafness in these genes would be close enough to the SNPs that

recombina

disequilib

this study

dog bree

will hav

inherita

This m

not the

pheno

findin

neith

the r

alre

both

dea

of v

wh

loc

co

hav

pos

have

recombination between them has not occurred. This is a reasonable assumption since the disequilibrium of loci 50 kb apart, a distance similar to the genomic sizes of the genes in this study, does not decay appreciably for thousands of years, longer than most modern dog breeds have been established.[8] It is also assumed that a mutation causing deafness will have occurred only once and that deafness in this breed is due to a founder effect by inheritance from a single common ancestor; therefore no allelic heterogeneity exists. This means that such a mutation should be associated with only one allele of a SNP and not the other. Finally, it is assumed that only one gene locus is involved, there are no phenocopies, and gene conversion has not occurred. Under these assumptions, the finding that dogs homozygous for either allele of these SNPs can be deaf suggests that neither of these genes contain a mutation causing deafness. It is possible, however, that the mutations causing the SNPs in these genes happened after the deafness mutation was already established in the population, meaning that deafness could be associated with both alleles. Therefore, these genes can't be conclusively excluded as candidates for deafness. Recently, however, the *EDNRB* and *KIT* genes have been excluded as the basis of white spotting in the Border Collie.[6] Since deafness is believed to be associated with white spotting and Jack Russell Terriers have inherited the piebald allele at the spotting locus, this is further evidence that these genes are not involved in deafness.

The possibility does exist that some of the genes in this study have multiple copies in the genome and that these alternate copies contain mutations. Multiple copies have not been identified in other species for *MITF*, *KIT*, or *KITLG*, although the possibility still exists for multiple copies in the dog. For *EDNRB*, however, subtypes have been identified clinically by differential binding affinity for ET3 competitors in

some species, including dogs.[1] In the quail, these subtypes have been sequenced, but were found to share only 74% homology at the amino acid level and so are likely produced by different genes.[4] In this study, two different sequences were found within one portion of the canine *EDNRB* gene. These consisted of 14 base changes in a 52 bp region of overlap between two PCR fragments and would be predicted to cause 6 amino acid changes. This may potentially represent *EDNRB* subtypes present in the dog. Alternately, there may be an *EDNRB* pseudogene in the canine genome. One of the fragments can be amplified from genomic DNA, whereas the other cannot. The use of RNA that had been treated with DNase, however, means that preferential amplification of a genomic pseudogene could not have occurred with this fragment. Further study of this region is necessary to clarify what is actually occurring, which may include Southern blots to determine if more than one *EDNRB* gene exists.

A potential pseudogene has been identified for *MITF*, however. The apparent presence of three different sequences for this pseudogene cannot be explained at present and requires further study. The extent of the pseudogene is also not currently known. The sequence acquired to date covers much of the coding region of the real *MITF* gene. If this sequence extends further upstream, it is possible that this might actually be a copy of the *MITF* gene that can be expressed. The presence of nonsense and frameshift mutations would result in a nonfunctional protein that might have a dominant negative effect. Even if this is the case, however, an association with deafness is unlikely. One of the dogs in which the proposed pseudogene sequence appeared normal was deaf. As with *EDNRB*, Southern blots should be used to determine whether multiple copies or pseudogenes of *MITF* exist in the canine genome. Besides the potential pseudogene, it is

possible that one of the known *MITF* isoforms is involved in deafness, particularly those that are expressed in melanocytes. In this study, the specific exon 1 sequences could only be obtained for 2 *MITF* isoforms. Attempts should be made to obtain the 5' ends of the other isoforms so that they may be screened for mutations.

As the investigation of the candidate genes in this study was primarily performed by PCR and sequencing, it is not known whether altered expression of one of these genes might play a role in deafness. Defects in a regulatory gene might lead to changes in the level or timing of expression of one of the candidate genes. Although these genes continue to be expressed even after birth, they are specifically required for melanocyte development in even the earliest embryonic stages. If possible, fetal tissues should be examined to determine if there is altered expression at this time. It is also possible that altered expression may only occur in certain tissues. The dogs used in this study were privately owned and euthanization was not an option in most cases. Therefore, in many cases the tissues used were reproductive organs that were removed when the dogs were sterilized. Attempts should be made to obtain tissues from more relevant locations, particularly the inner ear, to investigate gene expression in those areas.

Although further studies are required in order to provide conclusive evidence, it seems most likely at this time that none of the genes studied are responsible for hereditary deafness in dogs, at least in the breeds studied. Additional candidate genes remain based on phenotypic similarity to other species, however, namely *EDN3*, *PAX3*, *SOX10*, and *RET*. In the event that these genes are also excluded as candidates, other methods will have to be employed to determine the true cause. During the course of this study, substantial pedigrees were acquired for the Jack Russell Terrier and Catahoula

Leopard Dog breeds. Although not ideal in their current state, with further cooperation from breeders and owners they could be completed to the point where they would be useful for linkage studies. If deafness could be linked to a particular region of the canine genome, positional cloning could be used to identify new candidate genes based on genetic information.

**References**


1. Brooks DP, DePalma PD, Pullen M, Gellai M, Nambi P. Identification and function of putative $ET_B$ receptor subtypes in the dog kidney. J Cardiovasc Pharmacol 26 Suppl 3:S322-S325, 1995.

2. Canine Radiation Mapping Project, Universite de Rennesl, France. World Wide Web URL: http://www-recomgen.univ-rennes1.fr/Dogs/maquette.html. Retrieved January 6, 2003.

3. Fuse N, Yasumoto K, Takeda K, Amae S, Yoshizawa M, Udono T, Takahashi K, Tamai M, Tomita Y, Tachibana M, Shibahara S. Molecular cloning of cDNA encoding a novel microphthalmia-associated transcription factor isoform with a distinct amino-terminus. J Biochem (Tokyo) 126:1043-1051, 1999.

4. Lecoin L, Sakurai T, Ngo MT, Abe Y, Yanagisawa M, Le Douarin NM. Cloning and characterization of a novel endothelin receptor subtype in the avian class. Proc Natl Acad Sci U S A 95:3024-3029, 1998.

5. Mellersh CS, Hitte C, Richman M, Vignaux F, Priat C, Jouquand S, Werner P, André C, DeRose S, Patterson DF, Ostrander EA, Galibert F. An integrated linkage-radiation hybrid map of the canine genome. Mamm Genome 11:120-130, 2000.

6. Metallinos D, Rine J. Exclusion of EDNRB and KIT as the basis for white spotting in Border Collies. Genome Biol 1:RESEARCH0004, 2001.

7. Schmutz SM, Moker JS, Yuzbasiyan-Gurkan V, Zemke D, Sampson J, Lingaas F, Dunner S, Dolf G. DCT and EDNRB map to DogMap linkage group L07. Anim Genet 32:321, 2001.

8. Suarez BK, Hampe CL. Linkage and association. Am J Hum Genet 54:554-559, 1994.

# CHAPTER 3

Zemke D, Yuzbasiyan-GurkanV. A single nucleotide polymorphism and a (GA)*n* microsatellite in intron 6 of the canine endothelin receptor B (*EDNRB*) gene. Anim Genet 30:390, 1999.

*Source/description*: Consensus PCR primers to the published human and mouse sequences were designed to amplify the intron between exons 6 and 7 of the canine endothelin receptor B (*EDNRB*) gene. The numbering of the exons is the same as for the published human and murine sequences[1,2]. A total of 700 bp of canine sequence was obtained from the resulting PCR product, including the entire intron and both 5' and 3' exonic sequences. The intron sequence (GenBank accession no. AF134188) matched that of an intron previously sequenced by others[3] and reported to lie between exons 4 and 5 (Genbank accession no. AF026088). The two sequences were nearly identical, including a (GA)*n* microsatellite, except for the presence of an extra G at base 235 in AF026088. Comparison of the surrounding exonic sequences reported by Liu *et al.* (1998)[3] with the nearly complete canine *EDNRB* cDNA sequence obtained by this laboratory (Genbank accession no.AF034530) confirmed that this intron indeed lies between exons 6 and 7. During sequencing, a single nucleotide polymorphism (SNP) was found, resulting in a G-A transition ≈ 40 nucleotides downstream of the polymorphic microsatellite (GenBank accession no. AF134188).

*Primer Sequences*:

Forward primer, F: 5'-AGACGGGAAGTGGCCAAAAC-3'

Reverse primer, R: 5'-GAGGCCATATTGATGCCGAT-3'

SNP detection primer, S: 5'-GACCAGTGATAAAGTCAAAAATCAT-3'

Microsatellite forward primer, $M_F$: 5'-GAGAATTGGGCATGGGCAGA-3'

Microsatellite reverse primer, $M_R$: 5'-TGACTTTATCACTGGTCTTTG-3'

*PCR conditions*: All PCR reactions were carried out in 25 μL reactions containing 0.6 U *Taq* polymerase, 0.8 μM of each primer, 1.5 mM $MgCl_2$, and 100 μM dNTPs. Reactions were denatured at 94°C for 4 min, followed by 35 cycles of 94°C for 1 min, the chosen annealing temperature for 2 min, and 72°C for 3 min, followed by a final extension at 72°C for 8 min. The initial PCR was performed using primers F and R and 3 μL of genomic DNA at a 66°C annealing temperature. The resulting band was sampled by stabbing into the gel with a pipette tip and transferring it to 15 μL of water. Three microliters of this sample was used as template in the second PCR with primers S and R for SNP detection and primers $M_F$ and $M_R$ for microsatellite sizing, both at a 60°C annealing temperature. The expected size of the initial product was 740 bp, the SNP detection product was 170 bp, and the microsatellite product ≈ 131 bp. The SNP detection primer was designed to introduce a partial *BspHI* restriction site next to the single nucleotide polymorphism, which is completed when the polymorphic base is A and not completed if the polymorphic base is G. Following *BspHI* digestion, the *G* allele is represented as a 170-bp band and the *A* allele as two bands of ≈ 146 and 24 bp.

*Polymorphism*: Genomic DNA from 36 dogs, representing 11 mixed bred animals and 25 different pure breeds was tested for both the GA and the SNP polymorphisms. Four alleles were observed with the GA microsatellite and two with the SNP. The observed heterozygosity (HET) was 0.42 for the microsatellite and 0.36 for the SNP. The third largest (GA)*n* microsatellite repeat allele was found to be associated in all cases with an A at the SNP site. All other repeat alleles were associated with a G at this site.

*Chromosomal Location*: Unknown.

*Mendelian inheritance*: Testing of a family of dogs (Fig. 1) segregating for both the SNP and the microsatellite supported the inheritance of both of these variations in a Mendelian fashion.

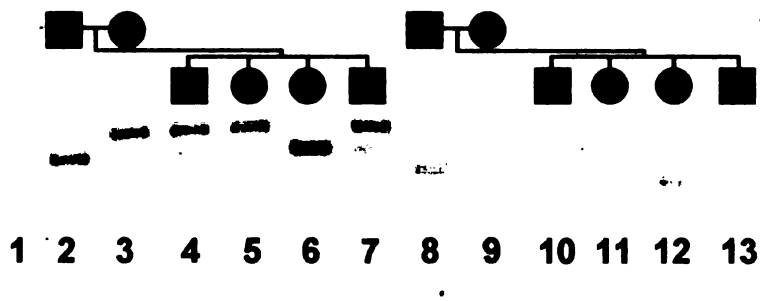


**Fig. 1.** Two percent agarose gel showing SNP (lanes 2-7) and microsatellite (lanes 8-13) results for a family of six dogs. The sire (lanes 2 and 8) was homozygous for the *A* SNP allele and the third largest microsatellite allele. The dam (lanes 3 and 9) was heterozygous for both SNP alleles and the second and third largest microsatellite alleles. The offspring are shown in lanes 4-7 and 10-13. Lane 1 contains a 100-bp DNA ladder.

*Acknowledgments*: This work was supported in part by grants from the American Kennel Club Canine Health Foundation, the Dalmatian Club of America and the Jaqua Foundation.

*References*

1 Elshourbagy N.A. *et al.* (1993) *J Biol Chem* **268**, 3873-3879.

2 Hosoda K. *et al.* (1994) *Cell* **79**, 1267-1276.

3 Liu P-C. *et al.* (1998) *Anim Genet* **29,** 236.

Correspondence: V. Yuzbasiyan-Gurkan (e-mail: yuzbasiyan@cvm.msu.edu)

# CHAPTER 4

# PREFACE TO EVALUATION OF *KIT* MUTATIONS IN MAST CELL TUMORS

Many dog breeds appear to exhibit an increased risk for the development of cancer when compared to other breeds. It is possible that the cause of the increased risk in these breeds has a genetic component. The Boxer in particular has a high incidence of many types of cancer, especially mast cell tumors.[2] Besides its role in the development of melanocytes, *KIT* also controls the development of mast cells.[1] Human mast cell leukemia has been linked to mutations in *KIT*, and mouse mastocytoma cell lines have been shown to have *Kit* mutations.[3,6] It was hypothesized that mutations in *KIT* might be responsible for mast cell tumors in dogs as well.

Since the *KIT* gene had already been sequenced in the dog as part of the investigation into hereditary deafness, most of the materials required for a study of this gene in mast cell tumors were already available. It was therefore decided to pursue this study as an adjunct to the main project on deafness. While in the preliminary stages of the investigation, our suspicions were confirmed by the publication of two articles reporting the discovery of mutations in the juxtamembrane domain of *KIT* in mast cell tumors.[4,5] At this point, a female Boxer had been acquired that had previously been treated for a mast cell tumor and was later euthanized after the development of numerous additional tumors. The following two chapters constitute reprints of published manuscripts resulting from studies of this dog and additional mast cell tumor cases.[7,8]

**References**


1. Broudy VC. Stem cell factor and hematopoiesis. Blood 90:1345-1364, 1997.
2. Cohen D, Reif JS, Brodey RS, Keiser H. Epidemiological analysis of the most prevalent sites and types of canine neoplasia observed in a veterinary hospital. Cancer Res 34:2859-2868, 1974.

3. Furitsu T, Tsujimura T, Tono T, Ikeda H, Kitayama H, Koshimizu U, Sugahara H, Butterfield JH, Ashman LK, Kanayama Y, Matsuzawa Y, Kitamura Y, Kanakura Y. Identification of mutations in the coding sequence of the proto-oncogene c-*kit* in a human mast cell leukemia cell line causing ligand-independent activation of c-*kit* product. J Clin Invest 92:1736-1744, 1993.

4. London CA, Galli SJ, Yuuki T, Hu ZQ, Helfand SC, Geissler EN. Spontaneous canine mast cell tumors express tandem duplications in the proto-oncogene c-*kit*. Exp Hematol 27:689-697, 1999.

5. Ma Y, Longley BJ, Wang X, Blount JL, Langley K, Caughey GH. Clustering of activating mutations in *c-KIT*'s juxtamembrane coding region in canine mast cell neoplasms. J Invest Dermatol 112:165-170, 1999.

6. Tsujimura T, Furitsu T, Morimoto M, Isozaki K, Nomura S, Matsuzawa Y, Kitamura Y, Kanakura Y. Ligand-independent activation of c-*kit* receptor tyrosine kinase in a murine mastocytoma cell line P-815 generated by a point mutation. Blood 83:2619-2626, 1994.

7. Zemke D, Yamini B, Yuzbasiyan-Gurkan V. Characterization of an undifferentiated malignancy as a mast cell tumor using mutation analysis in the proto-oncogene c-*KIT*. J Vet Diagn Invest 13:341-345, 2001.

8. Zemke D, Yamini B, Yuzbasiyan-Gurkan V. Mutations in the juxtamembrane domain of c-*KIT* are associated with higher grade mast cell tumors in dogs. Vet Pathol 39:529-535, 2002.

# CHAPTER 5

Zemke D, Yamini B, Yuzbasiyan-Gurkan V. Characterization of an undifferentiated malignancy as a mast cell tumor using mutation analysis in the proto-oncogene c-*KIT*. J Vet Diagn Invest 13:341-345, 2001.

**Abstract.** A 6.5-year-old female Boxer was euthanized and presented for necropsy following rapid clinical decline concomitant with the development of numerous tumor masses. The largest of these masses was in the same location as a mast cell tumor that had been previously removed from this dog. Gross examination revealed the presence of nodules from 5-200 mm in diameter throughout the body, including the lymph nodes. Histologic analysis showed an influx of round cells with no granules, leading to the provisional diagnosis of systemic lymphosarcoma. Immunohistochemical staining for B- and T-lymphocyte antigens was negative. Molecular tests were used to identify a tandem duplication in the c-*KIT* proto-oncogene from both the earlier mast cell tumor and the current nodules, implicating a common origin. Addition of molecular testing to conventional necropsy evaluations allowed a definitive diagnosis of mast cell tumors.

Mast cell tumors, or mastocytomas, are one of the most common types of skin cancer seen in dogs, accounting for an estimated 7-21% of all cases.[3,10,17] Although mast cell tumors are rare and generally nonthreatening in humans,[17] they are often more aggressive and constitute a significant health risk in dogs. Canine mast cell tumors develop swiftly, are quick to metastasize, and frequently recur after having been removed.[17] Moreover, certain breeds such as the Boxer appear to have some predisposition toward their development.[3] To investigate the possibility that the Boxer breed has an inherited increased susceptibility to certain types of cancer, particularly mast cell tumors, cases of mast cell tumors in Boxers were solicited and examined.

A 6.5- year-old female Boxer had a growth removed from the left shoulder in April 1998. This growth was diagnosed as a grade II mast cell tumor by routine histopathologic analysis. In early 1999, numerous additional nodules developed rapidly over the entire body in a matter of a few weeks, according to the owner and the veterinarian, and the dog was euthanized. The body was frozen and placed in storage until it could be transferred to Michigan State University, after which it was thawed for study. Postmortem examination revealed multiple round to oval nodules from 10-30 mm in diameter on the skin of the medial and caudal thighs, perineal region, humerus, femur, and thoracic and abdominal walls. Subcutaneous nodules 10-50 mm in diameter were found in the inguinal region (Fig. 1A). Multiple nodules 10-20 mm in diameter were present in the lateral and caudal musculature of the hip. A very large mass about 200 mm in diameter was found in the left subscapular region, approximately the same site from which the original mast cell tumor had been removed; this mass extended deep into the thoracic musculature. Nodules 5-30 mm in diameter were also found in the heart (Fig.

1B), liver (Fig. 1C), kidney (Fig. 1D), and lungs. The mesenteric and mediastinal lymph nodes were enlarged. Samples of nodules from the skin, liver, a lymph node and samples from the large subscapular mass were taken for both microscopic examination and molecular studies.

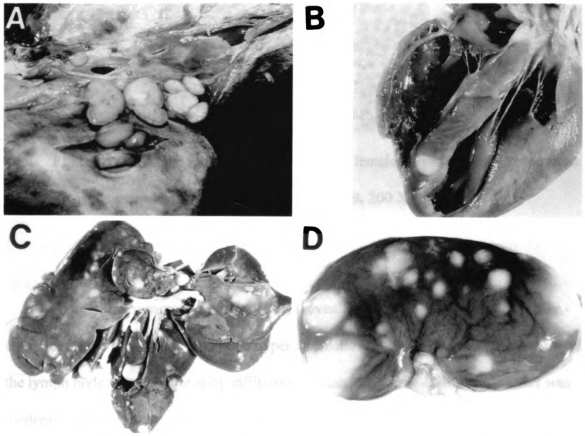


**Figure 1.** Macroscopic lesions observed in a 6.5-year-old female Boxer. Note white, firm nodules of various sizes in inguinal region (**A**), heart (**B**), liver (**C**) and kidney (**D**).

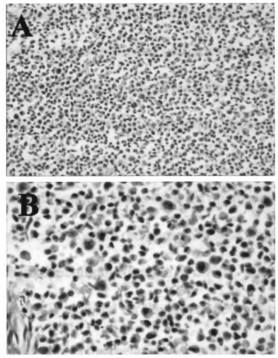


**Figure 2.** Hepatic nodule from a 6.5-year-old female Boxer. Round cells have no intracytoplasmic granules. Giemsa stain. **A.** 100 X. **B.** 200 X.

Histologic examination of the nodules revealed a diffuse infiltration of medium-sized neoplastic round cells with large hyperchromatic nuclei. The normal architecture of the lymph node was obliterated by infiltration of neoplastic cells. The mitotic index was moderate, with an average of 5 mitoses/high-power field. No eosinophils were observed during the microscopic examination. Special stains (Giemsa, toluidine blue) were used, and no mast cell granules were identified (Fig. 2). The absence of granules in sections stained with hematoxylin and eosin and with special stains and the extent and pattern of nodules found during the gross examination resulted in a preliminary diagnosis of malignant round cell tumor, highly suggestive of systemic lymphosarcoma. For

confirmation, immunohistochemical immunophenotyping for B and T lymphocytes was performed. Formalin-fixed, paraffin-embedded sections of neoplastic tissues were tested. Monoclonal antibodies to CD79a for B lymphocytes and polyclonal antibodies to CD3 for T cell lymphocytes were used, with negative results. Molecular testing was therefore utilized in an attempt to clarify the diagnosis.

Tissue samples from the same nodules used for microscopic examination and a sample of spleen that appeared to contain only normal tissue were chosen to search for potential mutations in the juxtamembrane domain of c-*KIT*. The c-*KIT* gene encodes for a receptor tyrosine kinase that is required for the proper development, survival, and maturation of hematopoietic stem cells, melanocytes, and mast cells.[2,12,18] The receptor consists of an extracellular domain of 5 immunoglobulin-like folds and an intracellular kinase domain separated by transmembrane and juxtamembrane domains.[11,19] Point mutations, deletions, and duplications have been identified in the juxtamembrane domain of c-*KIT* in certain canine mast cell tumors and mast cell tumor cell lines.[6,8] Some of these changes have been shown to result in constitutive activation of c-*KIT* in the absence of binding of its normal ligand, alternatively known as Steel factor, mast cell growth factor, or stem cell factor.[2] Activating mutations have also been identified in both human[4] and rodent[14-16] mast cell tumor cell lines, and *in situ* in cases of human mastocytosis associated with other disorders.[7,9] Similar mutations cause factor- independent cell growth and aggressive behavior characteristic of tumor formation in murine cell lines.[5]

Molecular characterization of normal and tumor tissue from this dog was carried out as follows. A guanidinium-based solution (Trizol[a]) was used for the isolation of genomic DNA and total RNA from fresh tissue, following the manufacturer's protocol. Contaminating genomic DNA was removed from the RNA preparation by treatment with RNase-free DNase as previously described[13]. The sample was precipitated in ethanol and resuspended in deionized water to the same volume originally obtained from the extraction procedure. The RNA was then reverse transcribed using random hexamers as primers. A reaction mixture was prepared containing 10 mM DTT, 2.4 μg of random hexamers, 0.32 mM dNTPs, 1X first-strand buffer[a], 8 μL of RNA, and 800 U of Moloney murine leukemia virus reverse transcriptase[a] in 100 μL total volume. All reagents except the first-strand buffer and enzyme were combined and incubated at 70 C for 5 minutes to denature the RNA secondary structure and then placed on ice for 5 minutes. The buffer and enzyme were then added, and the entire mixture was incubated for 1 hour at 37 C, followed by inactivation at 90 C for 5 minutes.

Primers were designed for polymerase chain reaction (PCR) amplification of the juxtamembrane domain of c-*KIT* based upon the published canine sequence (GenBank no. AF099030).[6] Amplifications were performed with the forward primer 5'-ACAAATCCATCCCCACACCCTGTTCAC-3' and the reverse primer 5'-CACTTTCCCGAAGGCACCAGCACCCA-3'. PCR reactions were in a total volume of 25 μL consisting of 1X PCR buffer,[a] 1.5 mM $MgCl_2$, 0.2 mM dNTPs, 20 pmol of each primer, 0.625 U of *Taq* polymerase,[a] and either 3 μL of cDNA template or 5 μL of genomic DNA template. Cycling conditions included an initial denaturation of 4 minutes

at 95 C followed by 35 cycles of 95 C for 1 minute, 66 C for 2 minutes, and 72 C for 3 minutes and a final polymerization step of 8 minutes at 72 C. The expected size of the amplified fragment was 267 bp from cDNA and 645 bp from genomic DNA.

Amplified products were separated on 2% agarose gels in Tris-acetate-ethylenediaminetetraacetic acid (EDTA) buffer and purified using a commercial gel extraction kit.[b] Extracted bands were eluted in 30 μL of 10 mM Tris (pH 8), and 5 μL was used for manual sequencing using a commercial dideoxy kit with $^{33}$P-radiolabelled terminators,[c] using the manufacturer's protocol. For the cDNA fragments, the same primers used for PCR amplification were used for the sequencing. For the genomic DNA templates, an additional internal primer, 5'-GAGGAGATCAATGGAAACAA-3' was used to sequence the entire fragment.

For archived tumors, a slight modification of a microwave-based lysis method[1] was used to extract DNA. A sample of approximately 1-3 mm$^3$ was removed from each paraffin block and placed into 400 μL of a solution of 50 mM Tris (pH 8.5), 1mM EDTA, and 0.5% Tween. The samples were heated to 95 C for 10 minutes and then microwaved twice for 30 seconds each, with vortexing between each heating step. The samples were allowed to cool, and 75 μg of proteinase K was added to each. After incubation overnight at 42 C, the enzyme was inactivated by heating to 95 C for 10 minutes. The samples were centrifuged for 10 minutes at 12,000 rpm in a microcentrifuge, and the supernatant was transferred to a clean tube. The amount of DNA obtained was variable; therefore, multiple dilutions of each sample were tested until PCR was successful. Typical samples amplified correctly at a 1:25 or 1:50 dilution of the

original DNA. This diluted DNA was used for PCR and sequencing as described for DNA from fresh tissue.

Amplification of both cDNA and genomic DNA templates from normal tissue produced a single band of the expected size, whereas tumor tissue produced two bigger bands in addition to the expected band, approximately 30 and 50 bp bigger than expected (Fig. 3). In both cDNA and genomic DNA templates, sequencing of the band from normal tissue confirmed that it contained the normal canine sequence. Sequencing of the

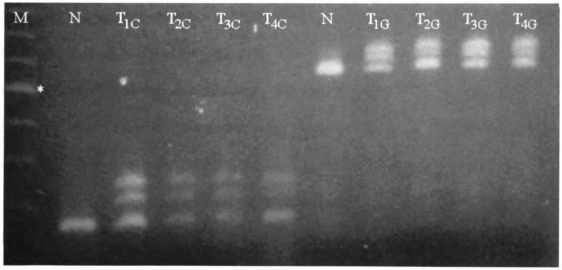


**Figure 3.** Separation of amplified bands from the juxtamembrane domain of c-*KIT* in a female Boxer. Lane 1 contains a 100-bp DNA ladder, with the 600-bp marker (*) to the right. Sample lanes represent PCR products from normal spleen (lanes 2 and 7) and 4 tumor nodules from various locations (lanes 3-6, 8-11). Amplifications from cDNA are shown in lanes 2-6, and those from genomic DNA are in lanes 7-11. M = molecular weight marker; N = normal tissue, T = tumor, with subscripts C and G indicating cDNA and genomic DNA templates, respectively.

3 bands obtained from tumor tissue determined that they represented 1) the normal sequence, 2) a sequence with a 45-bp tandem duplication, and 3) a mixture of the 2 sequences. The duplication was similar to those previously seen in canine mast cell tumors and in approximately the same location, consisting of bases 1721-1765, as per the canine c-KIT sequence.[6] This suggested that the tumor in the presented case was a mast cell tumor rather than a lymphosarcoma, as initially diagnosed.

To test the possibility that such mutations might also occur in lymphosarcomas, paraffin-embedded samples of mast cell tumors and lymphosarcomas, including the original mast cell tumor from the Boxer, were selected from the archives in the Animal Health and Diagnostic Laboratory at Michigan State University. RNA was not obtainable from the tissue blocks; therefore, only genomic DNA was studied for these cases. A total of 31 lymphosarcomas and 15 mast cell tumors were successfully amplified. None of the lymphosarcomas contained duplications in this region of c-*KIT*; however, 2 of the mast cell tumors, including the original mast cell tumor from the Boxer, had tandem duplications. The duplication from the original Boxer tumor was identical to that from fresh tissue in the tumor nodules. It is not known whether or not this particular duplication causes constitutive activation of c-*KIT*; however, it appears that duplications in this region can be used as markers to positively identify mast cell tumors in some cases, regardless of their implication as the cause of the tumor.

The results suggest that the tumor and nodules in this Boxer represent a highly undifferentiated and aggressive mast cell tumor that resembles systemic lymphosarcoma. Highly undifferentiated grade III mast cell tumors have a significantly decreased number of granules;[17] however, the granules in the present tumors were completely absent. To

rule out the possibility that the absence of granules was due to the freezing and thawing process and was not the original state of the tumor, a sample from a newly diagnosed mast cell tumor was subjected to similar conditions of freezing and thawing. No change in granule content was observed in this sample tumor even after 2 months of storage in the freezer, indicating that the tumor in this Boxer most likely never contained granules. Because the presence of granules is often key in the identification of mast cell tumors, it is reasonable to assume that the tumor could have been mistyped as a lymphosarcoma. However, the lymphocyte antigen staining results brought this diagnosis into question. Molecular tests appear to have produced a definitive determination of the actual tumor type seen in this dog. Because the duplication was only seen in tumor DNA and not in normal constitutive DNA, it must have arisen de novo in the tumor and was not an inherited trait. Because it is highly unlikely that 2 independent events would produce identical mutations in 2 different cell types, the current tumors must have been derived from the original tumor and therefore are mast cell tumors.

This case illustrates a potentially beneficial role for the use of molecular tests to aid in diagnosis when the results of conventional tests are in question. The exact test used in this study represents a rare situation that could not occur in all cases because it entailed the identification of a mutation and the availability of a sample from a primary tumor that had been definitively identified. However, results from a larger scale study currently underway appear to indicate that duplications such as that seen in this dog may be common in the more highly aggressive mast cell tumors, suggesting that molecular tests might be useful in these particular cases if the diagnosis is in doubt, even without a previous tumor for comparison. Furthermore, molecular testing may be useful as an

adjunct prognostic indicator and may be important in determining therapeutic options. However, such applications will require further studies. With the increasing number of genetic alterations known or suspected to cause neoplasms, the identification of many different tumor types could be facilitated in the near future by molecular testing.

*Acknowledgements*. We thank the AKC Canine Health Foundation and the Jaqua Foundation for their financial support, Dr. José A. Ramos-Vara (University of Missouri) for performing the lymphocyte antigen tests, and Ms. Marianne Balzer and Dr. Chris Jones for referring this case to our laboratory.

**Sources and manufacturers**

a. Gibco BRL, Gaithersburg, MD.

b. QIAEX II, Qiagen, Valencia, CA.

c. Thermo Sequenase Radiolabelled Terminator Cycle Sequencing Kit, USB, Cleveland, OH.

**References**

1. Banerjee SK, Makdisi WF, Weston AP, Mitchell SM, Campbell DR: 1995, Microwave-based DNA extraction from paraffin-embedded tissue for PCR amplification. Biotechniques 18: 768-70, 772-3.

2. Broudy VC: 1997, Stem cell factor and hematopoiesis. Blood 90: 1345-1364

3. Cohen D, Reif JS, Brodey RS, Keiser H: 1974, Epidemiological analysis of the most prevalent sites and types of canine neoplasia observed in a veterinary hospital. Cancer Res 34: 2859-2868.

4. Furitsu T, Tsujimura T, Tono T, et al.: 1993, Identification of mutations in the coding sequence of the proto-oncogene c-*kit* in a human mast cell leukemia cell line causing ligand-independent activation of c-*kit* product. J Clin Invest 92: 1736-1744.

5. Kitayama H, Kanakura Y, Furitsu T, et al.: 1995, Constitutively activating mutations of c-*kit* receptor tyrosine kinase confer factor-independent growth and tumorigenicity of factor-dependent hematopoietic cell lines. Blood 85: 790-798

6. London CA, Galli SJ, Yuuki T, et al.: 1999, Spontaneous canine mast cell tumors express tandem duplications in the proto-oncogene c-*kit*. Exp Hematol 27: 689-697.

7. Longley BJ, Tyrrell L, Lu S-Z, et al.: 1996, Somatic c-*KIT* activating mutation in urticaria pigmentosa and aggressive mastocytosis: establishment of clonality in a human mast cell neoplasm. Nature Genet 12: 312-314.

8. Ma Y, Longley BJ, Wang X, et al.: 1999, Clustering of activating mutations in c-*KIT*'s juxtamembrane coding region in canine mast cell neoplasms. J Invest Dermatol 112: 165-170.

9. Nagata H, Worobec AS, Oh CK, et al.: 1995, Identification of a point mutation in the catalytic domain of the protooncogene c-*kit* in peripheral blood mononuclear cells of patients who have mastocytosis with an associated hematologic disorder. Proc Natl Acad Sci USA 92: 10560-10564.

10. Priester WA: 1973, Skin tumors in domestic animals. Data from 12 United States and Canadian colleges of veterinary medicine. J Natl Cancer Inst 50: 457-466.

11. Qiu F, Ray P, Brown K, et al.: 1988, Primary structure of c-*kit*: relationship with the CSF-1/PDGF receptor kinase family - oncogenic activation of v-*kit* involves deletion of extracellular domain and C terminus. EMBO J 7: 1003-1011.

12. Serve H, Yee NS, Stella G, et al.: 1995, Differential roles of PI3-kinase and Kit tyrosine 821 in Kit receptor-mediated proliferation, survival and cell adhesion in mast cells. EMBO J 14: 473-483.

13. Tabor S and Struhl K: 1989, Endonucleases. *In:* Current protocols in molecular biology, ed. Ausubel FM, Brent R, Kingston RE, et al., vol. 1, pp. 3.12.5-3.12.6. John Wiley & Sons, New York, NY.

14. Tsujimura T, Furitsu T, Morimoto M, et al: 1994, Ligand-independent activation of c-*kit* receptor tyrosine kinase in a murine mastocytoma cell line P-815 generated by a point mutation. Blood 83: 2619-2626.

15. Tsujimura T, Furitsu T, Morimoto M, et al.: 1995, Substitution of an aspartic acid results in constitutive activation of c-*kit* receptor tyrosine kinase in a rat tumor mast cell line RBL-2H3. Int Arch Allergy Immunol 106: 377-385.

16. Tsujimura T, Morimoto M, Hashimoto K, et al.: 1996, Constitutive activation of c-*kit* in FMA3 murine mastocytoma cells caused by deletion of seven amino acids at the juxtamembrane domain. Blood 87: 273-283.

17. Vail DM: 1996, Mast cell tumors. *In:* Small animal clinical oncology, eds. Withrow SJ, MacEwen EG, 2nd ed., pp. 192-210. WB Saunders, Philadelphia, PA.

18. Valent P, Spanblöchl E, Sperr WR, et al.: 1992, Induction of human mast cells from bone marrow and peripheral blood mononuclear cells by recombinant human stem cell factor / *kit*-ligand in long-term culture. Blood 80: 2237-2245.

19. Yarden Y, Kuang W-J, Yang-Feng T, et al.: 1987, Human proto-oncogene c-*kit*: a new cell surface receptor tyrosine kinase for an unidentified ligand. EMBO J 6: 3341-3351.

# CHAPTER 6

Zemke D, Yamini B, Yuzbasiyan-Gurkan V. Mutations in the Juxtamembrane Domain of c-*KIT* are Associated with Higher Grade Mast Cell Tumors in Dogs. Vet Pathol 39:529-535, 2002.

**Abstract.** Mast cell tumors are among the most commonly seen tumors of the skin in dogs and are more highly aggressive than mast cell tumors of other species. Some breeds display a markedly higher incidence of mast cell tumor development than others and appear to have some genetic predisposition. Recently, mutations have been found in canine mast cell tumor tissues and cell lines within the juxtamembrane domain of the proto-oncogene c-*KIT*. In previous studies utilizing a small number of cases, no association between the presence of a mutation and the breed of dog or grade of the tumor could be identified. An expanded study with a larger sample set was performed in order to explore this possibility. The juxtamembrane domain of c-*KIT* was amplified using the polymerase chain reaction from genomic DNA preparations of 88 paraffin-embedded mast cell tumors from selected breeds. Mutations, consisting of duplications and deletions, were found in 12 of the tumors. A significant association was found between the presence of a mutation and a higher grade of tumor but not between breed and grade or between breed and the presence of a mutation.

*Key words:* c-kit receptor; dogs; DNA; mastocytoma; mutation; polymerase chain reaction; sequence analysis; single nucleotide polymorphism.

Mast cell tumors are one of the most frequently seen skin neoplasms in dogs, accounting for up to 21% of cases.[5,12,18] Most of these tumors are benign, developing slowly and persisting for years without increasing in size or metastasizing. However, a large number are highly aggressive and present a significant threat to canine health.[18] In contrast, mast cell tumors in humans are rare and usually benign.[18] Some dog breeds appear to be at relatively little risk, whereas others such as the Boxer have been reported to have a high incidence of mast cell tumor development.[5] This difference among breeds indicates a possible genetic influence on both susceptibility to tumors and tumor aggressiveness.

Mast cell tumors are usually graded on a histologic scale.[11] Grade I tumors are highly differentiated, with regular nuclei, rare or no mitotic figures, and a large number of metachromatic granules. They are generally considered to be benign. Grade III tumors are highly undifferentiated, with large misshapen nuclei, many mitotic figures, and few cytoplasmic granules. This is the most aggressive of the three grades. Grade II tumors are intermediate between the other two types. Mast cell tumors are often also identified by clinical stage based on the extent of their growth. Incompletely excised tumors are designated stage 0, single tumors without and with lymph node involvement are designated stage I and stage II, respectively, multiple tumors comprise stage III, and recurrent or metastatic tumors make up stage IV.[18] Both histologic grading and clinical staging are good predictive factors for the final outcome.[18]

The genes involved in the development of mast cell tumors are currently under study. Analyses of human[7] and rodent[15-17] mast cell tumor cell lines have revealed a

number of mutations in the proto-oncogene c-*KIT*. The c-*KIT* gene encodes for a cell surface receptor, which upon binding of its cognate ligand induces a signal transduction cascade responsible for the development, maturation, and survival of many cell lineages, including hematopoietic stem cells, melanocytes, and mast cells.[3,14,19] The c-*KIT* receptor consists of an extracellular domain of five immunoglobulin-like loops and an intracellular tyrosine kinase domain.[13,20] Mutations in the kinase domain or the neighboring juxtamembrane domain have been shown to cause constitutive activation of c-*KIT* in the absence of ligand binding. Constitutive activation of c-*KIT* in certain murine cell lines leads to the uncontrolled cell growth and aggressive behavior typical of tumor development.[8] The mutations identified to date in humans and rodents are confined to the kinase and juxtamembrane domains of c-*KIT* and consist of point mutations and small deletions. Many of these mutations cause constitutive activation of c-*KIT* in vitro and some have been identified in situ.

Mutations in canine c-*KIT* have only recently been identified, and all have been found exclusively in the juxtamembrane domain. Ma et al.[10] discovered point mutations and small deletions in three of seven tumors and a duplication in two of three cell lines. London et al.[9] found duplications in 5 of 11 tumors; however, they did not see any of the other types of mutations. Although the duplications encompassed approximately the same area of c-*KIT*, no two were identical. Both groups found mutations in approximately 50% of the animals studied. In a recent study, 2 of 15 mast cell tumors tested contained juxtamembrane domain duplications, and in one of these dogs, a recurrence of a tumor with the exact same duplication allowed molecular confirmation of the tumor type when the diagnosis based on pathology was questionable.[21] Because

duplications in the juxtamembrane domain of c-*KIT* as seen in canine mast cell tumors have not been identified in any other species to date, these duplications may be related in some way to the increased aggressiveness of these tumors in dogs. In the previous studies, the limited number of animals involved made it impossible to accurately determine the percentage of canine mast cell tumors with detectable mutations or to identify any correlation between the type of mutation seen and the breed of dog or the aggressiveness of the tumor. The present study of c-*KIT* duplications was conducted on a much larger scale to determine the significance of these mutations.

## Materials and Methods

### Sample selection

Mast cell tumor cases were selected from tissue samples submitted to the Michigan State University Animal Health and Diagnostic Laboratory (AHDL) during the period of 1998-1999. Cases were selected from breeds with the highest number of cases so that differences between breeds could be examined. The Boxer and Boston Terrier were chosen based on their suspected predisposition for mast cell tumors, whereas the Labrador Retriever, Golden Retriever, and mixed-breed dogs were not suspected to be predisposed and were chosen for comparison. The 15 dogs from the preliminary study were included; this group consisted of a Pit Bull in addition to the breeds listed above. For each dog, a single block of formalin-fixed, paraffin-embedded tumor tissue was retrieved from the AHDL archives.

**Paraffin block DNA isolation**

Sections of each block were cut and stained with hematoxylin and eosin. Stained sections were examined under a microscope by a certified veterinary pathologist (B. Yamini) to determine the borders of the tumor, which were marked on the block. A small piece of tissue approximately 2 mm in diameter was excised from each block within the boundaries of the tumor. DNA was isolated by a modified version of a previously described method.[1] The tissue was placed into 400 μL of digestion buffer (50 mM Tris, pH 8.5, 1 mM ethylenediaminetetraacetic acid (EDTA), 0.5% Tween). The paraffin in the samples was melted by heating at 95 C for 10 minutes and heating for 30 seconds twice in a microwave at full power, with thorough vortexing after each heating step. The samples were allowed to cool, and 5 μL of 15 mg/mL proteinase K was added to each. The samples were then incubated at 42 C overnight or until the piece of tissue was completely digested. The proteinase K was inactivated by heating at 95 C for 10 minutes, and the samples were centrifuged at 12,000 rpm in a microcentrifuge for 10 minutes. An aliquot of 200 μL was then transferred to a clean tube, avoiding the transfer of paraffin.

**Amplification of the juxtamembrane region of c-*KIT***

For each sample, the undiluted DNA preparation and dilutions of 1:10, 1:25, and 1:50 were used as templates for polymerase chain reaction (PCR) amplification of the juxtamembrane domain of c-*KIT*. PCRs with a total volume of 25 μL were set up using 5 μL of template, 20 pmol of each primer, 0.625 U *Taq* polymerase (Gibco BRL), and final

concentrations of 100 μM dNTPs, 1.5 mM $MgCl_2$, 50 mM Tris-Cl (pH 8.3), and 10 mM KCl. Amplification was performed using primers JuxtF and JuxtR (Fig. 1). PCR conditions consisted of an initial denaturation step of 4 minutes at 94 C, followed by 35 cycles of 1 minute at 94 C, 2 minutes at 66 C, and 3 minutes at 72 C, and a final extension step of 8 minutes at 72 C.

**Purification of amplification products**

The PCR amplification products were separated on 2% agarose gels in Tris-acetate-EDTA buffer. Individual bands were stabbed with a pipette tip and transferred to 15 μL of water, 5 μL of which was used as a template in an additional PCR with the same conditions as the initial amplification. The secondary amplification products were separated on 2% agarose gels, and the resulting bands were excised and purified using the QIAEX II kit (Qiagen) following the manufacturer's protocol, with each sample resuspended in a final volume of 30 μL of 10 mM Tris, pH 8.

**Sequencing of purified bands**

Manual sequencing was performed using the Thermo Sequenase radiolabelled terminator cycle sequencing kit (USB). Samples were sequenced from both the JuxtF and JuxtR primers used for PCR amplification, plus an internal primer JuxtM (Fig. 1). Sequencing followed the manufacturer's standard protocol for the dGTP termination mix except for an annealing temperature of 50 C, using 5 μL of template DNA and 0.5 pmol of primer per sample. The reaction products were separated on 6% denaturing polyacrylamide gels and visualized by exposure to x-ray film.

**Fig. 1.** Genomic sequence of the juxtamembrane domain of canine c-*KIT* and flanking regions (amino acids 518-606). The amino acid sequence of the exons is given beneath the DNA sequence. Single nucleotide polymorphisms are shown in boxed letters (R = A or G; Y = C or T; K = G or T). Primers used for amplification and sequencing are shown in bold type, with arrows indicating the direction of the primer. Exon sequences are shown in uppercase letters; intron sequences are in lowercase letters. Deletions are denoted by open bars; duplications are denoted by solid bars.

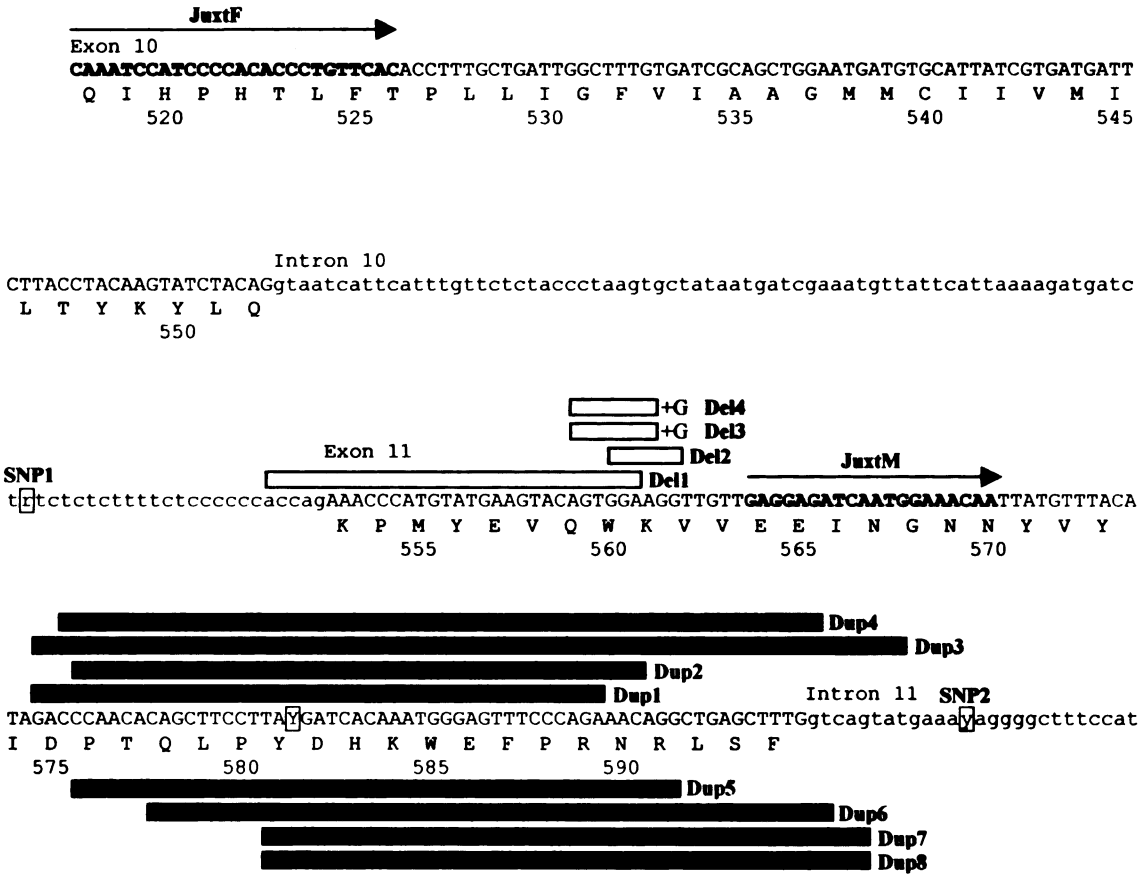
JuxtF
Exon 10
CAAATCCATCCCCACACCCTGTTCACACCTTTGCTGATTGGCTTTGTGATCGCAGCTGGAATGATGTGCATTATCGTGATGATT
Q I H P H T L F T P L L I G F V I A A G M M C I I V M I
520 525 530 535 540 545
Intron 10
CTTACCTACAAGTATCTACAGgtaatcattcatttgttctctaccctaagtgctataatgatcgaaatgttattcattaaaagatgatc
L T Y K Y L Q
550
+G Del4
+G Del3
Del2
Exon 11
Del1
JuxtM
SNP1
trtctctcttttctcccccaccagAAACCCATGTATGAAGTACAGTGGAAGGTTGTTGAGGAGATCAATGGAAACAATTATGTTTACA
K P M Y E V Q W K V V E E I N G N N Y V Y
555 560 565 570
Dup4
Dup3
Dup2
Dup1
Intron 11 SNP2
TAGACCCAACACAGCTTCCTTAYGATCACAAATGGGAGTTTCCCAGAAACAGGCTGAGCTTTGgtcagtatgaaaygaggggctttccat
I D P T Q L P Y D H K W E F P R N R L S F
575 580 585 590
Dup5
Dup6
Dup7
Dup8
gtaacctttttgtgtacgtgtaacaatgactttagggaaccccattagcttcctttgttctgttccaactgagacaataagtattttct
SNP3
SNP4
gtgaagtttcatcaytttttgatagattcckcataaagcaccttatagagaaatgtccttagctggatttgtccttaattccttaacaat
SNP5
Exon 12
tccttgattgttgactttgaaattacccagatgctcctttggtcctaycaccacccccttactcttttcttcctttctgcagGGAAAACT
G K T
595
JuxtR
TTGGGTGCTGGTGCCTTCGGGAAAGTG
L G A G A F G K V
600 605

Automated sequencing was performed on an ABI Prism 377 DNA Sequencer using Big Dye terminators. Samples were sequenced from JuxtF and, when readable length produced was insufficient, JuxtM. Cycle sequencing was performed using 10 μL of template DNA and 3.2 pmol of primer per sample, following the manufacturer's protocol. Unincorporated terminators were removed by isopropanol precipitation following the manufacturer's protocol, except for the addition of 1 μL of 20 mg/mL glycogen as a carrier. Samples were resuspended in 4 μL of loading dye, 2 μL of which was loaded onto the gel.

**Results**

The juxtamembrane domain of c-*KIT* was successfully amplified from a total of 88 canine mast cell tumor cases. The number of dogs of each breed and the grade distribution of tumors within those breeds is shown in Table 1. PCR amplification revealed that 8 of the 88 cases contained two larger bands in addition to the expected band when separated on agarose gels, indicating possible duplications. An additional case also contained two extra bands, one below and one above the expected band, indicating a possible deletion. All bands from these cases were purified and sequenced manually. For each sample, the three bands represented the normal sequence, either a duplication or deletion, and a mixture of the two sequences. Figure 2 shows an example of a duplication and a deletion as seen on an agarose gel. The remaining samples were sequenced either manually or with an automated sequencer to screen for mutations too small to be seen as separate bands. Three additional deletions were found during the course of this sequencing.

**Table 1.** Grade distribution of mast cell tumors in various dog breeds.

| Breed | No. Tumors | Grade I | Grade II | Grade III |
|---|---|---|---|---|
| Boston Terrier | 8 | 2 | 6 | 0 |
| Boxer | 29 | 7 | 20 | 2 |
| Golden Retriever | 13 | 1 | 10 | 2 |
| Labrador Retriever | 18 | 6 | 11 | 1 |
| Pit Bull | 1 | 1 | 0 | 0 |
| Mixed Breed | 19 | 7 | 11 | 1 |

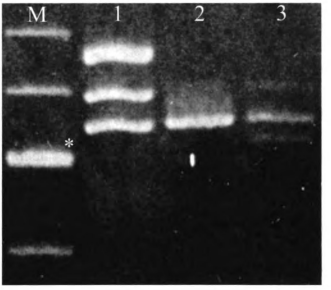


**Fig. 2.** Agarose gel showing products obtained by amplification of the juxtamembrane region of c-*KIT* from different sources. Lane M contains a 100 bp DNA ladder. The 600-bp band is marked with an asterisk. For lane 1, the lower band contains normal sequence and the middle band contains a 45-bp duplication (Dup2). The upper band is a heteroduplex of normal and mutant sequence. Lane 2 is an example of amplification from normal tissue. In lane 3, the lower band contains a 30-bp deletion (Del1), the middle band is normal, and the upper band is a heteroduplex of normal and mutant sequence.

Figure 1 shows a portion of the juxtamembrane domain sequence (GenBank accession Nos. AF448146, AF448147, and AF448148) with the positions of the duplications indicated. The duplications were all in frame, ranged in size from 44 to 69 base pairs (bp), and were located near the 3' end of exon 11, with five of them (Dup3, Dup4, Dup6, Dup7, Dup8) extending into the neighboring intron 11. In two of the dogs, the duplicated sequences (Dup7 and Dup8) were identical. Three of the duplications cause tandem repeats within the protein sequence: Dup1, residues $Asp_{575}$ - $Arg_{589}$; Dup2, residues $Pro_{576}$ - $Asn_{590}$; Dup5, residues $Pro_{576}$ - $Arg_{591}$. Dup4 resulted in the insertion of a Gly residue after $Phe_{594}$, followed by a direct repeat of residues $Pro_{576}$ - $Phe_{594}$. The numbering of the amino acid residues is based on the normal canine c-*KIT* cDNA sequence (GenBank accession No. AF448148). The remaining four duplications involve duplication of part or all of the consensus splice sequence at the 5' end of intron 11, creating the potential for alternative splicing events. For all four duplications, no change to the protein is made if the upstream site is used. If the downstream site is used, then Dup3 causes an insertion of Gly-Gln-Tyr plus a repeat of residues $Asp_{575}$ - $Phe_{594}$, Dup6 causes an insertion of Gly plus a repeat of residues $Gln_{578}$ - $Phe_{594}$, and Dup7/Dup8 cause an insertion of Gly-Gln plus a repeat of residues $Tyr_{581}$ - $Phe_{594}$, with the insertion occurring after $Phe_{594}$ in all four cases. RNA studies are required to determine the splicing pattern in these tumors.

Figure 1 also shows the location of the identified deletions. Del1 encompasses 30 bp, including the last few bases of intron 10 and part of the 5' end of exon 11. Because the deletion removes part of the 3' splice site sequence for intron 10, the exact effect of

this deletion on the protein is not known. If the first AG following the deletion is used for splicing, the result would be a deletion of $Lys_{553}$ - $Lys_{561}$; however, other potential splice acceptors are present in the area. A study of the RNA from such cases is necessary to determine which of these sites, if any, is used. Del2 removes 6 bp and causes the substitution of a Phe residue for $Trp_{560}$ - $Val_{562}$ in the protein sequence. Del3 and Del4 remove 7 bp but are followed by the insertion of a single G, so no frameshift is created. They cause the substitution of an Arg residue for $Gln_{559}$ - $Lys_{561}$.

The distributions of the different mutation types by breed and tumor grade are shown in Tables 2 and 3. None of the mutations identified were from grade I tumors. All of the deletions were found within grade II tumors, and equal numbers of duplications were found in grade II and grade III tumors. The mutation frequencies for the three grades were significantly different from each other as determined by a minimum chi-square analysis ($\chi^2 = 21.68$, 95% confidence level = 9.49). With respect to breed, two of the four deletions were found in Labrador Retrievers (Table 3). Half of the duplications were identified in Boxers, and the remaining half consisted of single tumors in each of the other breeds. No significant association was seen between presence of a mutation and the breed of dog ($\chi^2 = 6.06$, 95% confidence level = 18.31).

**Table 2.** Grade distribution of duplications and deletions in c-*KIT* among canine mast cell tumors.

| Grade | No. Tumors | Duplications | Deletions |
|---|---|---|---|
| I | 24 | 0 | 0 |
| II | 58 | 4 | 4 |
| III | 6 | 4 | 0 |

**Table 3.** Distribution of duplications and deletions in c-*KIT* among different dog breeds.

| Breed | No. Tumors | Duplications | Deletions |
|---|---|---|---|
| Boston Terrier | 8 | 1* | 1* |
| Boxer | 29 | 4† | 0 |
| Golden Retriever | 13 | 1‡ | 1‡ |
| Labrador Retriever | 18 | 1§ | 2§ |
| Pit Bull | 1 | 0 | 0 |
| Mixed Breed | 19 | 1‖ | 0 |

* Dup5 and Del1
† Dup2, Dup3, Dup7, Dup8
‡ Dup6 and Del4
§ Dup4, Del2, Del3
‖ Dup1

During the course of sequencing work on c-*KIT* for this and other projects, a number of single nucleotide polymorphisms (SNPs) were found throughout the gene, six of which are located in the region shown in Figure 1. Five of these SNPs are located in introns and have no effect on the protein. The allele frequencies of the SNPs among 61 of the dogs in this study were evaluated and determined to be 35.2% A + 64.8% G for SNP1, 49.2%T + 50.8% C for SNP2, 48.4% C + 51.6% T for SNP3, 48.4% G + 51.6% T for SNP4, and 47.5% C + 52.5% T for SNP5. The sixth SNP is located within exon 11, but is silent, causing no amino acid change. The allele frequency of this SNP was 24.6% T + 75.4% C.

## Discussion

Duplications and deletions of sufficient size can readily be distinguished by agarose gel electrophoresis (Fig. 2). The smaller 6 or 7-bp deletions were only

identifiable by direct sequencing. All of the duplications and the largest of the deletions identified in this study produced a pattern of three bands similar to the examples in Figure 2. The lower two bands represent the normal and mutant sequences, indicating that the tumors were heterozygous for their respective mutations. The uppermost band represents heteroduplexes containing one strand each of normal and mutant DNA, as determined by sequencing. In heteroduplexes, unpaired bases in one of the strands form a bulge in the DNA, which retards the migration of the heteroduplexes during electrophoresis and causes them to appear as if they were larger fragments.[2]

The results of this study suggest that there is a relationship between tumor grade and the presence of c-*KIT* juxtamembrane domain mutations, particularly duplications. No mutations were found in any of the grade I tumors tested, and <10% of the grade II tumors had mutations (Table 2). Among grade III tumors, however, four of six contained mutations in the juxtamembrane domain. Equal numbers of duplications were seen in grade II and grade III tumors, in spite of the fact that nearly 10 times more grade II tumors than grade III tumors were tested. Juxtamembrane duplications appear to be associated with only the most aggressive tumors.

With respect to breed, there does not appear to be an association between the presence of mutations and the breed of dog in which they were identified (Table 3), and no significant association was observed between breed and tumor grade ($\chi^2 = 7.97$, 95% confidence level = 18.31). This finding is in contrast to those of previous studies in which a higher percentage of mast cell tumors in Boxers were of a low grade as compared with other breeds. A compilation of records for all cases submitted to AHDL during 1999 revealed that the tumor grade distribution in Boxers was nearly identical to

that seen in mixed-breed dogs. Of 69 mast cell tumors in Boxers, 29.0% were grade I, 62.3% grade II, and 8.7% grade III. The distribution for 99 mixed-breed dogs was 29.3% grade I, 62.6% grade II, and 8.1% grade III.

In both of the previous studies, the canine mastocytoma cell line C2 containing a c-*KIT* juxtamembrane domain duplication exhibited constitutive phosphorylation of c-*KIT*.[9,10] Because the duplications identified in this study all overlap with the duplication found in that cell line, the present duplications probably also would cause activation of c-*KIT*. Mouse cell lines with c-*KIT*-activating mutations can induce growth behavior typical of tumor formation.[8] Uncontrolled growth seen in tumors should be expected when a receptor regulating cell growth is constitutively active. This finding implicates the duplications found in this study as potential causes of the aggressiveness of the tumors in which they were identified. The role of the deletions requires further investigation.

In the present study, approximately 13.6% of canine mast cell tumors tested contained mutations within the coding region for the juxtamembrane domain of c-*KIT*. This frequency is much lower than those reported by Ma et al.,[10] who found mutations in three of seven tumors and two of three cell lines, and London et al.,[9] who found duplications in 5 of 11 tumors. Our study was based upon a larger sample set, which is less susceptible to ascertainment bias, and tumors of all grades were included. London et al.[9] studied only grade II tumors, some of which may have been at the higher end of that range (borderline grade III). If that were the case, our finding of mutations in four of six grade III tumors would agree more closely with the results of London et al. The grades of the tumors studied by Ma et al. were not reported.[10]

A significant portion of canine mast cell tumors currently have no identified genetic defect in the juxtamembrane domain of c-*KIT*. In addition to the possibility that other genes are involved, there is also the chance that some of these tumors may contain other mutations in c-*KIT*. In this study and that of London et al.,[9] only the juxtamembrane domain was screened for mutations; however, Ma et al.[10] also tested the phosphotransferase domain. The phosphotransferase domain of c-*KIT* has been reported to harbor mutations in some human[7] and rodent[15-17] mast cell tumors. In addition to the duplications and deletions, our identification of numerous SNPs in c-*KIT*, both in the juxtamembrane domain and in other regions of the c-*KIT* gene, suggests that c-*KIT* as a whole may be a hotspot for mutations in dogs, with the potential for mutations in mast cell tumors outside of the juxtamembrane domain.

Our finding of c-*KIT* mutations in grade II and grade III but not grade I tumors indicates that c-*KIT* may be a good marker for tumor status and suggests a role for c-*KIT* in at least part of the tumorigenic process, providing a potential target for intervention. Tyrosine kinase inhibitors are currently in development for treatment of a number of cancer types. Very recently, one of these tyrosine kinase inhibitors, STI-571[6] (Gleevec, Novartis Pharmaceuticals), has been approved by the Food and Drug Administration for the treatment of chronic myologenous leukemia (CML) in humans. In CML, a translocation causes a hybrid tyrosine kinase made up of parts of the genes *bcr* and *abl* to be constitutively active.[6] This drug may also be a good inhibitor of c-*KIT*.[4] c-*KIT* inhibitors such as these and others could be used on tumors both with and without mutations to evaluate their effect on tumor growth and their potential as therapeutic agents. We are planning to launch such studies at the molecular and cellular level,

followed by clinical studies. If reduced tumor growth were observed, c-*KIT* activation, such as that caused by these mutations, would be considered important for the development of mast cell tumors. These findings would pave the way for an additional medical treatment for the management of these tumors.

**Acknowledgements**

We thank Dr. Joseph Hauptman for assistance with the statistical analyses. This work was funded in part by the Jaqua Foundation, the Animal Health and Diagnostic Laboratory, and the Elizabeth Eddy Fund of Michigan State University.

**References**

1. Banerjee SK, Makdisi WF, Weston AP, Mitchell SM, Campbell DR: Microwave-based DNA extraction from paraffin-embedded tissue for PCR amplification. Biotechniques **18:**768-73, 1995

2. Bhattacharyya A, Lilley, DMJ: The contrasting structures of mismatched DNA sequences containing looped-out bases (bulges) and multiple mismatches (bubbles). Nucleic Acids Res **17:**6821-6840, 1989

3. Broudy VC: Stem cell factor and hematopoiesis. Blood **90:**1345-1364, 1997

4. Buchdunger E, Cioffi CL, Law N, Stover D, Ohno-Jones S, Druker BJ, Lydon NB: Abl protein-tyrosine kinase inhibitor STI571 inhibits in vitro signal transduction mediated by c-Kit and platelet-derived growth factor receptors. J Pharm Exp Ther **295:**139-145, 2000

5. Cohen D, Reif JS, Brodey RS, Keiser H: Epidemiological analysis of the most prevalent sites and types of canine neoplasia observed in a veterinary hospital. Cancer Res **34:**2859-2868, 1974

6. Druker BJ, Lydon NB: Lessons learned from the development of an Abl tyrosine kinase inhibitor for chronic myelogenous leukemia. J Clin Invest **105:**3-7, 2000

7. Furitsu T, Tsujimura T, Tono T, Ikeda H, Kitayama H, Koshimizu U, Sugahara H, Butterfield JH, Ashman LK, Kanayama Y, Matsuzawa Y, Kitamura Y, Kanakura Y: Identification of mutations in the coding sequence of the proto-oncogene c-*kit* in a human mast cell leukemia cell line causing ligand-independent activation of c-*kit* product. J Clin Invest **92:**1736-1744, 1993

8. Kitayama H, Kanakura Y, Furitsu T, Tsujimura T, Oritani K, Ikeda H, Sugahara H, Mitsui H, Kanayama Y, Kitamura Y, Matsuzawa Y: Constitutively activating mutations of c-*kit* receptor tyrosine kinase confer factor-independent growth and tumorigenicity of factor-dependent hematopoietic cell lines. Blood **85:**790-798, 1995

9. London CA, Galli SJ, Yuuki T, Hu Z, Helfand SC, Geissler EN: Spontaneous canine mast cell tumors express tandem duplications in the proto-oncogene c-*kit*. Exp Hematol **27:**689-697, 1999

10. Ma Y, Longley BJ, Wang X, Blount JL, Langley K, Caughey GH: Clustering of activating mutations in c-*KIT*'s juxtamembrane coding region in canine mast cell neoplasms. J Invest Dermatol **112:**165-170, 1999

11. Patnaik AK, Ehler WJ, MacEwen EG: Canine cutaneous mast cell tumor: morphologic grading and survival time in 83 dogs. Vet Pathol **21:**469-474, 1984

12. Priester WA: Skin tumors in domestic animals. Data from 12 United States and Canadian colleges of veterinary medicine. J Natl Cancer Inst **50:**457-466, 1973

13. Qiu F, Ray P, Brown K, Barker PE, Jhanwar S, Ruddle FH, Besmer P: Primary structure of c-*kit*: relationship with the CSF-1/PDGF receptor kinase family - oncogenic activation of v-*kit* involves deletion of extracellular domain and C terminus. EMBO J **7:**1003-1011, 1988

14. Serve H, Yee NS, Stella G, Sepp-Lorenzino L, Tan JC, Besmer P: Differential roles of PI3-kinase and Kit tyrosine 821 in Kit receptor-mediated proliferation, survival and cell adhesion in mast cells. EMBO J **14:**473-483, 1995

15. Tsujimura T, Furitsu T, Morimoto M, Isozaki K, Nomura S, Matsuzawa Y, Kitamura Y, Kanakura Y: Ligand-independent activation of c-*kit* receptor tyrosine kinase in a murine mastocytoma cell line P-815 generated by a point mutation. Blood **83:**2619-2626, 1994

16. Tsujimura T, Furitsu T, Morimoto M, Kanayama Y, Nomura S, Matsuzawa Y, Kitamura Y, Kanakura Y: Substitution of an aspartic acid results in constitutive activation of c-*kit* receptor tyrosine kinase in a rat tumor mast cell line RBL-2H3. Int Arch Allergy Immunol **106**:377-385, 1995

17. Tsujimura T, Morimoto M, Hashimoto K, Moriyama Y, Kitayama H, Matsuzawa Y, Kitamura Y, Kanakura Y: Constitutive activation of c-*kit* in FMA3 murine mastocytoma cells caused by deletion of seven amino acids at the juxtamembrane domain. Blood **87**:273-283, 1996

18. Vail DM: Mast cell tumors. *In:* Small Animal Clinical Oncology, eds. Withrow SJ, MacEwen EG, 2nd ed., pp. 192-210. W.B. Saunders, Philadelphia, 1996

19. Valent P, Spanblöchl E, Sperr WR, Sillaber C, Zsebo KM, Agis H, Strobl H, Geissler K, Bettelheim P, Lechner K: Induction of human mast cells from bone marrow and peripheral blood mononuclear cells by recombinant human stem cell factor / *kit*-ligand in long-term culture. Blood **80**:2237-2245, 1992

20. Yarden Y, Kuang W, Yang-Feng T, Coussens L, Munemitsu S, Dull TJ, Chen E, Schlessinger J, Francke U, Ullrich A: Human proto-oncogene c-*kit*: a new cell surface receptor tyrosine kinase for an unidentified ligand. EMBO J **6**:3341-3351, 1987

21. Zemke D, Yamini B, Yuzbasiyan-Gurkan V: Characterization of an Undifferentiated Malignancy as a Mast Cell Tumor Using Mutation Analysis in the Proto-oncogene c-*KIT*. J Vet Diagn Invest **13**:341-345, 2001

Request reprints from Dr. Yuzbasiyan-Gurkan, D-208 Veterinary Medical Center,

Michigan State University, East Lansing, MI 48824-1314, (USA).

E-mail: yuzbasiyan@cvm.msu.edu

# CHAPTER 7

# SUMMARY, CONCLUSIONS, AND FUTURE DIRECTIONS

The genes examined in this study have multiple roles and affect different cell types, meaning that defects in these genes could have effects on many systems of the body. These genes share a common role in the development and maintenance of melanocytes, cells that control pigmentation in many parts of the body and that were hypothesized to also be involved in some aspect of normal hearing. The examination of these genes in dogs with hereditary hearing loss found no mutations within the coding regions. In the *MITF* gene, splice sites were also evaluated and no mutations were found. Future studies will involve examination of the splice sites in the *EDNRB* and *KIT* genes, for which intronic sequences have been obtained. The absence of mutations within the genes studied reduces the likelihood that any of them are involved in hereditary deafness in the breeds studied, although important regions of these genes outside of the coding region have yet to be studied. The involvement of *EDNRB* and *KIT* in deafness in the Jack Russell Terrier is particularly unlikely given the lack of an association between deafness and markers within these genes. This breed shows inheritance of the piebald allele at the canine spotting locus. In addition to the spotting locus, the merle locus is also possibly linked with deafness in dogs. The Catahoula Leopard Dog, which shows inheritance of the merle locus, is currently being tested with these markers to determine whether they are associated with deafness in that breed.

Although no potential cause for deafness was found, the study of these genes identified several features that may be useful for future studies. The *EDNRB* and *MITF* genes had not been sequenced in the dog prior to this study, and probable errors in the published sequences of *KIT* were identified. Furthermore, polymorphisms were found within the *EDNRB* and *KIT* genes. These polymorphisms can be used as markers both

for linkage studies and for mapping of the genes. Using a polymorphism found in *EDNRB*, this gene was mapped to canine Chromosome 22.[9] Mapping efforts are currently underway for *KIT* and *MITF*. The study of these genes also identified other interesting sequence features, namely a potential pseudogene for *MITF* and a sequence variation in *EDNRB* that is currently unexplained. Further examination of these features is important for the full characterization of these genes.

Besides melanocytes, the *KIT* gene is also important for the development of mast cells. Investigation of this gene has determined that mutations within it are found in some mast cell tumors in the dog. Most of these mutations involved duplications of a particular region of the gene and are predicted to cause constitutive activation of the receptor. This study provided evidence for association of these mutations with high grade tumors. Any role that *KIT* possible plays in deafness is probably unrelated to mast cell tumors. Deafness, and the lack of pigmentation that is associated with it, are most likely the result of a loss of function in a particular gene. Mast cell tumors, on the other hand, appear to involve the constitutive activation of KIT.[5,6] Another group has recently published a study of mast cell tumors in a number of dogs and also found that duplications were more frequent in high grade tumors.[2] However, this difference was not determined to be significant. Further studies are necessary to determine the role of such mutations in mast cell tumors. In fact, a prospective study is being planned incorporating mutation studies in *KIT*, studies of proliferation markers and other histological attributes, and the biological behavior of mast cell tumors in dogs.

The identification of duplication events at the same site in independent cases is of interest. While it is likely that these events are selected for, the exact nature of how

duplications within this particular region of *KIT* are generated is currently unknown. An oncogene that was identified in a feline sarcoma virus shows considerable homology to a portion of the *KIT* gene.[1] The duplications found in *KIT* are in approximately the same region where this viral homology exists.[6] It is possible that sequences mediating recombination exist in this area and are responsible for the creation of duplications. This does not explain, however, why the majority of the duplications have different endpoints from each other. It also does not explain the deletions found in this study that lie upstream of this region. The effect of these mutations in *KIT* and their role in mast cell tumor development is also unclear. Studies have shown that one canine mast cell tumor cell line with a *KIT* duplication exhibits constitutive phosphorylation of the receptor.[6,8] This is likely to be true for other duplications in the same region as well. The juxtamembrane domain has been proposed to contain an α-helix that inhibits receptor phosphorylation.[7] Duplications may disrupt this structure and lead to activation. The effect of deletions in this region is not known at present. Activating mutations of *KIT* in other species have been shown to result in tumor formation.[5] These mutations differ in type and location from those seen in the dog, however. The phosphotransferase domain of *KIT*, one location where these mutations are seen in other species, was found not to contain mutations in canine tumors.[8] Future evaluation of such mutations in experimental systems will need to be carried out to further define the role of such mutations in mast cell tumor development and behavior.

In the mouse, mutations in the *Mitf* gene are responsible for the microphthalmia phenotype.[4] Many of the known *Mitf* alleles result in abnormal pigmentation.

Depending on the particular allele, the phenotype may also include microphthalmia, deafness, or other abnormalities.[11] Microphthalmia is prevalent in a number of dog breeds, including those that have inherited the merle trait, and can be associated with white coat color and deafness.[3] Based on the similarity to the mouse phenotype, it is possible that microphthalmia in the dog is also due to mutations in the *MITF* gene. This gene is currently being screened in dogs from a number of affected breeds to determine if this is the case. The microphthalmia black-eyed white allele in mice is the result of the insertion of a LINE element within one of the introns of *Mitf*.[12] It has been suggested that the merle trait in dogs may be due to a transposable element.[10] It is possible that this may also be responsible for deafness and microphthalmia in these dogs. As well as the coding region and the splice sites, efforts should be made to obtain full sequences for the introns, so that they can be examined as well.

Besides the genes involved in this study, focus should also be placed on other candidate genes for deafness. The *PAX3* gene was originally included in this study, however difficulties prevented sufficient progress from being obtained. The *EDN3* gene was also attempted without success. Work should be continued on these genes, and other genes such as *SOX10* should be investigated as well. Genes that modify the activity of the current candidiates should be studied. Attempts should also be made to build a pedigree of dogs with deafness that could be used for linkage studies. With linkage results, positional cloning could be employed and the number of candidate genes to be studied should be reduced. It would also allow the identification of candidates that so far have not presented themselves. With the current state of knowledge of the canine genome and the number of genetic markers being produced, this is far more feasible now

than it was when this study was initiated. Finally, the examination of the candidate genes to this point has been primarily at the sequence level. Studies of expression and large-scale genomic studies such as Northern and Southern blots should be performed to determine whether other levels are involved in deafness.

## References


1. Besmer P, Murphy JE, George PC, Qiu F, Bergold PJ, Lederman L, Snyder HW Jr, Brodeur D, Zuckerman EE, Hardy WD. A new acute transforming feline retrovirus and relationship of its oncogene v-*kit* with the protein kinase gene family. Nature 320:415, 1986.

2. Downing S, Chien MB, Kass PH, Moore PE, London CA. Prevalence and importance of internal tandem duplications in exons 11 and 12 of c-*kit* in mast cell tumors of dogs. Am J Vet Res 63:1718-1723, 2002.

3. Gwin RM, Wyman M, Lim DJ, Ketring K Jr, Werling K. Multiple ocular defects associated with partial albinism and deafness in the dog. J Am Anim Hosp Assoc 17:401-408, 1981.

4. Hodgkinson CA, Moore KJ, Nakayama A, Steingrímsson E, Copeland NG, Jenkins NA, Arnheiter H. Mutations at the mouse microphthalmia locus are associated with defects in a gene encoding a novel basic-helix-loop-helix-zipper protein. Cell 74:395-404, 1993.

5. Kitayama H, Kanakura Y, Furitsu T, Tsujimura T, Oritani K, Ikeda H, Sugahara H, Mitsui H, Kanayama Y, Kitamura Y, Matsuzawa Y. Constitutively activating mutations of c-*kit* receptor tyrosine kinase confer factor-independent growth and tumorigenicity of factor-dependent hematopoietic cell lines. Blood 85:790-798, 1995.

6. London CA, Galli SJ, Yuuki T, Hu ZQ, Helfand SC, Geissler EN. Spontaneous canine mast cell tumors express tandem duplications in the proto-oncogene c-*kit*. Exp Hematol 27:689-697, 1999.

7. Ma Y, Cunningham ME, Wang X, Ghosh I, Regan L, Longley BJ. Inhibition of spontaneous receptor phosphorylation by residues in a putative α-helix in the KIT intracellular juxtamembrane region. J Biol Chem 274:13399-13402, 1999.

8. Ma Y, Longley BJ, Wang X, Blount JL, Langley K, Caughey GH. Clustering of activating mutations in *c-KIT*'s juxtamembrane coding region in canine mast cell neoplasms. J Invest Dermatol 112:165-170, 1999.

9. Schmutz SM, Moker JS, Yuzbasiyan-Gurkan V, Zemke D, Sampson J, Lingaas F, Dunner S, Dolf G. DCT and EDNRB map to DogMap linkage group L07. Anim Genet 32:321, 2001.

10. Sponenberg DP. Germinal reversion of the merle allele in Australian shepherd dogs. J Hered 75:78, 1984.

11. Steingrímsson E, Moore KJ, Lamoreux ML, Ferré-D'Amaré AR, Burley SK, Zimring DCS, Skow LC, Hodgkinson CA, Arnheiter H, Copeland NG, Jenkins NA. Molecular basis of mouse *microphthalmia* (*mi*) mutations helps explain their developmental and phenotypic consequences. Nat Genet 8:256-263, 1994.

12. Yajima I, Sato S, Kimura T, Yasumoto K, Shibahara S, Goding CR, Yamamoto H. An L1 element intronic insertion in the black-eyed white (Mitf[mi-bw]) gene: the loss of a single Mitf isoform responsible for the pigmentary defect and inner ear deafness. Hum Mol Genet 8:1431-1441, 1999.

# CHAPTER 8

# MATERIALS AND METHODS

**Genomic DNA Isolation From Tissue**

Genomic DNA was obtained from frozen tissues using either a guanidine isothiocyanate solution (Trizol, Gibco BRL) or a guanidine-detergent solution (DNAzol, Gibco BRL).

For isolation with Trizol, approximately 200-400 mg of tissue was homogenized in 3 mL of Trizol with a glass homogenizer and allowed to sit for 5 minutes at room temperature. The homogenized tissue was split into 4 microcentrifuge tubes and 150 µL of chloroform was added to each. The tubes were shaken by hand for 15 seconds, allowed to sit for 3 minutes at room temperature, and then centrifuged at 4 °C for 15 minutes at 12,000 rpm. The upper phase was removed and the lower two phases were mixed with 225 µL of 95% ethanol by inversion. The samples were allowed to sit for 3 minutes at room temperature, then centrifuged at 4 °C for 5 minutes at 2000 rpm. The supernatant was removed and 750 µL of 0.1 M sodium citrate in 10% ethanol was added. The samples were allowed to sit for 30 minutes at room temperature with periodic mixing by inversion, then centrifuged at 4 °C for 5 minutes at 2000 rpm. The supernatant was removed and a second wash with the sodium citrate solution was performed. After removal of the supernatant, 1.5 mL of 75% ethanol was added to each pellet, allowed to sit for 20 minutes at room temperature with periodic mixing by inversion, then centrifuged at 4 °C for 5 minutes at 2000 rpm. The supernatant was removed, the pellets were air-dried for 10 minutes, and then resuspended in 300 µL of 8 mM NaOH. The 4 tubes were then combined for a total volume of 1.2 mL of DNA from each tissue sample.

. For isolation with DNAzol, approximately 50-100 mg of tissue was homogenized in 1 mL of DNAzol with a glass homogenizer in as few strokes as possible.

The homogenized tissue was transferred to a microcentrifuge tube and spun at 4 °C for 10 minutes at 10,000 rpm. The supernatant was transferred to a clean tube and mixed with 500 µL of 95% ethanol by inversion. The sample was allowed to sit for three minutes at room temperature, then a pipette tip was used to spool up the DNA and transfer it to a clean tube. The DNA was washed twice by adding 1 mL of 75% ethanol, mixing by inversion, allowing the DNA to settle to the bottom of the tube by gravity, then removing the supernatant. The pellet was air-dried for a few seconds and resuspended in 1 mL of 8 mM NaOH.

**Genomic DNA Isolation From Cheek Swabs**

A sterile cytology brush was placed between the lip and gum and used to brush the inside surface of the cheek for approximately 15 seconds. The brush was then stored in the original packaging until the DNA was isolated. The tip of each swab was cut off and placed into a microcentrifuge tube containing 600 µL of 50 mM NaOH. The tube was mixed by vortexing, heated at 95 °C for 5 minutes, and mixed again. The tube was spun briefly, followed by the addition of 60 µL of 1 M Tris, pH 8.

**Total RNA Isolation**

Total RNA was isolated from frozen tissues using a solution of guanidine isothiocyanate and phenol (Trizol, Gibco BRL). Approximately 200-400 mg of tissue was homogenized in 3 mL of Trizol with a glass homogenizer and allowed to sit for 5 minutes at room temperature. The homogenized tissue was split into 4 microcentrifuge tubes and 150 µL of chloroform was added to each. The tubes were shaken by hand for

15 seconds, allowed to sit for 3 minutes at room temperature, and then centrifuged at 4 °C for 15 minutes at 12,000 rpm. The upper phase was transferred to a clean tube and 375 μL of isopropanol was added. The samples were mixed by inversion, allowed to sit for 10 minutes at room temperature, then centrifuged at 4 °C for 10 minutes at 12,000 rpm. The supernatant was removed and 750 μL of 75% ethanol was added to each pellet. The samples were mixed by vortexing and centifuged at 4 °C for 5 minutes at 7500 rpm. The supernatant was removed, the pellets were air-dried for 10 minutes, and were resuspended in 75 μL of water each. The 4 tubes were then combined for a total volume of 300 μL total RNA from each tissue sample.

**DNase Treatment of Total RNA Samples**

A 400 μL reaction mixture was set up containing 300 μL RNA, 50 mM Tris pH 7.5, 10 mM $MgCl_2$, 50 μg/mL bovine serum albumin, and 40 U RNase-free DNase I (Boehringer Mannheim). The mixture was incubated for 30 minutes at 37 °C, then ethanol precipitated and resuspended in 300 μL deionized water.

**Reverse Transcription**

A 76 μL reaction mixture was prepared containing 10 mM DTT, 2.4 μg random hexamers, 0.32 mM dNTPs, and 8 μL of RNA. This mixture was incubated at 70 °C for 5 minutes to denature the RNA secondary structure, then placed on ice for 5 minutes. After incubation on ice, 20 μL first strand buffer and 800 U MMLV reverse transcriptase (Gibco BRL) were added for a total volume of 100 μL, and the entire mixture was incubated for 1 hour at 37 °C, followed by inactivation at 90 °C for 5 minutes.

**Polymerase Chain Reaction**

Standard PCR reactions had a total volume of 25 μL and contained 20 pmol of each primer, 0.625 U *Taq* polymerase (Gibco BRL/Invitrogen), and final concentrations of 100 μM dNTPs, 1.5 mM $MgCl_2$, 50 mM Tris-Cl (pH 8.3), and 10 mM KCl. Typically, 3 μL of template were used for amplification from cDNA and 5 μL of template were used for amplification from genomic DNA. Standard PCR conditions consisted of an initial denaturation step of 4 minutes at 94 °C, followed by 35 cycles of 1 minute at 94 °C, 2 minutes at the appropriate annealing temperature, and 3 minutes at 72 °C, with a final extension step of 8 minutes at 72 °C.

**Gel Purification of Amplified Bands**

Amplification products were separated on agarose gels, and the resulting bands were excised. DNA was isolated from the excised gel slices using a system based on silica beads and chaotropic salts (QIAEX II, Qiagen). Each gel slice was placed into a microcentrifuge tube, to which 500 μL of buffer QX1 and 5 μL of beads were added. The samples were incubated for 10 minutes at 55 °C, with mixing by vortexing every 2 minutes. The samples were then spun briefly in a microcentrifuge at maximum speed. The supernatant was removed, the pellet was resuspended in 500 μL of buffer QX1 by vortexing, and the sample was spun briefly again. This step was repeated two more times using buffer QX2. The supernatant was removed, the pellet was air-dried for 10 minutes, then resuspended in 30 μL of 10 mM Tris, pH 8 by vortexing. The sample was allowed to sit at room temperature for 5 minutes then spun briefly in a microcentrifuge at maximum speed. The supernatant containing DNA was then transferred to a clean tube.

**Sequencing of Purified DNA**

Manual sequencing was performed based on a modified version of the Sanger sequencing method using dideoxy terminators labeled with $^{33}P$ (Thermo Sequenase kit, USB). A 20 μL reaction mixture was prepared containing 5-15 μL of template DNA, 2 μL of reaction buffer, 0.5 pmol of primer, and 2 μL of Thermo Sequenase enzyme. A 4.5 μL aliquot of this mixture was transferred to each of 4 separate tubes containing 2 μL of dNTP solution and 0.5 μL (approximately 225 nCi) of labeled ddNTP. The samples were cycled for 30 cycles of 95 °C for 30 seconds, 50 °C for 30 seconds, and 72 °C for 1 minute. In the case of template sequences containing sequence compressions, a dNTP solution containing dITP instead of dGTP was used and the samples were cycled at 95 °C for 30 seconds, 50 °C for 30 seconds, and 60 °C for 10 minutes. The reaction products were mixed with 4 μL of stop solution, denatured at 70 °C for 2-10 minutes, and 4 μL of each was electrophoresed on a 6% polyacrylamide/7 M urea gel at a constant 60 W. The gel was transferred onto Whatman 3MM paper, dried under vacuum at 80 °C, and visualized by exposure to x-ray film.

Automated sequencing was performed by the author on an ABI Prism 377 DNA Sequencer using Big Dye terminators. A 20 μL sequencing reaction was prepared containing 8 μL of the Big Dye reaction mix, 5-10 μL of template DNA, and 3.2 pmol of primer. Samples were cycled for 25 cycles of 96 °C for 30 seconds, 50 °C for 15 seconds, and 60 °C for 4 minutes. Unincorporated terminators were removed by precipitation with 75% isopropanol plus 1 μL of 20 mg/mL glycogen as a carrier. A solution of 25 mM EDTA pH 8 + 50 mg/mL blue dextran was mixed with 5 volumes of

deionized formamide to create a loading buffer. Each sample was resuspended in 8 μL of loading buffer, denatured for 2 minutes at 95 °C, and a 1.5 μL aliquot was loaded onto the gel.

**Preparation of Radioactive Probes by the Incorporation of $^{32}$P-labeled dCTP**

A 28 μL mixture containing 9.6 μg of random DNA hexamers and 200 ng of probe DNA was boiled for 3 minutes then placed on ice. To this sample, 5 μL of a mixture containing 0.5 mM each of dGTP, dATP, and dTTP was added. Next, 5 μL of Klenow buffer, 8 U of Klenow fragment, and 50 μCi $^{32}$P-labeled dCTP were added and the reaction brought up to a total volume of 50 μL. The reaction was incubated for 4 hours at 37 °C, then stopped by the addition of 2 μL 0.5 M EDTA and 200 μL TE.

**DNA Isolation From BAC Clones**

A bacterial stock containing each clone was used to inoculate 2 mL of LB broth containing 20 μg/mL chloramphenicol, which was incubated at 37 °C overnight with shaking at 250 rpm. The overnight cultures were spun at 1000 G for 10 minutes at room temperature, and the cell pellet was resuspended in 300 μL of 15 mM Tris pH 8, 10 mM EDTA, 100 μg/mL RNase. To each sample, 300 μL of 0.2 N NaOH, 1% SDS was added. Each tube was mixed by inversion and placed at room temperature for 5 minutes. This was followed by the addition of 300 μL of 3 M KOAc pH 5.5 to each tube, mixing by inversion, and incubation on ice for 5 minutes. The samples were spun at 12,000 rpm for 10 minutes in a microcentrifuge at 4 °C. The supernatant was transferred to a tube containing 0.8 mL of ice-cold isopropanol. The samples were mixed by inversion,

incubated on ice for 5 minutes, then spun for 15 minutes at 4 °C. The supernatant was removed and the pellets were washed with 500 µL of 70% ethanol, then spun at for 5 minutes at 4 °C, followed by removal of the supernatant. The pellets were air dried and resuspended in 40 µL TE.

**Genomic DNA Isolation From Paraffin-Embedded Mast Cell Tumors**

Sections of the embedded tumor were stained with haematoxylin and eosin, and viewed by a veterinary pathologist to determine the borders of the tumor. DNA was isolated from the tumors by a microwave-based method similar to that initially developed by Banerjee, *et al.* A modified protocol was developed that is summarized as follows. A small piece of tissue approximately 2 mm in diameter was excised from each block within the boundaries of the tumor. The tissue was placed into 400 µL of digestion buffer (50 mM Tris pH 8.5, 1 mM EDTA, 0.5% Tween). The paraffin in the samples was melted by heating them to 95 °C for 10 minutes, then heating for 30 seconds twice in a microwave at full power, mixing thoroughly by vortexing after each heating step. The samples were allowed to cool, and 5 µL of 15 mg/mL proteinase K was added to each. The samples were then incubated at 42 °C overnight or until the piece of tissue was completely digested. The proteinase K was inactivated by heating at 95 °C for 10 minutes, and the samples were centrifuged at 12,000 rpm in a microcentrifuge for 10 minutes. An aliquot of 200 µL was then transferred to a clean tube, avoiding the transfer of paraffin as best as possible.

# APPENDIX

# APPENDIX A

Schmutz SM, Moker JS, Yuzbasiyan-Gurkan V, Zemke D, Sampson J, Lingaas F, Dunner S, Dolf G. DCT and EDNRB map to DogMap linkage group L07. Anim Genet 32:321, 2001.

*Source/description:* Dopachrome tautomerase (dopachrome-isomerase, tyrosine-related protein 2) is the gene referred to as slaty in the mouse[1] which is thought to dilute eumelanin from black to grey[2].

*Primer sequences:* Published dog primer sequences for a microsatellite in an intron of DCT[3] were used. EDNRB[4], CXX.279[5], FH2109[6], and LEI005[7], were also genotyped and mapped to the L07 linkage group[8].

*Chromosomal location:*

All the DogMap families[8] were genotyped for this purpose by various members. CRI-MAP was used to analyse linkage data. DCT was found to be linked to all four markers previously mapped to L07 with a LOD > 3. The sex averaged map generated by CRI-MAP was CXX.279 - LEI005 - DCT - FH2109 - EDNRB. DCT maps to human chromosome 13q31-q32[9], to mouse chromosome 14[1], to cattle chromosome 12[10], and to pig 11[11]. EDNRB, another coat colour gene, has also been mapped to cattle chromosome 12q22 by in situ hybridization[12] and to human 13q22-q31[13].

Recently painting of dog chromosomes with human chromosome-specific paints and painting of human chromosomes with dog-specifc chromosome paints[14,15] suggests human 13q21-qter is homologous to the entirety of dog chromosome 22. At the ISAG 2000 meeting, the DogMap workshop endorsed the chromosome numbering system proposed by the International Committee for the Standardization of the dog Karyotype[14].

Therefore, the linkage mapping of DCT reported here suggests that L07 from the DogMap studies is assigned to dog chromosome 22.

*Comment:* An autosomal recessive disease, Black Hair Follicular Dysplasia which alters black pigmented hair to grey in addition to other abnormalities, did not segregate concordantly with DCT in a family of Large Munsterlanders affected with this condition[10]. EDNRB alleles did not segregate with pups that were plated (recessive) vs. ticked (dominant) following the terminology of Little[16] for T locus phenotypes.

*Acknowledgements:* The Natural Science and Engineering Research Council provided funding in Canada and the AKC Canine Health Foundation provided funding in the USA.

**References**

1 Jackson I.J. *et al.* (1992) *EMBO* **11**, 527-35.

2 Budd P. & Jackson I.J. (1995) *Genomics* **29**, 35-43.

3 Liu P.-C. *et al.* (1998) *Anim Genet* **29**, 327.

4 Zemke D. & Yuzbasiyan-Gurkan V. (1999) *Anim Genet* **30**, 390.

5 Ostrander E. *et al.* (1993) *Genomics* **16**, 207-13.

6 Francisco L.V. *et al.* (1996) *Mamm Genome* **7**, 359-62.

7 Lingaas F. *et al.* (1997) *Mamm Genome* **8**, 218-21.

8 Lingaas F. *et al.* (2001) *J Anim Breed Genet* **118**, 3-19.

9 Sturm R.A. *et al.* (1994) *Genomics* **21**, 293-6.

10 Schmutz S.M. *et al.* (1998) *Can Vet J* **39**, 644-6.

11 Chowdhary B.P. *et al.* (1993) *Chromosome Res* **1**, 175-9.

12 Schläpfer J. *et al.* (1997) *Mamm Genome* **8**, 380-1.

13 Cyr C. *et al.* (1991) *Biochem Biophys Res Commun* **181**, 184-90.

14 Breen M. *et al.* (1999) *Genomics* **61**, 141-55.

15 Yang F. *et al.* (1999) *Genomics* **62**, 189-202.

16 Little C.C. (1957) *The Inheritance of Coat Color in Dogs*. Howell, New York.

*Correspondence:* S. Schmutz (e-mail: schmutz@sask.usask.ca)

# REFERENCES

Amae S, Fuse N, Yasumoto K, Sato S, Yajima I, Yamamoto H, Udono T, Durlu YK, Tamai M, Takahashi K, Shibahara S. Identification of a novel isoform of microphthalmia-associated transcription factor that is enriched in retinal pigment epithelium. Biochem Biophys Res Commun 247:710-715, 1998.

American Kennel Club. The complete dog book, 19th ed., pp. 19-23. Howell Book House, New York, NY, 1997.

Amiel J, Attié T, Jan D, Pelet A, Edery P, Bidaud C, Lacombe D, Tam P, Simeoni J, Flori E, Nihoul-Fékété C, Munnich A, Lyonnet S. Heterozygous endothelin receptor B (EDNRB) mutations in isolated Hirschsprung disease. Hum Mol Genet 5:355-357, 1996.

Anderson DM, Williams DE, Tushinski R, Gimpel S, Eisenman J, Cannizzaro LA, Aronson M, Croce CM, Huebner K, Cosman D, Lyman SD. Alternate splicing of mRNAs encoding human mast cell growth factor and localization of the gene to chromosome 12q22-q24. Cell Growth Differ 2:373-378, 1991.

Anderson H, Henricson B, Lundquist PG, Wedenberg E, Wersall J. Genetic hearing impairment in the Dalmatian dog. Acta Otolaryngol (Stockh) Suppl 232:1-34, 1968.

Arai H, Nakao K, Takaya K, Hosoda K, Ogawa Y, Nakanishi S, Imura H. The human endothelin-B receptor gene. Structural organization and chromosomal assignment. J Biol Chem 268:3463-3470, 1993.

Asher JH Jr, Friedman TB. Mouse and hamster mutants as models for Waardenburg syndromes in humans. J Med Genet 27:618-626, 1990.

Attié T, Till M, Pelet A, Amiel J, Edery P, Boutrand L, Munnich A, Lyonnet S. Mutation of the endothelin-receptor B gene in Waardenburg-Hirschsprung disease. Hum Mol Genet 4:2407-2409, 1995.

Banerjee SK, Makdisi WF, Weston AP, Mitchell SM, Campbell DR. Microwave-based DNA extraction from paraffin-embedded tissue for PCR amplification. Biotechniques 18:768-773, 1995.

Besmer P, Murphy JE, George PC, Qiu F, Bergold PJ, Lederman L, Snyder HW Jr, Brodeur D, Zuckerman EE, Hardy WD. A new acute transforming feline retrovirus and relationship of its oncogene v-*kit* with the protein kinase gene family. Nature 320:415, 1986.

Bhattacharyya A, Lilley DM. The contrasting structures of mismatched DNA sequences containing looped-out bases (bulges) and multiple mismatches (bubbles). Nucleic Acids Res 17:6821-6840, 1989.

Bondurand N, Pingault V, Goerich DE, Lemort N, Sock E, Caignec CL, Wegner M, Goossens M. Interaction among *SOX10*, *PAX3* and *MITF*, three genes altered in Waardenburg syndrome. Hum Mol Genet 9:1907-1917, 2000.

Brizzi MF, Dentelli P, Rosso A, Yarden Y, Pegoraro L. STAT protein recruitment and activation in c-Kit deletion mutants. J Biol Chem 274:16965-16972, 1999.

Brooks DP, DePalma PD, Pullen M, Gellai M, Nambi P. Identification and function of putative $ET_B$ receptor subtypes in the dog kidney. J Cardiovasc Pharmacol 26 Suppl 3:S322-S325, 1995.

Brooks M, Sargan DR. Genetic aspects of disease in dogs. *In:* The genetics of the dog, ed. Ruvinsky A, Sampson J, pp. 191-266. CABI, New York, NY, 2001.

Broudy VC. Stem cell factor and hematopoiesis. Blood 90:1345-1364, 1997.

Buchdunger E, Cioffi CL, Law N, Stover D, Ohno-Jones S, Druker BJ, Lydon NB. Abl protein-tyrosine kinase inhibitor STI571 inhibits in vitro signal transduction mediated by c-kit and platelet-derived growth factor receptors. J Pharmacol Exp Ther 295:139-145, 2000.

Budd PS, Jackson IJ. Structure of the mouse tyrosinase-related protein-2/dopachrome tautomerase (*Tyrp2/Dct*) gene and sequence of two novel slaty alleles. Genomics 29:35-43, 1995.

Canine Radiation Mapping Project, Universite de Rennesl, France. World Wide Web URL: http://www-recomgen.univ-rennes1.fr/Dogs/maquette.html. Retrieved January 6, 2003.

Cattanach B. The 'dalmatian dilemma': white coat colour and deafness. J Small Anim Pract 40:193-200, 1999.

Ceccherini I, Zhang AL, Matera I, Yang G, Devoto M, Romeo G, Cass DT. Interstitial deletion of the endothelin-B receptor gene in the spotting lethal (sl) rat. Hum Mol Genet 4:2089-2096, 1995.

Cheng HF, Su YM, Yeh JR, Chang KJ. Alternative transcript of the nonselective-type endothelin receptor from rat brain. Mol Pharmacol 44:533-538, 1993.

Cohen D, Reif JS, Brodey RS, Keiser H. Epidemiological analysis of the most prevalent sites and types of canine neoplasia observed in a veterinary hospital. Cancer Res 34:2859-2868, 1974.

Copeland NG, Gilbert DJ, Cho BC, Donovan PJ, Jenkins NA, Cosman D, Anderson D, Lyman SD, Williams DE. Mast cell growth factor maps near the steel locus on mouse chromosome 10 and is deleted in a number of steel alleles. Cell 63:175-183, 1990.

d'Auriol L, Mattei MG, Andre C, Galibert F. Localization of the human c-*kit* protooncogene on the q11-q12 region of chromosome 4. Hum Genet 78:374-376, 1988.

Deol MS. The origin of the acoustic ganglion and effects of the gene dominant spotting ($W^V$) in the mouse. J Embryol Exp Morph 23:773-784, 1970.

Downing S, Chien MB, Kass PH, Moore PE, London CA. Prevalence and importance of internal tandem duplications in exons 11 and 12 of c-*kit* in mast cell tumors of dogs. Am J Vet Res 63:1718-1723, 2002.

Druker BJ, Lydon NB. Lessons learned from the development of an abl tyrosine kinase inhibitor for chronic myelogenous leukemia. J Clin Invest 105:3-7, 2000.

Elshourbagy NA, Korman DR, Wu HL, Sylvester DR, Lee JA, Nuthalaganti P, Bergsma DJ, Kumar CS, Nambi P. Molecular characterization and regulation of the human endothelin receptors. J Biol Chem 268:3873-3879, 1993.

Evans HE. The ear. *In:* Miller's anatomy of the dog, ed. Evans HE, Miller ME, 3rd ed., pp. 988-1008. WB Saunders, Philadelphia, PA, 1993.

Famula TR, Oberbauer AM, Sousa CA. A threshold model analysis of deafness in Dalmatians. Mamm Genome 7:650-653, 1996.

Fischel-Ghodsian N, Falk RE. Deafness. *In:* Emery and Rimoin's Principles and Practice of Medical Genetics, ed. Rimoin DL, Connor JM, Pyeritz RE, 3rd ed., vol. I, pp. 1149-1170. Churchill Livingstone, New York, NY, 1996.

Flanagan JG, Leder P. The *kit* ligand: a cell surface molecule altered in Steel mutant fibroblasts. Cell 63:185-194, 1990.

Furitsu T, Tsujimura T, Tono T, Ikeda H, Kitayama H, Koshimizu U, Sugahara H, Butterfield JH, Ashman LK, Kanayama Y, Matsuzawa Y, Kitamura Y, Kanakura Y. Identification of mutations in the coding sequence of the proto-oncogene c-*kit* in a human mast cell leukemia cell line causing ligand-independent activation of c-*kit* product. J Clin Invest 92:1736-1744, 1993.

Fuse N, Yasumoto K, Takeda K, Amae S, Yoshizawa M, Udono T, Takahashi K, Tamai M, Tomita Y, Tachibana M, Shibahara S. Molecular cloning of cDNA encoding a novel microphthalmia-associated transcription factor isoform with a distinct amino-terminus. J Biochem (Tokyo) 126:1043-1051, 1999.

Geissler EN, Ryan MA, Housman DE. The dominant-white spotting (*W*) locus of the mouse encodes the c-*kit* proto-oncogene. Cell 55:185-192, 1988.

Geneste O, Bidaud C, De Vita G, Hofstra RMW, Tartare-Deckert S, Buys CHCM, Lenoir GM, Santoro M, Billaud M. Two distinct mutations of the RET receptor causing Hirschsprung's disease impair the binding of signalling effectors to a multifunctional docking site. Hum Mol Genet 8:1989-1999, 1999.

Giebel LB, Spritz RA. Mutation of the *KIT* (mast/stem cell growth factor receptor) protooncogene in human piebaldism. Proc Natl Acad Sci U S A 88:8696-8699, 1991.

Giuffra E, Evans G, Törnsten A, Wales R, Day A, Looft H, Plastow G, Andersson L. The Belt mutation in pigs is an allele at the Dominant white (*I/KIT*) locus. Mamm Genome 10:1132-1136, 1999.

Greibrokk T. Hereditary deafness in the Dalmatian: relationship to eye and coat color. J Am Anim Hosp Assoc 30:170-176, 1994.

Gwin RM, Wyman M, Lim DJ, Ketring K Jr, Werling K. Multiple ocular defects associated with partial albinism and deafness in the dog. J Am Anim Hosp Assoc 17:401-408, 1981.

Halaban R, Moellmann G. White mutants in mice shedding light on humans. J Invest Dermatol 100(2 Suppl):176S-185S, 1993.

Hemesath TJ, Price ER, Takemoto C, Badalian T, Fisher DE. MAP kinase links the transcription factor Microphthalmia to c-Kit signalling in melanocytes. Nature 391:298-301, 1998.

Hodgkinson CA, Moore KJ, Nakayama A, Steingrímsson E, Copeland NG, Jenkins NA, Arnheiter H. Mutations at the mouse microphthalmia locus are associated with defects in a gene encoding a novel basic-helix-loop-helix-zipper protein. Cell 74:395-404, 1993.

Hofstra RMW, Osinga J, Tan-Sindhunata G, Wu Y, Kamsteeg EJ, Stulp RP, van Ravenswaaij-Arts C, Majoor-Krakauer D, Angrist M, Chakravarti A, Meijers C, Buys CHCM. A homozygous mutation in the endothelin-3 gene associated with a combined Waardenburg type 2 and Hirschsprung phenotype (Shah-Waardenburg syndrome). Nat Genet 12:445-447, 1996.

Holliday TA, Nelson HJ, Williams DC, Willits N. Unilateral and bilateral brainstem auditory-evoked response abnormalities in 900 Dalmatian dogs. J Vet Intern Med 6:166-174, 1992.

Hosoda K, Hammer RE, Richardson JA, Baynash AG, Cheung JC, Giaid A, Yanagisawa M. Targeted and natural (piebald-lethal) mutations of endothelin-B receptor gene produce megacolon associated with spotted coat color in mice. Cell 79:1267-1276, 1994.

Igarashi M, Alford BR, Cohn AM, Saito R, Watanabe T. Inner ear anomalies in dogs. Ann Otol Rhinol Laryngol 81:249-255, 1972.

Johnsson LG, Hawkins JE Jr, Muraski AA, Preston RE. Vascular anatomy and pathology of the cochlea in Dalmatian dogs. *In:* Vascular Disorders and Hearing Defects, ed. de Lorenzo AJD, pp. 249-295. University Park Press, Baltimore, MD, 1973.

Kapur RP, Sweetser DA, Doggett B, Siebert JR, Palmiter RD. Intercellular signals downstream of endothelin receptor-B mediate colonization of the large intestine by enteric neuroblasts. Development 121:3787-3795, 1995.

Karne S, Jayawickreme CK, Lerner MR. Cloning and characterization of an endothelin-3 specific receptor (ETC receptor) from Xenopus laevis dermal melanophores. J Biol Chem 268:19126-19133, 1993.

Kitayama H, Kanakura Y, Furitsu T, Tsujimura T, Oritani K, Ikeda H, Sugahara H, Mitsui H, Kanayama Y, Kitamura Y, Matsuzawa Y. Constitutively activating mutations of c-*kit* receptor tyrosine kinase confer factor-independent growth and tumorigenicity of factor-dependent hematopoietic cell lines. Blood 85:790-798, 1995.

Lahav R, Ziller C, Dupin E, Le Douarin NM. Endothelin 3 promotes neural crest cell proliferation and mediates a vast increase in melanocyte number in culture. Proc Natl Acad Sci U S A 93:3892-3897, 1996.

Lahav R, Heffner G, Patterson PH. An endothelin receptor B antagonist inhibits growth and induces cell death in human melanoma cells *in vitro* and *in vivo*. Proc Natl Acad Sci U S A 96:11496-11500, 1999.

Lecoin L, Sakurai T, Ngo MT, Abe Y, Yanagisawa M, Le Douarin NM. Cloning and characterization of a novel endothelin receptor subtype in the avian class. Proc Natl Acad Sci U S A 95:3024-3029, 1998.

Liu PC, Chen YW, Shibuya H, Katz ML, Lubahn DB, Johnson GS. A polymorphic (GA)n microsatellite in an intron of the canine endothelin-B receptor gene. Anim Genet 29:236, 1998.

London CA, Galli SJ, Yuuki T, Hu ZQ, Helfand SC, Geissler EN. Spontaneous canine mast cell tumors express tandem duplications in the proto-oncogene c-*kit*. Exp Hematol 27:689-697, 1999.

Longley BJ, Tyrrell L, Lu SZ, Ma YS, Langley K, Ding TG, Duffy T, Jacobs P, Tang LH, Modlin I. Somatic c-*KIT* activating mutation in urticaria pigmentosa and aggressive mastocytosis: establishment of clonality in a human mast cell neoplasm. Nat Genet 12:312-314, 1996.

Lurie MH. The membranous labyrinth in the congenitally deaf Collie and Dalmatian dog. Laryngoscope 58:279-287, 1948.

Ma Y, Cunningham ME, Wang X, Ghosh I, Regan L, Longley BJ. Inhibition of spontaneous receptor phosphorylation by residues in a putative α-helix in the KIT intracellular juxtamembrane region. J Biol Chem 274:13399-13402, 1999.

Ma Y, Longley BJ, Wang X, Blount JL, Langley K, Caughey GH. Clustering of activating mutations in *c-KIT*'s juxtamembrane coding region in canine mast cell neoplasms. J Invest Dermatol 112:165-170, 1999.

Marklund S, Kijas J, Rodriguez-Martinez H, Rönnstrand L, Funa K, Moller M, Lange D, Edfors-Lilja I, Andersson L. Molecular basis for the dominant white phenotype in the domestic pig. Genome Res 8:826-833, 1998.

Marklund S, Moller M, Sandberg K, Andersson L. Close association between sequence polymorphism in the KIT gene and the roan coat color in horses. Mamm Genome 10:283-288, 1999.

Martin FH, Suggs SV, Langley KE, Lu HS, Ting J, Okino KH, Morris CF, McNiece IK, Jacobsen FW, Mendiaz EA, Birkett NC, Smith KA, Johnson MJ, Parker VP, Flores JC, Patel AC, Fisher EF, Erjavec HO, Herrera CJ, Wypych J, Sachdev RK, Pope JA, Leslie I, Wen D, Lin C, Cupples RL, Zsebo KM. Primary structure and functional expression of rat and human stem cell factor DNAs. Cell 63:203-211, 1990.

Masaki T, Ninomiya H, Sakamoto A, Okamoto Y. Structural basis of the function of endothelin receptor. Mol Cell Biochem 190:153-156, 1999.

Mellersh CS, Hitte C, Richman M, Vignaux F, Priat C, Jouquand S, Werner P, André C, DeRose S, Patterson DF, Ostrander EA, Galibert F. An integrated linkage-radiation hybrid map of the canine genome. Mamm Genome 11:120-130, 2000.

Metallinos D, Rine J. Exclusion of EDNRB and KIT as the basis for white spotting in Border Collies. Genome Biol 1:RESEARCH0004, 2001.

Morris D. Dogs. The ultimate dictionary of over 1,000 breeds, pp. 7-12. Trafalgar Square, North Pomfret, VT, 2001.

Morton CC. Genetics, genomics and gene discovery in the auditory system. Hum Mol Gen 11:1229-1240, 2002.

Mouse Genome Database (MGD), Mouse Genome Informatics Web Site, The Jackson Laboratory, Bar Harbor, Maine. World Wide Web URL: http://www.informatics.jax.org/. Retrieved January 8, 2003.

Muhle AC, Jaggy A, Stricker C, Steffen F, Dolf G, Busato A, Kornberg M, Mariscoli M, Srenk P, Gaillard C. Further contributions to the genetic aspect of congenital sensorineural deafness in Dalmatians. Vet J 163:311-318, 2002.

Nagata H, Worobec AS, Oh CK, Chowdhury BA, Tannenbaum S, Suzuki Y, Metcalfe DD. Identification of a point mutation in the catalytic domain of the protooncogene c-*kit* in peripheral blood mononuclear cells of patients who have mastocytosis with an associated hematologic disorder. Proc Natl Acad Sci U S A 92:10560-10564, 1995.

Oboki K, Morii E, Kataoka TR, Jippo T, Kitamura Y. Isoforms of *mi* transcription factor preferentially expressed in cultured mast cells of mice. Biochem Biophys Res Commun 290:1250-1254, 2002.

Patnaik AK, Ehler WJ, MacEwen EG. Canine cutaneous mast cell tumor: morphologic grading and survival time in 83 dogs. Vet Pathol 21:469-474, 1984.

Priester WA: 1973, Skin tumors in domestic animals. Data from 12 United States and Canadian colleges of veterinary medicine. J Natl Cancer Inst 50: 457-466.

Puffenberger EG, Hosoda K, Washington SS, Nakao K, deWit D, Yanagisawa M, Chakravart A. A missense mutation of the endothelin-B receptor gene in multigenic Hirschsprung's disease. Cell 79:1257-1266, 1994.

Qiu FH, Ray P, Brown K, Barker PE, Jhanwar S, Ruddle FH, Besmer P. Primary structure of c-*kit*: relationship with the CSF-1/PDGF receptor kinase family--oncogenic activation of v-*kit* involves deletion of extracellular domain and C terminus. EMBO J 7:1003-1011, 1988.

Sakamoto A, Yanagisawa M, Sakurai T, Takuwa Y, Yanagisawa H, Masaki T. Cloning and functional expression of human cDNA for the $ET_B$ endothelin receptor. Biochem Biophys Res Commun 178:656-663, 1991.

Sato S, Roberts K, Gambino G, Cook A, Kouzarides T, Goding CR. CBP/p300 as a co-factor for the Microphthalmia transcription factor. Oncogene 14:3083-3092, 1997.

Schaible RH, Brumbaugh JA. Electron microscopy of pigment cells in variegated and nonvariegated, piebald-spotted dogs. *In:* Pigment Cell, vol. 3. Proceedings of the 9th International Pigment Cell Conference, Houston, Texas, January 13-17, 1975, ed. Riley V, pp. 191-200. Karger, Basel, NY, 1996.

Schmutz SM, Moker JS, Yuzbasiyan-Gurkan V, Zemke D, Sampson J, Lingaas F, Dunner S, Dolf G. DCT and EDNRB map to DogMap linkage group L07. Anim Genet 32:321, 2001.

Schrott A, Spoendlin H. Pigment anomaly-associated inner ear deafness. Acta Otolaryngol (Stockh) 103:451-457, 1987.

Seitz JJ, Schmutz SM, Thue TD, Buchanan FC. A missense mutation in the bovine *MGF* gene is associated with the roan phenotype in Belgian Blue and Shorthorn cattle. Mamm Genome 10:710-712, 1999.

Serve H, Yee NS, Stella G, Sepp-Lorenzino L, Tan JC, Besmer P. Differential roles of PI3-kinase and Kit tyrosine 821 in Kit receptor-mediated proliferation, survival and cell adhesion in mast cells. EMBO J 14:473-483, 1995.

Sponenberg DP. Germinal reversion of the merle allele in Australian shepherd dogs. J Hered 75:78, 1984.

Sponenberg DP. Inheritance of the harlequin color in Great Dane dogs. J Hered 76:224-225, 1985.

Sponenberg DP, Lamoreux ML. Inheritance of tweed, a modification of merle, in Australian shepherd dogs. J Hered 76:303-304, 1985.

Spritz RA, Beighton P. Piebaldism with deafness: Molecular evidence for an expanded syndrome. Am J Med Genet 75:101-103, 1998.

Steel KP, Barkway C. Another role for melanocytes: their importance for normal stria vascularis development in the mammalian inner ear. Development 107:453-463, 1989.

Steingrímsson E, Moore KJ, Lamoreux ML, Ferré-D'Amaré AR, Burley SK, Zimring DCS, Skow LC, Hodgkinson CA, Arnheiter H, Copeland NG, Jenkins NA. Molecular basis of mouse *microphthalmia* (*mi*) mutations helps explain their developmental and phenotypic consequences. Nat Genet 8:256-263, 1994.

Strain GM. Aetiology, prevalence, and diagnosis of deafness in dogs and cats. Br Vet J 152:17-36, 1996.

Strain GM. Congenital deafness in dogs and cats. The Compendium on Continuing Education for the Small Animal Practitioner 13:245-251, 1991.

Strain GM. Congenital deafness and its recognition. Vet Clin North Am Small Anim Pract 29:895-907, 1999.

Suarez BK, Hampe CL. Linkage and association. Am J Hum Genet 54:554-559, 1994.

Tabor S, Struhl K. Endonucleases. *In:* Current protocols in molecular biology, ed. Ausubel FM, Brent R, Kingston RE, Moore DD, Seidman JG, Smith JA, Struhl K, vol. 1, pp. 3.12.5-3.12.6. John Wiley & Sons, New York, NY, 1989.

Tachibana M, Perez-Jurado LA, Nakayama A, Hodgkinson CA, Li X, Schneider M, Miki T, Fex J, Francke U, Arnheiter H. Cloning of *MITF*, the human homolog of the mouse *microphthalmia* gene and assignment to chromosome 3p14.1-p12.3. Hum Mol Genet 3:553-557, 1994.

Tachibana M. MITF: a stream flowing for pigment cells. Pigment Cell Res 13:230-240, 2000.

Takeda K, Yasumoto K, Kawaguchi N, Udono T, Watanabe K, Saito H, Takahashi K, Noda M, Shibahara S. Mitf-D, a newly identified isoform, expressed in the retinal pigment epithelium and monocyte-lineage cells affected by Mitf mutations. Biochim Biophys Acta 1574:15-23, 2002.

Takemoto CM, Yoon YJ, Fisher DE. The identification and functional characterization of a novel mast cell isoform of the microphthalmia-associated transcription factor. J Biol Chem 277:30244-30252, 2002.

Tsujimura T, Furitsu T, Morimoto M, Isozaki K, Nomura S, Matsuzawa Y, Kitamura Y, Kanakura Y. Ligand-independent activation of c-*kit* receptor tyrosine kinase in a murine mastocytoma cell line P-815 generated by a point mutation. Blood 83:2619-2626, 1994.

Tsujimura T, Furitsu T, Morimoto M, Kanayama Y, Nomura S, Matsuzawa Y, Kitamura Y, Kanakura Y. Substitution of an aspartic acid results in constitutive activation of c-*kit* receptor tyrosine kinase in a rat tumor mast cell line RBL-2H3. Int Arch Allergy Immunol 106:377-385, 1995.

Tsujimura T, Morimoto M, Hashimoto K, Moriyama Y, Kitayama H, Matsuzawa Y, Kitamura Y, Kanakura Y. Constitutive activation of c-*kit* in FMA3 murine mastocytoma cells caused by deletion of seven amino acids at the juxtamembrane domain. Blood 87:273-283, 1996.

Udono T, Yasumoto K, Takeda K, Amae S, Watanabe K, Saito H, Fuse N, Tachibana M, Takahashi K, Tamai M, Shibahara S. Structural organization of the human microphthalmia-associated transcription factor gene containing four alternative promoters. Biochim Biophys Acta 1491:205-219, 2000.

Vail DM. Mast cell tumors. *In:* Small animal clinical oncology, ed. Withrow SJ, MacEwen EG, 2nd ed., pp. 192-210. WB Saunders, Philadelphia, PA, 1996.

Valent P, Spanblöchl E, Sperr WR, Sillaber C, Zsebo KM, Agis H, Strobl H, Geissler K, Bettelheim P, Lechner K. Induction of differentiation of human mast cells from bone marrow and peripheral blood mononuclear cells by recombinant human stem cell factor/*kit*-ligand in long-term culture. Blood 80:2237-2245, 1992.

Willis MB. Genetics of the Dog, pp. 69-70. Howell Book House, New York, NY, 1989.

Yajima I, Sato S, Kimura T, Yasumoto K, Shibahara S, Goding CR, Yamamoto H. An L1 element intronic insertion in the black-eyed white (Mitf[mi-bw]) gene: the loss of a single Mitf isoform responsible for the pigmentary defect and inner ear deafness. Hum Mol Genet 8:1431-1441, 1999.

Yanagisawa M, Kurihara H, Kimura S, Tomobe Y, Kobayashi M, Mitsui Y, Yazaki Y, Goto K, Masaki T. A novel potent vasoconstrictor peptide produced by vascular endothelial cells. Nature 332:411-415, 1988.
Yang GC, Croaker D, Zhang AL, Manglick P, Cartmill T, Cass D. A dinucleotide mutation in the endothelin-B receptor gene is associated with lethal white foal syndrome (LWFS); a horse variant of Hirschsprung disease. Hum Mol Genet 7:1047-1052, 1998.

Yarden Y, Kuang WJ, Yang-Feng T, Coussens L, Munemitsu S, Dull TJ, Chen E, Schlessinger J, Francke U, Ullrich A. Human proto-oncogene c-*kit*: a new cell surface receptor tyrosine kinase for an unidentified ligand. EMBO J 6:3341-3351, 1987.

Yasumoto K, Mahalingam H, Suzuki H, Yoshizawa M, Yokoyama K. Transcriptional activation of the melanocyte-specific genes by the human homolog of the mouse *Microphthalmia* protein. J Biochem (Tokyo) 118:874-881, 1995.

Zemke D, Yamini B, Yuzbasiyan-Gurkan V. Characterization of an undifferentiated malignancy as a mast cell tumor using mutation analysis in the proto-oncogene c-*KIT*. J Vet Diagn Invest 13:341-345, 2001.

Zemke D, Yamini B, Yuzbasiyan-Gurkan V. Mutations in the Juxtamembrane Domain of c-*KIT* are Associated with Higher Grade Mast Cell Tumors in Dogs. Vet Pathol 39:529-535, 2002.